

Revision: Baseline/Revision Level	Document Number: SNP-DOC-0046
Effective Date: 07/01/2024	Page: 1 of 149
Title: Parahydrogen Thermophysical Properties V05 Final Report	



National Aeronautics and  
Space Administration

SNP-DOC-0046  
BASELINE  
EFFECTIVE DATE: 07/01/2024

---

**George C. Marshall Space Flight Center**  
Marshall Space Flight Center, Alabama 35812

ST-23

SPACE NUCLEAR PROPULSION (SNP)

**PARAHYDROGEN  
THERMOPHYSICAL  
PROPERTIES V05**

Revision: Baseline/Revision Level	Document Number: SNP-DOC-0046
Effective Date: 07/01/2024	Page: 2 of 149
Title: Parahydrogen Thermophysical Properties V05 Final Report	

## PARAHYDROGEN THERMOPHYSICAL PROPERTIES V05 SNP PROJECT

*Prepared By:*

\_\_\_\_\_  
**Jonathan P. McDonald**  
Systems Analysis and Integration Lead  
KBR, Inc.

\_\_\_\_\_  
**Date**

\_\_\_\_\_  
**Corey D. Smith**  
Senior Nuclear Engineer  
Analytical Mechanics Associates, Inc.

\_\_\_\_\_  
**Date**

\_\_\_\_\_  
**Adam D. Boylston**  
Senior Aerospace Engineer  
Analytical Mechanics Associates, Inc.

\_\_\_\_\_  
**Date**

*Approved By:*

\_\_\_\_\_  
**Chris Garrett**  
Systems Engineering and Integration Manager  
Jacobs Space Exploration Group (ESSCA)

\_\_\_\_\_  
**Date**

Revision: Baseline/Revision Level	Document Number: SNP-DOC-0046
Effective Date: 07/01/2024	Page: 3 of 149
Title: Parahydrogen Thermophysical Properties V05 Final Report	

### REVISION AND HISTORY PAGE

Status	Revision No.	Change No.	Description	Effective Date
Baseline	–		Baseline (SNP ECB 02 May 2024)	07/01/2024

Revision: Baseline/Revision Level	Document Number: SNP-DOC-0046
Effective Date: 07/01/2024	Page: 4 of 149
Title: Parahydrogen Thermophysical Properties V05 Final Report	

## TABLE OF CONTENTS

PARAGRAPH	PAGE
1.0 SUMMARY .....	8
2.0 DOCUMENTS.....	8
2.1 Applicable Documents.....	8
2.2 Reference Documents .....	8
3.0 INTRODUCTION .....	9
3.1 Why A New Database?.....	9
3.1.1 Dataset Must be Consistent with NIST REFPROP.....	10
3.2 Brief Note on Verification and Validation.....	13
3.3 Revision History .....	13
3.3.1 Original Release – Version 03b (v03b).....	14
3.3.2 Version 04 – Never Officially Released for Use.....	14
3.3.3 Version 05 .....	14
4.0 OVERVIEW OF DIHYDROGEN AND THE CURRENT DATABASE.....	17
4.1 Dihydrogen Spin Isomers .....	17
4.1.1 Spin Isomer Equilibrium Distribution - Variation with Temperature.....	17
4.1.2 Spin Isomer Distribution - Temporal Variation .....	19
4.2 Chemical Equilibrium.....	20
4.3 Some Guidance Regarding Usage - Limitations.....	20
4.3.1 Ionization.....	20
4.3.2 Very Low Density States.....	21
4.3.3 Extrapolation Below the Triple Point Temperature .....	22
5.0 DESCRIPTION.....	22
5.1 Zero-Pressure Backbone .....	22
5.2 Equation of State for High Temperature Calculations and Supporting Parameters .....	24
5.2.1 Collision Interaction Models .....	25
5.3 Thermodynamic Property Calculations .....	28
5.3.1 Dihydrogen Mole Fraction .....	28

Revision: Baseline/Revision Level	Document Number: SNP-DOC-0046
Effective Date: 07/01/2024	Page: 5 of 149
Title: Parahydrogen Thermophysical Properties V05 Final Report	

5.3.2	Density.....	29
5.3.3	Enthalpy.....	30
5.3.4	Entropy .....	31
5.3.5	Isobaric Specific Heat .....	32
5.3.6	Isochoric Specific Heat .....	34
5.3.7	Sound Speed .....	34
5.4	Shifting Enthalpy and Entropy to the REFPROP Reference State .....	35
5.5	Bridging High Temperature Thermodynamic Results to REFPROP .....	35
5.5.1	Bridging Temperature .....	36
5.5.2	Modification of PVT Surface to Enable Bridging.....	36
5.5.3	Bridging Parameter Variation Along Bridging Boundary .....	37
5.5.4	Bridging Parameter Variation with Temperature Internal to Bridging Region....	38
5.6	Transport Properties.....	40
5.6.1	Thermal Conductivity.....	40
5.6.2	Absolute Viscosity .....	43
5.6.3	Frozen Transport Properties .....	45
6.0	REFERENCES .....	46

Revision: Baseline/Revision Level	Document Number: SNP-DOC-0046
Effective Date: 07/01/2024	Page: 6 of 149
Title: Parahydrogen Thermophysical Properties V05 Final Report	

## TABLE OF APPENDICES

APPENDIX A.....	49
SYSTEMIC ENTROPY ERROR IN NBS-168 PARAHYDROGEN TABULATIONS .....	49
RATIONALE FOR EXCLUSION OF NBS-168 DATA FROM VALIDATION EFFORTS .....	49
IDEALIZED THRUST CHAMBER CALCULATIONS USING NBS-168 DATA.....	49
APPENDIX B.....	59
APPENDIX C.....	100
DERIVATION OF H-ATOM TEMPERATURE-VARYING FORCE CONSTANTS .....	100
APPENDIX D.....	118
VALIDATION OF THERMODYNAMIC PROPERTY RESULTS AGAINST CHEMICAL EQUILIBRIUM WITH APPLICATIONS.....	118
APPENDIX E.....	123
VALIDATION OF THERMODYNAMIC PROPERTY RESULTS AGAINST VARGAFTIK ET AL. (1996) TABULATIONS .....	123
APPENDIX F.....	127
VALIDATION OF TRANSPORT PROPERTY RESULTS .....	127
APPENDIX G.....	139
COMPARISON OF V05 WITH V03B .....	139
APPENDIX H.....	144
OVERVIEW OF THE BRIDGING PROCESS .....	144
APPENDIX I.....	149
PYTHON SOURCE CODE LISTING(S) .....	149

Revision: Baseline/Revision Level	Document Number: SNP-DOC-0046
Effective Date: 07/01/2024	Page: 7 of 149
Title: Parahydrogen Thermophysical Properties V05 Final Report	

### LIST OF TABLES

Table 5-1. REFPROP Zero-Pressure Model Constants ..... 23

### LIST OF FIGURES

Figure 3-1. Relative Error between NBS-168 and CEA for Sound Speed’s 100 kPa Isobar ..... 11  
Figure 3-2. Relative Error between NBS-168 and CEA for Entropy’s 100 kPa Isobar ..... 11  
Figure 3-3. Thermodynamic Property Calculation Method by Region (REFPROP vs. High-Temperature Methods)..... 16  
Figure 4-1. Equilibrium Variation of Spin Isomer Distribution with Temperature..... 18  
Figure 4-2. Variation of Isobaric Specific Heat with Temperature/Pressure..... 18  
Figure 4-3. Variation of Thermal Conductivity with Temperature/Pressure..... 19  
Figure 4-4. Error Associated with Exclusion of Ionization Effects..... 21  
Figure 5-1. Bridging Parameters between 10 kPa and 100 MPa ..... 38

Revision: Baseline/Revision Level	Document Number: SNP-DOC-0046
Effective Date: 07/01/2024	Page: 8 of 149
Title: Parahydrogen Thermophysical Properties V05 Final Report	

## 1.0 SUMMARY

The NASA Space Nuclear Propulsion (SNP) Program works to mature both nuclear electric and nuclear thermal propulsion capabilities. The nuclear thermal propulsion (NTP) sub-effort focuses on development of technologies enabling human exploration of Mars – with a nominal performance target of 900 second vacuum specific impulse ( $I_{vac}$ ). This  $I_{vac}$  target demands a hydrogen (molecular hydrogen, or dihydrogen) monopropellant NTP engine system, as other propellant choices fall well short of this target for realistically attainable reactor system temperatures ( $< 3000$  K).

Thus, SNP NTP development requires knowledge of the thermophysical properties for its dihydrogen propellant/working-fluid for temperatures up to roughly 3000 K. Pressure up to at least 35 MPa should be considered (rough upper end of historical pump outlet pressures), to not limit development space. Also, since the propellant is typically stored in a liquid state near its normal boiling point, the thermophysical properties must be for the parahydrogen nuclear spin state of the dihydrogen molecule.

The gold-standard for parahydrogen properties is the National Institute of Standards and Technology (NIST) Standard Database 23 usually accessed using the software tool REFPROP. For parahydrogen, this database covers temperatures from the triple point to 1000 K and pressures up to 2000 MPa. The present work extends REFPROP above its 1000 K upper bound and considers pressures up to 100 MPa. The resulting database covers temperature from the triple point to 6000 K and pressures from 1 Pa to 100 MPa. The present database includes mass-density, mass-specific enthalpy, mass-specific entropy, mass-specific isobaric specific heat capacity, mass-specific isochoric heat capacity, sound speed, absolute viscosity, thermal conductivity, and dihydrogen mole fraction. This database assumes a frozen parahydrogen nuclear spin state and chemical equilibrium for conditions where dissociation occurs. Chemically frozen values are provided, in addition to their chemical equilibrium values, for the transport properties – mass-specific isobaric specific heat and thermal conductivity.

The main body of the present document describes the database itself and provides some guidance regarding appropriate use and limitations. Various appendices cover topics that are deemed too detailed to include in the main body such as background on other candidate databases, verification/validation efforts for the present database, and source code listings.

## 2.0 DOCUMENTS

### 2.1 Applicable Documents

None.

### 2.2 Reference Documents

The following documents are the predecessors to the present document. This section also lists prior releases of the property dataset itself. A more complete discussion of the release history is found in Section 3.3

Revision: Baseline/Revision Level	Document Number: SNP-DOC-0046
Effective Date: 07/01/2024	Page: 9 of 149
Title: Parahydrogen Thermophysical Properties V05 Final Report	

JPID-FY18-00658      “Reconciling the Dihydrogen Property Calculations of McDonald (2017) to the REFPROP 9.1 Dataset” produced under:  
George C. Marshall Space Flight Center  
Engineering Services and Science Capability  
Augmentation Contract 80MSFC18C0011

ESSSA-FY17-2355      “Re-creation of the Calculations Behind the Dissociating  
[McDonald (2017) from      Dihydrogen Thermodynamic Property Tables of Vargaftik et al.  
JPID-FY18-00658]      (1996)” produced under:  
George C. Marshall Space Flight Center  
Science and Engineering  
Contract NNM12AA41C

Previous release history:

v03 – First release of thermodynamic properties only approved by the NTP Project Engineering Change Board on 27 March 2018.

v03b – Added transport properties to the v03b release.

v04 – Prepared for release, but some equation errors discovered which aborted the release in favor of moving on to a v05.

v05 - Submitted in December 2018 to the NEXUS Project office for release. Lost – never released – but copies likely exist within NASA so if v05 dated 2018 ever found - DO NOT USE.

### 3.0 INTRODUCTION

NTP system development activities underway within the SNP Program require knowledge of the thermophysical properties for its dihydrogen propellant/working-fluid for temperatures up to roughly 3000 K and pressures to at least 35 MPa. The parahydrogen nuclear spin state is of interest, since the propellant is stored in a near normal boiling point liquid state which results in it consisting almost entirely of the parahydrogen spin isomer. The current database considers temperatures up to 6000 K – much higher than the 3000 K need – because the lack of ionization up to 6000 K, except at very low pressure, allows ready extension of the chosen calculation methods to 6000 K. Pressures up to 100 MPa are considered since this is the upper bound considered by the original works on which the present calculations are based.

#### 3.1 Why A New Database?

Two key factors drove the creation of a new parahydrogen properties database. The first is the necessity that the National Institute of Standards and Technology (NIST) Standard Database 23, as accessed in via REFPROP 10 (NIST, 2018), serve as the basis of any database used by the Space Nuclear Propulsion (SNP) project. The second was the need to extend REFPROP above its 1000 K upper temperature limit in a manner that is thermodynamically seamless. Satisfying both demands together, essentially, demands a new database be created.

Revision: Baseline/Revision Level	Document Number: SNP-DOC-0046
Effective Date: 07/01/2024	Page: 10 of 149
Title: Parahydrogen Thermophysical Properties V05 Final Report	

### **3.1.1 Dataset Must be Consistent with NIST REFPROP**

The NIST Standard Database 23 is used extensively throughout NASA as a primary source for fluid thermophysical properties. Typically, this database, as accessed via the REFPROP interface (NIST, 2018), is the source for parahydrogen properties when dealing with LH<sub>2</sub>-fueled engine systems and vehicle main propulsion system analyses such as tank fill, expulsion, vent, etc.; and it is the source for properties used in support of Cryogenic Fluid Management development activities. Thus, the database to be used for SNP development activities should exactly match REFPROP within the temperature range of its applicability (up to 1000 K), or at least as close to 1000 K as possible when grafting a high temperature source onto the REFPROP dataset.

#### **3.1.1.1 Need to Extend REFPROP Above 1000 Kelvin**

The REFPROP tool provides parahydrogen properties up to 1000 K. Typical performance targets for NTP systems require propellant temperatures upwards of 3000 K, and higher temperatures are desirable from a vacuum specific impulse efficiency standpoint were they to be attainable. Thus, the database developed for use within the SNP program should have an upper limit of at least 3000 K. Of course, even higher temperatures are desirable so long as they are supported by available calculation methods and don't incur additional complications not relevant to SNP parahydrogen property needs (e.g. – SNP has no need to consider ionization effects).

#### **3.1.1.2 Data Sources Above 1000 Kelvin**

The following sources of higher temperature data were investigated for extension of the REFPROP database. Of course, it was hoped that one of these would match REFPROP well enough along its 1000 K upper isotherm to simply be added to the REFPROP dataset, but that did not prove to be the case.

##### **3.1.1.2.1 National Bureau of Standards – Monograph 168**

The predecessor to NIST, the National Bureau of Standards, published their Monograph 168 (McCarty, et al., 1981) which tabulates parahydrogen thermophysical properties up to 3000 K. When originally being considered back in 2016, this source appeared promising, when compared with REFPROP 9.1 along the 1000 K isotherm representing the REFPROP upper temperature bound, with the largest error of 1% occurring in entropy.

Yet, this source compares very poorly with results from Chemical Equilibrium with Applications (CEA, 2004) along a 100 kPa isobar – where real-gas effects should be modest enough that these two sources should agree well. Density between NBS-168 and CEA are in excellent agreement (error magnitude < 0.03%). Sound speed error becomes apparent around 2000 K, as depicted in Figure 3-1 below, and steadily increases to just over a magnitude of 2% at 3000 K.

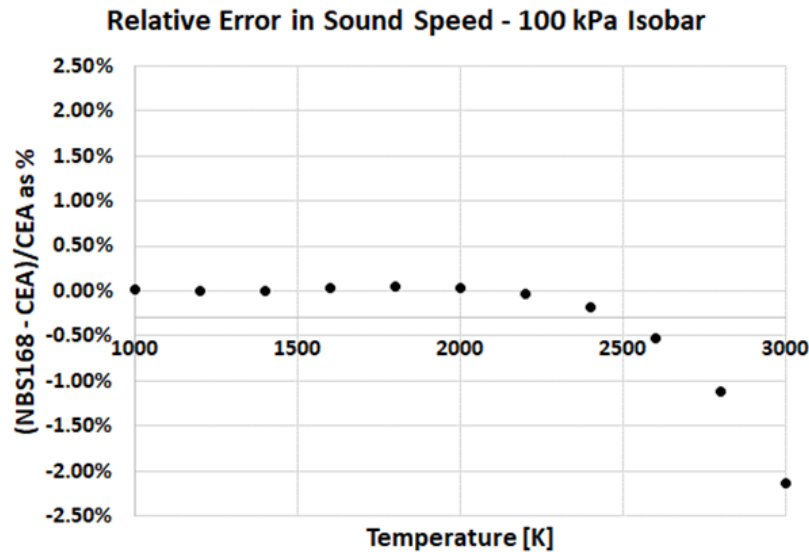


**Figure 3-1. Relative Error between NBS-168 and CEA for Sound Speed's 100 kPa Isobar**

The level of error in sound speed is not too much of an issue in itself, but the manner in which it grows steadily with increasing temperature while density remains in excellent agreement was deemed as possibly belying some other underlying issue with NBS -168. Ultimately, comparison of entropy between NBS-168 and CEA proved to be the reason for elimination of NBS-168 as a potential source of the needed high temperature parahydrogen data. As depicted in Figure 3-2 below, the local difference in entropy begins to diverge, also around 2000 K, and the relative error peaks around 54% at 2600 K.

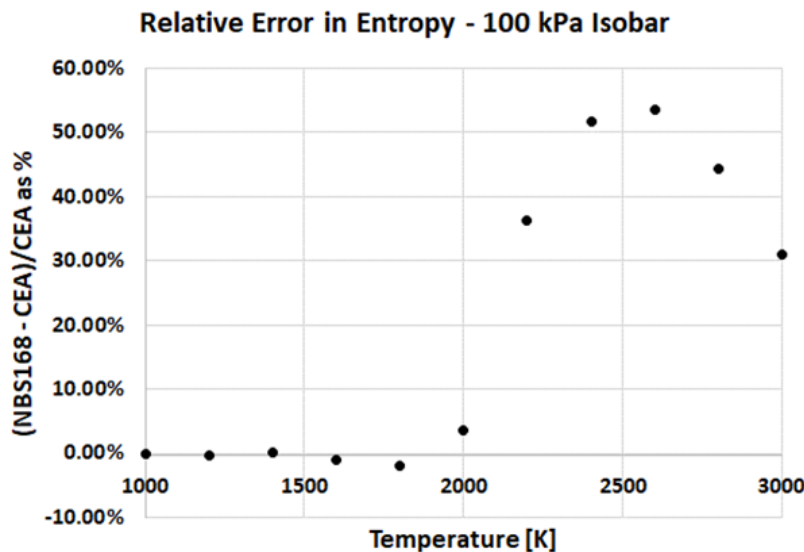


**Figure 3-2. Relative Error between NBS-168 and CEA for Entropy's 100 kPa Isobar**

Back in 2016, no explanation for this poor comparison between NBS-168 and CEA along the 100000 Pa isobar could be found, and there was too little person-hours available to pursue

Revision: Baseline/Revision Level	Document Number: SNP-DOC-0046
Effective Date: 07/01/2024	Page: 12 of 149
Title: Parahydrogen Thermophysical Properties V05 Final Report	

understanding the cause. While NBS-168 was eliminated as a source for high temperature data, it was still considered as a basis for validation of the v05 database that is the topic of this report – though NBS-168 entropy values were not considered for validation comparisons. Yet, while working validation of the v05 database calculations/results, the reason for the apparently erroneous entropy values from NBS-168 was discovered, and this discovery is documented in Appendix A of this report. Though it is not clear if the error detailed in Appendix A is also responsible for the suspicious behavior of sound speed from NBS-168, it is clear that NBS-168 is not a reliable source for the desired high temperature data, and of very limited value for validation of the SNP v05 parahydrogen database.

### **3.1.1.2.2 Department of Energy SESAME Database**

The name SESAME doesn't seem to be an acronym. The SESAME database consists of a wide range of solid and fluid substances and is distributed by the Department of Energy (DoE) Los Alamos National Laboratory (LANL). As of 2016, when access was first obtained by the present author, the hydrogen entry numbered 5250 was provided by LANL as most relevant to our NTP modeling needs. This hydrogen model compared rather unfavorably with REFPROP 9.1 along the 1000 K isotherm, but no worse so than found above for NBS-168. The key disadvantage found with the SESAME database were that access to the database is controlled and, thus, this might result in any database leveraging SESAME also having to be access controlled. Also, key references for hydrogen entries in SESAME point back to NBS work closely related to NBS-168 era efforts – and, thus, may also contain the same errors as those discussed in the last section.

### **3.1.1.2.3 Vargaftik et Alia**

The Handbook of Physical Properties of Liquids and Gases (Vargaftik et alia, 1996) tabulates real-gas properties for dissociating dihydrogen. Though not for parahydrogen, per se, the tabulations begin at 1500 K; and the properties for parahydrogen and normal hydrogen forms are the same above roughly 700 K. No glaring errors could be found in this dataset, except for numerous typographical errors in the tabulated values at isolated states. Thus, Vargaftik et al. (1996) was deemed the best option for high temperature properties; but this source begins at 1500 K, so it was not possible to directly append it to REFPROP. Thus, it was decided back in 2016 to recreate the calculation methods behind the Vargaftik et al. (1996) tabulations and use these methods as the basis for the needed property values above 1000 K.

### **3.1.1.3 Recreate the Vargaftik Methods and Append to REFPROP Results**

One of the two publications referenced by the Vargaftik et al. (1996) tabulation was found to be available in the form of a United States Air Force translation (Lykova, 1969a) of Russian language proceedings from a Union of Soviet Socialist Republics Heat and Mass Transfer conference held in Minsk, Belarus in 1968. McDonald (2017) provides additional background on how this led to recreation of the methods and constants used to calculate the tabulations of Vargaftik et al. (1996). The second of the two publications referenced by Vargaftik et al. (1996) is a doctoral dissertation (Gorykin, 1968) that should directly relate the actual methods used. The only copy of Gorykin (1968) found to date is held at a university library in Odesa, Ukraine, and repeated efforts to obtain a copy have failed due to copyright restrictions/rules. Yet, it is believed that the methods related

Revision: Baseline/Revision Level	Document Number: SNP-DOC-0046
Effective Date: 07/01/2024	Page: 13 of 149
Title: Parahydrogen Thermophysical Properties V05 Final Report	

in McDonald (2017) and deployed in McDonald (2018) are believed to be very close to those likely related in the Gorykin (1968) dissertation were it available for review. McDonald (2018) relates the first attempt at appending these methods to REFPROP results. The present work relates a similar, but considerably improved, process for ‘bridging’ the high temperature calculations to REFPROP results.

### **3.2 Brief Note on Verification and Validation**

Verification of the calculations in this work relies mostly on the validation process – if results compare well with existing sources of relevant property values, then the calculations were most likely implemented correctly. This noted, some of the more complex calculations were verified by manually executing similar calculations in Excel spreadsheets. Examples of these verification calculations were to confirm that the Python language numerical routine deployed to estimate derivatives was producing the desired results. To then confirm that the same differentiation routine delivered acceptable results for the case where it is used to estimate a derivative that itself depends on estimation of another derivative. And, lastly, to confirm proper functioning of a method used to ensure that numerical derivative estimates are not impacted by available numerical precision. The last item is the subtopic of Appendix I to this report.

Validation of the v05 results consists of comparing the results with available, trusted, sources of similar results. The main sources for validation data are the Vargaftik et al. (1996) real-gas tabulations already discussed briefly in Section 3.1.1.2.3 and ideal gas results from Chemical Equilibrium with Applications (CEA, 2004). Very limited validation use is made of NBS-168 tabulations for reasons related in Section 3.1.1.2.1 and Appendix A of this report. Lastly, the Vargaftik et al. (1996) sourced data actually used for the present validation purposes is that related in appendices to McDonald (2017), wherein the original tabulations were screened for errors and erroneous values were either corrected/deleted as appropriate. Validation is carried out separately for thermodynamic and transport quantities and the processes and results are related in appendices to the present report. This separation of validation efforts is to help ensure the reader doesn’t attempt to formulate conclusions about the validity of thermodynamic results on the basis of transport results, or vice-versa. While transport results depend on the thermodynamic calculations, the thermodynamic results do not depend on transport calculations. Additionally, the thermodynamic results are required to follow certain relationships as they transition from REFPROP to the high temperature region – but there is no such requirement imposed on the transport quantities absolute viscosity or thermal conductivity. The behavior of viscosity and conductivity as their computational bases transition from REFPROP to the high temperature methods is driven primarily by a need to avoid sudden changes that would prove troublesome to gradient-based solvers in tools that use this property database.

### **3.3 Revision History**

The revision naming convention is of the form ##\$ (e.g. – 00a, 01d, 99z). Simply put, major revisions advance the number and minor revisions advance the letter. As of the writing of this report, the revision in use within the SNP community is 03b. Revisions 00, 01, 02 were created in

Revision: Baseline/Revision Level	Document Number: SNP-DOC-0046
Effective Date: 07/01/2024	Page: 14 of 149
Title: Parahydrogen Thermophysical Properties V05 Final Report	

the 2016-2018 timeframe but never released for external use due to errors found in their review/validation process.

### 3.3.1 Original Release – Version 03b (v03b)

The first revision released for use was 03, but it only contained thermodynamic properties and was revised to 03b with the addition of transport properties.

### 3.3.2 Version 04 – Never Officially Released for Use

A v04 database was created and provided for limited review within the community, but never formally released since a community member at the Oak Ridge National Laboratory (Greenwood, 2018) found a few typographical errors in the mathematical relations used to calculate the database results. Instead of just revising v04, the present author thought there might be less of a chance for future confusion if v04 were left alone and never officially released (much less work also), and the needed corrections deployed in v05.

### 3.3.3 Version 05

A v05 database was prepared and provided in late 2018 to the then NTP development effort (not yet called SNP) for review/release. That process never proceeded due to the December 2018 to January 2019 federal shutdown, so it was decided to retain the v05 name for the effort reported here. The main creator of the database calculations pursued other career interests for several years before coming back to NTP development work and re-engaging with release of v05.

Version 03b is compared against v05 in Appendix H. The primary reason is to help users understand what impact deployment of v05 might have on their various analytical results.

#### 3.3.3.1 Correction of Errors from v03b

The original impetus to drop v04 and create a v05 was the discovery of a few typographical errors in the calculations of v03b, and the observation of a stair-step behavior in some properties for a few combinations of pressure and temperature. One of the typographical errors from v03b no longer exists because of other changes in v05 relative to v03b, but the single typographical correction that remains is to correct the following relation from Appendix C, page 15 of McDonald (2018):

dihydrogen fugacity term

$$\ln \gamma_{\text{H}_2}(T, P, \sigma_{\text{H}_2}, \epsilon_{\text{k}_\text{H}_2}) := \frac{1}{R_u \cdot T} \left[ B_{\text{H}_2}(T, \sigma_{\text{H}_2}, \epsilon_{\text{k}_\text{H}_2}) \cdot P + \frac{(C_{\text{H}_2}(T, \sigma_{\text{H}_2}, \epsilon_{\text{k}_\text{H}_2}) - B_{\text{H}_2}(T, \sigma_{\text{H}_2}, \epsilon_{\text{k}_\text{H}_2})^2) \cdot P^2}{R_u \cdot T} \cdot \frac{1}{1} \right]$$

wherein the ratio  $(P^2/1)$  should be  $(P^2/2)$  and is so corrected in the v05 calculations. The other equation update wasn't a typographical error, but rather just an instance where the algebraic form that falls most readily out of a derivation caused numerical precision issues. The following v03b relation for the equilibrium mole fraction of dihydrogen

Revision: Baseline/Revision Level	Document Number: SNP-DOC-0046
Effective Date: 07/01/2024	Page: 15 of 149
Title: Parahydrogen Thermophysical Properties V05 Final Report	

$$x_{H2}(T, P, \sigma_{H2}, \epsilon_{k_{H2}}) := 1 - \frac{2}{1 + \sqrt{1 + \frac{4 \cdot P}{K_p(KP0(T), T, P, \sigma_{H2}, \epsilon_{k_{H2}})}}}$$

yields a stair-step variation with respect to either pressure or temperature for cases where the sum term ( $4 \cdot P + K_p$ ) results in numerical truncation of the sum itself. Thus, for v05, this relation is recast in terms of the ratio  $P/K_p$  alone as follows:

Now, express dihydrogen mole fraction in terms of T and P only

$$x_{H2}(T, P, \sigma_{H2}, \epsilon_{k_{H2}}) := \frac{2 \cdot P + K_p(KP0(T), T, P, \sigma_{H2}, \epsilon_{k_{H2}}) - \sqrt{K_p(KP0(T), T, P, \sigma_{H2}, \epsilon_{k_{H2}}) \cdot (4 \cdot P + K_p(KP0(T), T, P, \sigma_{H2}, \epsilon_{k_{H2}}))}}{2 \cdot P}$$

repeat right-hand side below since it ran off page in working definition

$$\frac{2 \cdot P + K_p(KP0(T), T, P, \sigma_{H2}, \epsilon_{k_{H2}}) - \sqrt{K_p(KP0(T), T, P, \sigma_{H2}, \epsilon_{k_{H2}}) \cdot (4 \cdot P + K_p(KP0(T), T, P, \sigma_{H2}, \epsilon_{k_{H2}}))}}{2 \cdot P}$$

which eliminates the stair-step variation in  $x_{H2}$  its impact on other properties.

### 3.3.3.2 Move to Implement Methods in the Python Language

All computational work through v04 was executed in the Mathcad 15 computational software tool. The Mathcad parent company, Parametric Technologies Corporation, announced in 2021 that they would no longer allow use of Mathcad 15 after 01 January 2022. Even licensed users would no longer be allowed to open the application using their licenses. So, in the midst of development of v05 of this property database, the focus moved from the calculations themselves to porting those calculations to an open-source computational environment. The present author is not much of a programmer, so the SNP project retained the support of AMA, Inc staff (co-authors on this work) who were well-versed in use of the Python Language. Thus, the vast majority of the computations related to the v05 database are coded in Python.

### 3.3.3.3 What Else is New in v05?

In addition to the error corrections and porting to the Python Language, a few other major improvements/additions/potential-additions are discussed in the following sections.

#### 3.3.3.3.1 Improved Method for Bridging Results between REFPROP and High Temperature Calculations

Until v05, the lower temperature REFPROP results valid up to 1000 K were ‘bridged’ to the higher temperature calculations of McDonald (2017, 2018) which begin at 1500 K via methods related in McDonald (2018). The approach of McDonald (2018) worked great for pressures above roughly 30 MPa, good in the range 1 MPa to 30 MPa, and they became increasingly worse below 1 bar pressure with typical fractional errors on the order of  $1E-04$ . This author knew this behavior of increasing error with decreasing pressure was likely associated with small, though non-negligible, amounts of dissociation occurring at 1000 K for pressures below 1 bar; but there simply wasn’t time to address this systemic error in the v03b release. This error is addressed in v05 by making

the lower bound temperature of the ‘bridging’ region a function of pressure, such that the effect of dissociation at a given pressure is always = 1E-08 fractional contribution to isobaric specific heat. Thus, instead of the lower bound bridging temperature being 1000 K for all pressures, this lower bound is as depicted in Figure 3-3 below.

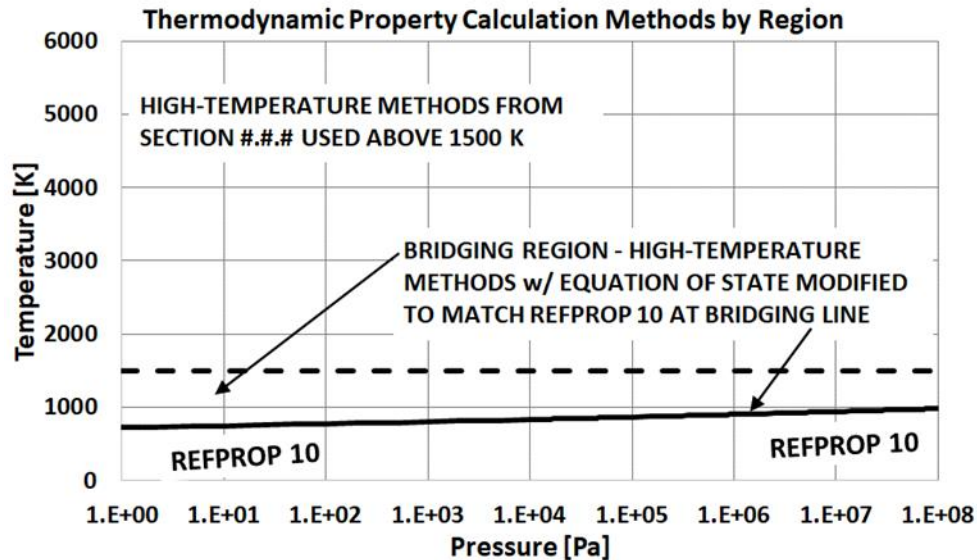


**Figure 3-3. Thermodynamic Property Calculation Method by Region (REFPROP vs. High-Temperature Methods)**

At and below this temperature curve, property results come directly from the REFPROP 10. The region between the lower temperature 'bridging' curve and 1500 K is the ‘bridging’ region wherein thermodynamic properties are obtained from the high temperature calculation methodology modified as discussed in Section 5.5.2.2 to match REFPROP 10 results along the bridging line and transition towards unmodified high temperature methods in a manner that preserves key thermodynamic relationships. At and above 1500 K, the high temperature methods are deployed without alteration.

### 3.3.3.3.2 Availability of Frozen Transport Properties

Some analytical tools commonly used within the propulsion community provide the user access to so-called 'frozen' values for some transport properties - typically isobaric specific heat and thermal conductivity. When calculating properties for systems assumed to be in thermodynamic equilibrium, the equilibrium property value may be thought of as being comprised of a 'frozen' part which excludes terms containing derivatives of product species mole fractions, and a "reaction"/"reacting"/"shifting" part which accounts for changes in composition. Typical examples of tools that offer access to 'frozen' properties are Chemical Equilibrium with Applications (CEA, 2004) and its "CEC" predecessor which may be found embedded in other tools such as Solid Rocket Motor Performance Program (SPP) or Two-Dimensional Kinetics (TDK). The 'frozen' properties made available by the present real-gas database will be slightly different than those output by these other tools since those tools assume ideal gas behavior.

Revision: Baseline/Revision Level	Document Number: SNP-DOC-0046
Effective Date: 07/01/2024	Page: 17 of 149
Title: Parahydrogen Thermophysical Properties V05 Final Report	

### 3.3.3.4 Customized Output and Possible Future Improvements

The present database is primarily defined by its methodology and the fact that it is anchored to REFPROP 10. A data tabulation suitable for most engineering calculations is provided with v05, but customized versions can be provided on request for those willing to work, patiently, with the development team. One such custom version of the v03b database was created for integration into the Loci-CHEM tool used extensively within the Fluid Dynamics Branch of the Marshall Space Flight Center Propulsion Department (NASA/MSFC/ER42).

The high temperature calculations used for the present database apply force constants for dihydrogen and atomic hydrogen based on theoretical and experimental work that is over 50 years old as of this writing. Similarly, some of the needed collision integral and dimensionless virial coefficient curves are from an even older source (Hirschfelder et al. 1966). Though updating these constants/curves will likely not impact the usefulness of this database as a property source for engineering calculations; the impact of updating these inputs isn't known and may be investigated at some point.

Given that the v05 database calculations are coded in the Python language, it may also be possible to provide a means of allowing one to directly access the underlying calculation methods instead of having to deploy the database as a sort of static data tabulation. Though not a goal of this v05 release, use of Python makes this a possibility.

## 4.0 OVERVIEW OF DIHYDROGEN AND THE CURRENT DATABASE

The term hydrogen is most often used in reference to the diatomic molecule consisting of two hydrogen atoms (dihydrogen) that naturally exists near standard temperature. As it is typically stored in a near normal boiling point liquid state for use in an engine system, dihydrogen is assumed to be in its parahydrogen spin state. Which brings us to the next section.

### 4.1 Dihydrogen Spin Isomers

Spin is a quantum mechanical property. Each hydrogen atom in dihydrogen has a proton and each proton exhibits the quantum property known as spin. This spin has a sense/direction of either up or down. Proton spin typically has no discernable impact on macroscale thermodynamic properties such as density, enthalpy, entropy for molecules; but this is not true for dihydrogen where its simplicity allows exhibition of the effect of proton spin. When the proton spins are of the same sense, or aligned, the resulting dihydrogen spin isomer is called orthohydrogen, and when of opposite sense the isomer is called parahydrogen.

#### 4.1.1 Spin Isomer Equilibrium Distribution - Variation with Temperature

The amount of each spin isomer present depends on temperature, as depicted in Figure 4-1 below from Fegley (2013). Stored near its normal boiling point, as is the case in most propulsion system applications, liquid hydrogen consists of about 99.8% parahydrogen, and the proportion of parahydrogen decreases with increasing temperature until it asymptotically approaches 25% (essentially reached by room temperature of 300 K) in a mixture commonly referred to as normal hydrogen.

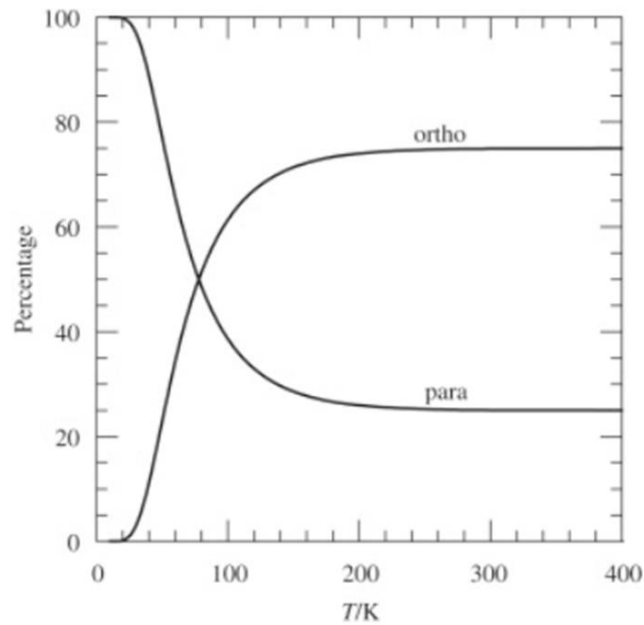


**Figure 4-1. Equilibrium Variation of Spin Isomer Distribution with Temperature**

Figure 4-2 depicts variation of isobaric specific heat variation with temperature - units are Base SI unless otherwise noted. Supporting data is from REFPROP 10 (NIST, 2018). While pressure does not impact the ortho/para distribution, curves representing atmospheric pressure and 100 atmospheres are provided since pressure does impact specific heat itself. As readily seen, the impact of spin isomer distribution on specific heat becomes quite large below room temperature.

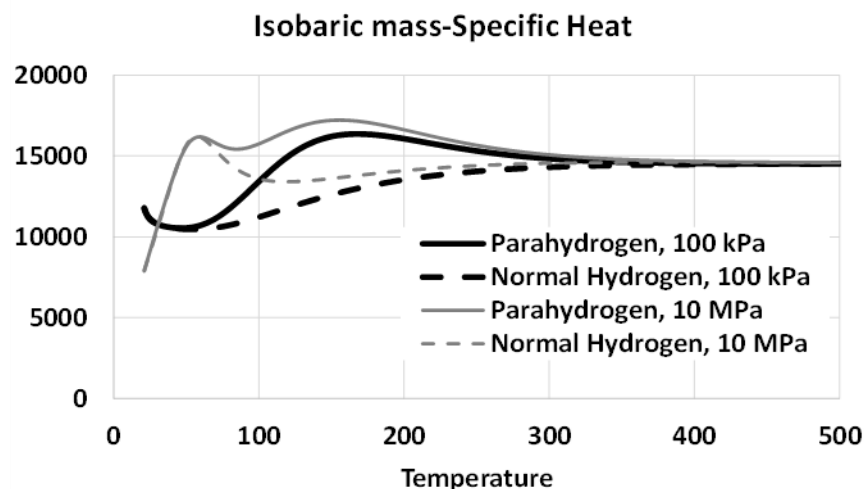


**Figure 4-2. Variation of Isobaric Specific Heat with Temperature/Pressure**

The effect of spin isomer distribution also has a substantial impact on thermal conductivity, as depicted in Figure 4-3 below. The impact of spin isomer distribution impacts other properties, but

Revision: Baseline/Revision Level	Document Number: SNP-DOC-0046
Effective Date: 07/01/2024	Page: 19 of 149
Title: Parahydrogen Thermophysical Properties V05 Final Report	

it is the impacts on specific heat and thermal conductivity that are large enough to be of interest to most engineering applications.

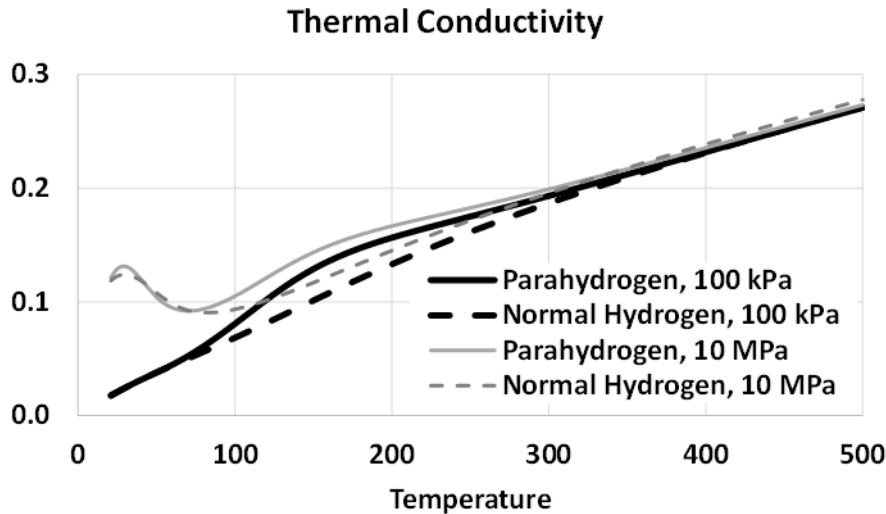


**Figure 4-3. Variation of Thermal Conductivity with Temperature/Pressure**

#### 4.1.2 Spin Isomer Distribution - Temporal Variation

The last section related how the equilibrium distribution of dihydrogen spin isomers vary with temperature; but just how long does it take for dihydrogen to attain this equilibrium distribution or to re-equilibrate after a sudden change in temperature? Typically, equilibration takes many hours, or even tens of hours, but the time may be shorter for small changes in temperature, in the presence of a suitable catalyst, in the presence of various forms of radiation, and/or under conditions resulting in dissociation. Except for substantial dissociation, even the hastened conversion half-times (time to reduce parahydrogen concentration to half its starting value) due to other noted effects are on the order of magnitude of minutes (Pyper and Briggs, 1977).

##### 4.1.2.1 Dissociation Effects

The impact of dihydrogen dissociation on spin isomer distribution has been estimated going back to Farkas and Farkas (1935) and is also discussed in Pyper and Briggs (1977). The energy level difference between the two forms results in a bias towards formation of orthohydrogen - para-to-ortho favored by a factor of 3 relative to the ortho-to-para - as a result of the recombination of H atoms to again form dihydrogen. Thus, it is possible that a measurable shift from parahydrogen towards normal-hydrogen can occur in a fuel cooling channel - especially in the boundary layer where both high dihydrogen temperature and long local fluid residence times are present. Though it would have to be the subject of a suitably detailed Computational Fluid Dynamics analysis, it might even be possible to completely achieve normal hydrogen by the exit of a fuel cooling channel for a sufficiently high performing fuel technology (temperature well above 3000 K), low chamber pressure, and long fuel cooling channel. This possibility noted, typical residence time in an NTP engine system is on the order of 10's of milliseconds and residence time in a typical fuel cooling

Revision: Baseline/Revision Level	Document Number: SNP-DOC-0046
Effective Date: 07/01/2024	Page: 20 of 149
Title: Parahydrogen Thermophysical Properties V05 Final Report	

channel where dissociation might occur is on the order of a few milliseconds. Even spontaneous conversion between spin isomer forms above roughly 700 K has no impact on thermodynamic properties except for the spin isomer form itself, since specific heats are identical for the two spin isomers above this temperature. Thus, for most any conceivable analytical purpose, it is appropriate to assume dihydrogen to be 100% parahydrogen throughout an NTP engine system.

#### **4.1.2.2 A Possible Caveat - Possibly not the Only One**

One exception to it being safe to assume parahydrogen throughout an NTP engine system, though possibly not the only such exception, might be a system where dihydrogen is extracted from the thrust chamber. A flow where dissociation in a fuel cooling channel might result in meaningful levels of para-to-ortho conversion as discussed in the last section – possibly for the purpose of pressurizing a liquid hydrogen storage tank. Though this para-to-ortho conversion would not impact tank pressurization thermodynamics, if the gaseous pressurant were then chilled back to a liquid state (e.g. - via a cryogenic fluid management system), the spin isomer effect on thermodynamic properties would become necessary to consider.

## **4.2 Chemical Equilibrium**

The present database assumes chemical equilibrium in all its property calculations. In addition to their equilibrium values, values for isobaric specific heat and thermal conductivity are reported that exclude the effects of the reaction coordinate - 'frozen' values. Yet, the relative dihydrogen and atomic hydrogen concentrations used to calculate these 'frozen' values are the equilibrium concentrations for the state of interest.

Most equilibrium solvers used within the propulsion community assume product species to interact as ideal gases when calculating their equilibrium concentrations. The present work accounts for real-gas effects on the equilibrium composition, so one may find dihydrogen mole fraction in the present database to increasingly differ from that reported by other sources as one moves towards the 100 MPa and 6000 K corner of this database.

## **4.3 Some Guidance Regarding Usage - Limitations**

For the most part, this document simply intends to relate assumptions and methods the user needs to understand to make responsible use of the database; and it is up to the user to be responsible in its use. Yet, a few bits of 'guidance' are offered in the next sections.

### **4.3.1 Ionization**

For pressures above 1 bar, even at 6000 K, ionization has a negligible impact on properties - typically tenths of a percent or less. The state point with greatest ionization potential in the present database is 1 Pa, 6000 K, and properties at this point are greatly impacted by the fact that this database does not include ionization effects (e.g. - the present database underpredicts isobaric specific heat by a factor of 4x, overpredicts sound speed by 1.18x, but overpredicts density by only 1.02x). Some commonly used properties most impacted by ionization are depicted as lines in pressure-temperature space along which each of these properties errs by 1% as estimated using CEA (2009). Points below and to the right of each curve incur error less than 1%. Due to the

Revision: Baseline/Revision Level	Document Number: SNP-DOC-0046
Effective Date: 07/01/2024	Page: 21 of 149
Title: Parahydrogen Thermophysical Properties V05 Final Report	

logarithmic pressure scale, it appears as if a lot of pressure-temperature space incurs error greater than 1%; but the vast majority of pressures of practical interest are above 100000 Pa where ionization is negligible. For the lowest pressure considered by the present database, ionization results in 1% error in isobaric specific heat at around 4200 K - a temperature well above the range of present practical interest to nuclear thermal propulsion system development.

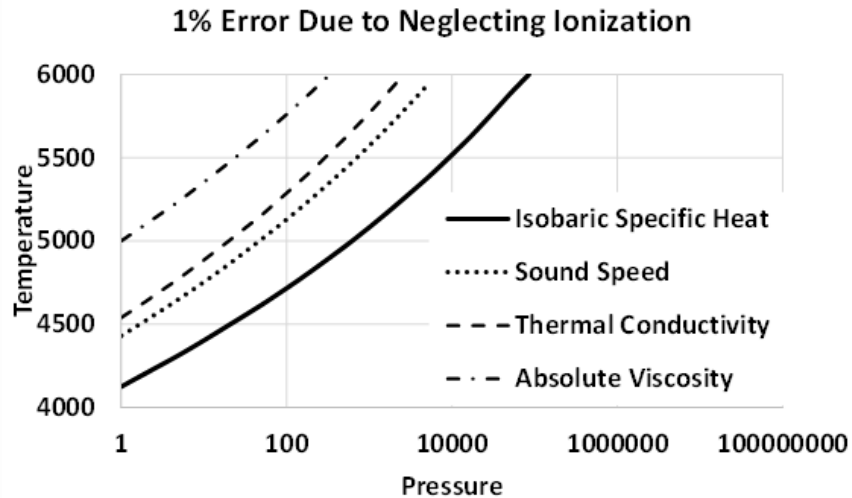


**Figure 4-4. Error Associated with Exclusion of Ionization Effects**

#### 4.3.2 Very Low Density States

The present database provides access to property values to pressure as low as 1 Pa and temperature as low as the parahydrogen triple point temperature of 13.8 K. For Knudsen Number,  $Kn \leq 0.01$ , a flow condition of interest may be comfortably treated as continuum in nature; where Knudsen Number may be estimated from properties tabulated in this present database as:

$$Kn = \frac{\mu}{\rho \cdot L \cdot a} \cdot \sqrt{\frac{c_p}{c_v} \cdot \frac{\pi}{2}}$$

where  $\mu$  is the absolute viscosity,  $\rho$  is density,  $L$  is characteristic length scale for the flow of interest,  $a$  is sound speed,  $c_p$  is mass-specific isobaric specific heat, and  $c_v$  is mass-specific isochoric specific heat. At 1 Pa and 13.8 K, Knudsen Number based on a 1 meter characteristic length scale is  $Kn = 1.9E-4$ . Cast another way, the smallest characteristic length for which a flow is continuum in nature ( $Kn \leq 0.01$ ) is 0.02 meters. Thus, many flows are non-continuum at 1 Pa and 13.8 K, though along a 13.8 K isotherm most flows of practical interest are continuum in nature for pressures above 10 Pa. The present database can readily produce property data for states that likely correspond to non-continuum flow regimes, and the user is cautioned to take care when considering conditions that result in very low densities.

Revision: Baseline/Revision Level	Document Number: SNP-DOC-0046
Effective Date: 07/01/2024	Page: 22 of 149
Title: Parahydrogen Thermophysical Properties V05 Final Report	

### 4.3.3 Extrapolation Below the Triple Point Temperature

In as much as REFPROP 10 (NIST, 2018) serves as the basis for all low temperature properties in the present database, the lowest temperature considered by the present database is the same as that applied in REFPROP 10 - the parahydrogen triple point temperature of 13.8 K. This leaves a region between this triple point boundary/isotherm and the sublimation line where one may choose to extrapolate to obtain properties (though no such functionality is inherent in the v05 database). One may use REFPROP 10 to estimate pressure-temperature pairs along the sublimation line using the call form =REFPROP("T","parahydrogen","PSUBL","Mass Base SI", Input Pressure Value), and the following (Pa,K) pairs are provided down to the 1 Pa lower limit of the v05 database to aid the user with defining the sublimation line:

(1,6.68), (2,6.98), (5,7.41), (10,7.77), (20,8.16), (50,8.74), (100,9.23), (200,9.77), (500,10.58), (1000,11.29), (2000,12.08), (5000,13.29), (7041,13.80)

where the last pair is the parahydrogen triple point. Should a user decide they need to extrapolate into this gaseous region below 13.8 K, note that the best mathematical-physics forms for such extrapolation are driven by the fact that this region behaves like an ideal gas with constant specific heat - at least until the sublimation line is reached. The user is entirely on their own below the 13.8 K minimum temperature associated with the REFPROP 10 representation of parahydrogen.

## 5.0 DESCRIPTION

National Institute of Standards and Technology Database 23, in the form of REFPROP 10 (NIST, 2018), serves as the basis for the present work which grafts values resulting from statistical mechanics methods onto the REFPROP 10 values in a manner that preserves the most relevant thermodynamic interrelationships between the two different sources. Since a recipient of this v05 SNP developed database may not have access to REFPROP 10, some key references regarding the REFPROP 10 parahydrogen model, as provided internal to the REFPROP 10 application, are:

Equation of State - Leachman et al. (2009)

Viscosity - Muzny et al. (2013)

Thermal Conductivity - Assael et al. (2011)

Much related here is the same as background from McDonald (2017, 2018) but it is hopefully better-related than in those earlier works; and some of the details here are new as well.

### 5.1 Zero-Pressure Backbone

The basis for any fluid property dataset is how the substance under consideration behaves in the absence of meaningful interactions - even with itself - or its ideal-gas/zero-pressure behavior. Real-gas properties are then obtained by application of relevant thermodynamic relations over a suitable pressure-volume-temperature mathematical surface (equation of state). Such zero-pressure property data is the topic of many compendium sources, two of the most familiar of which are the NIST-JANNAF Thermochemical Tables (Chase, 1998) and Thermodynamic Properties of Individual Substances (Gurvich et al., 1989). The present work bridges the REFPROP 10 property

Revision: Baseline/Revision Level	Document Number: SNP-DOC-0046
Effective Date: 07/01/2024	Page: 23 of 149
Title: Parahydrogen Thermophysical Properties V05 Final Report	

dataset to high temperature calculations and, thus, the first step is to bridge the underlying zero-pressure properties between these low and high temperature sources.

The zero-pressure isobaric molar specific heat model used for parahydrogen in REFPROP 10 is related in Leachman et al. (2009) and has the form:

$$\frac{c_p^0}{R} = 2.5 + \sum_{k=1}^N u_k \left( \frac{v_k}{T} \right)^2 \frac{\exp(v_k/T)}{[\exp(v_k/T) - 1]^2}$$

where  $C_p0$  is the zero-pressure isobaric molar specific heat,  $R$  is the molar gas constant,  $T$  is temperature, and  $u_k$  and  $v_k$  are fit parameters tabulated below.

**Table 5-1. REFPROP Zero-Pressure Model Constants**

Parahydrogen		
$k$	$u_k$	$v_k$
1	4.302 56	499
2	13.028 9	826.5
3	-47.736 5	970.8
4	50.001 3	1166.2
5	-18.626 1	1341.4
6	0.993 973	5395
7	0.536 078	10185

The above relation can be integrated to obtain zero-pressure enthalpy and entropy changes. The zero-pressure properties needed for the high-temperature calculations are taken from Gurvich et al. (1989). Many sources for zero-pressure properties exist, but Gurvich et al. (1989) was chosen as it lists values for both spin isomers (orthohydrogen, parahydrogen) and the case in which they are in equilibrium at each tabulated temperature value. This allows one to discern the temperature above which zero-pressure isobaric specific heat is the same for the two spin isomer forms (700 K). Gurvich et al. (1989) also provides extensive discussion of calculation methods / assumptions.

Ultimately, only zero-pressure enthalpy and entropy (referenced to 1 bar) are needed for the present work. Zero-pressure isobaric heat capacity isn't used explicitly, but it should be accurately extractable from the zero-pressure enthalpy model since this process is implicit to how real-gas specific heats are calculated. The high temperature calculations apply zero-pressure curves where enthalpy ( $h$ ) = entropy ( $s$ ) = 0 at 0 K, and the final real-gas  $h$  and  $s$  values are shifted to match the REFPROP 10 default reference state. The zero-pressure enthalpy and entropy curves used for this work apply the following curve fit form for  $C_p0$ :

$$C_p0 = am6 \cdot T^{-6} + am5 \cdot T^{-5} + am4 \cdot T^{-4} + am3 \cdot T^{-3} + am2 \cdot T^{-2} + am1 \cdot T^{-1} \\ + a0 + a1 \cdot T + a2 \cdot T^2 + a3 \cdot T^3 + a4 \cdot T^4 + a5 \cdot T^5 + a6 \cdot T^6 + a7 \cdot T^7 + a8 \cdot T^8 + a9 \cdot T^9$$

Revision: Baseline/Revision Level	Document Number: SNP-DOC-0046
Effective Date: 07/01/2024	Page: 24 of 149
Title: Parahydrogen Thermophysical Properties V05 Final Report	

This basic fit form was stolen from CEA (2009) and expanded by adding both negative and positive power terms in T to allow it to accurately represent the entire range of current interest -  $700 \text{ K} \leq T \leq 6000 \text{ K}$ . This form is explicitly integrable to obtain zero-pressure enthalpy (H0) and entropy at 1 bar (S0\_1bar) with the addition of integration constants. The needed fit and integration constants are obtained by constraining the above relation for Cp0 to match the REFPROP 10 Cp0 representation over the range  $700 \text{ K} \leq T \leq 1000 \text{ K}$ , to be guided by a weighted average of REFPROP 10 and Gurvich et al. (1989) values in the range  $1000 \text{ K} < T < 1500 \text{ K}$ , and to reproduce values from Gurvich et al. (1989) in the range  $1500 \text{ K} \leq T \leq 6000 \text{ K}$  within their tabulated precision. Simultaneous with these Cp0 constraints, constraints were applied to reproduce H0 and S0 from Gurvich et al. (1989) in the range  $1500 \text{ K} \leq T \leq 6000 \text{ K}$  within tabulated precision. The details of this process and results are related in Appendix B.

Though zero-pressure properties for atomic hydrogen are very straightforward to obtain, as its Cp0 value is constant for all temperatures in the range  $700 \text{ K} < T < 6000 \text{ K}$ , Appendix B also develops and relates mathematical models for atomic hydrogen zero-pressure molar enthalpy and molar entropy at 1 bar that are used in the real-gas calculations instead of the Gurvich et al. (1989) tabulations themselves.

## 5.2 Equation of State for High Temperature Calculations and Supporting Parameters

Calculation of real-gas properties other than specific volume (or its inverse, density) requires a suitable real-gas equation of state. The present work uses the same virial forms used in McDonald (2017, 2018), and also used in the works on which those works were built. While overall the SNP v05 database represents parahydrogen, discussion of the high temperature region calculation methods refer to dihydrogen as they are generally applicable to any mixture of spin isomers above 700 K as noted in Section 4.1.2.1 above.

### Dihydrogen

$$V_{H_2} = \frac{Ru \cdot T}{P} + B_{H_2} + \frac{C_{H_2} - B_{H_2}^2}{Ru \cdot T} \cdot P$$

### Atomic Hydrogen

$$V_H = \frac{Ru \cdot T}{P} + B_H$$

where H2 refers to dihydrogen and H to atomic hydrogen, Ru is the molar gas constant, B is the second virial coefficient, and C is the third virial coefficient. The efforts on which this work and that from McDonald (2017, 2018) are based found the 3-term model necessary to represent dihydrogen, while the 2-term model is sufficient for atomic hydrogen so long as BH accounts for quantum effects.

Revision: Baseline/Revision Level	Document Number: SNP-DOC-0046
Effective Date: 07/01/2024	Page: 25 of 149
Title: Parahydrogen Thermophysical Properties V05 Final Report	

## 5.2.1 Collision Interaction Models

The virial coefficients B and C are functions of temperature only. Their values depend on the interaction potential deployed in their calculation. The present work is based around the common Lennard-Jones 6-12 interaction potential, details of which are readily available in the literature, but which depends on two 'force' constants typically referred to as effective collision diameter,  $\sigma$ , and well-depth (a.k.a. - dispersion energy),  $\epsilon$ . The dispersion energy is commonly used as its ratio to the Boltzmann Constant, k, with this ratio,  $\epsilon/k$ , being referred to as the characteristic temperature of the well-depth. Virial coefficients are calculated via integration of appropriate statistical mechanics relationships using a normalized form of an interaction potential, such that these curves of normalized virial coefficient variation with temperature can approximate different species/particles with proper selection of  $\sigma$  and  $\epsilon/k$ . Thus, virial coefficients are usually supplied as tabulations versus temperature instead of recalculating them each time.

### 5.2.1.1 Dihydrogen

For dihydrogen, the following force constant values are obtained from Lykova (1968b):

effective collision diameter -  $\sigma_{H_2} = 2.934 \text{ Angstrom}$

and characteristic temperature -  $\left(\frac{\epsilon}{K}\right)_{H_2} = 34.1 \text{ K}$

McDonald (2017) attempts to relate how these values were found and are believed to be those used to calculate the dissociating hydrogen tabulations in Vargaftik et al. (1996). The short version is that the sources referenced by Vargaftik et al. (1996) for its dissociating hydrogen tabulations are an S.F. Gorykin Doctoral Dissertation from the Lomonosov Odesa Technical Institute (Gorykin, 1968) and a conference publication co-authored by S.F. Gorykin and P.M. Kessel'man - both from 1968. Lykova (1968b) containing the above constants was from the same conference, and P.M. Kessel'man received their doctoral degree from the Lomonosov Odesa Technical Institute in 1966. Thus, while the Gorykin dissertation is not available for review, it seems highly likely that Gorykin (1968) would have used the above values when developing the calculations behind the tabulation of Vargaftik et al. (1996).

### 5.2.1.2 Atomic Hydrogen (with Quantum Corrections)

McDonald (2017) attempted to deduce from available literature sources the methods used by Gorykin (1968) to calculate the dissociating hydrogen tabulations of Vargaftik et al. (1996). Without access to Gorykin (1968), the atomic hydrogen model used in that work remains unknown – though sources contemporary to Gorykin (1968) note that accounting for quantum corrections is necessary when modeling atomic hydrogen. Ultimately, McDonald (2017) used a Lennard-Jones 6-12 potential with quantum corrections (Boyd, 1971) as it provides sufficient flexibility to recreate the only insight currently available into the method of Gorykin (1968) - a tabulation of atomic hydrogen second virial coefficient from the Lykova et al. (1968b). This model approach is certainly not the one actually used by Gorkyin (1968), but it works for the present purposes. Appendix C relates the details of this approach to modeling atomic hydrogen along with details touched upon in the next few sections about special methods applied to allow the models for

Revision: Baseline/Revision Level	Document Number: SNP-DOC-0046
Effective Date: 07/01/2024	Page: 26 of 149
Title: Parahydrogen Thermophysical Properties V05 Final Report	

dihydrogen and atomic hydrogen self-interaction to be joined to model the unlike interaction potential for interaction of dihydrogen with atomic hydrogen.

### 5.2.1.3 Dihydrogen <-> Atomic Hydrogen Unlike Interaction Model

The dihydrogen self-interaction model used in this work is based on a simple Lennard-Jones 6-12 potential. The atomic hydrogen self-interaction model is derived using a combination of a quantum corrected Lennard-Jones 6-12 potential and tabulated values for atomic hydrogen second virial coefficient based on an unknown potential model from the unavailable Gorykin (1968) dissertation. The key point here is that these two self-interaction models have different interaction potential models as their basis and, thus, their force constants cannot be directly combined for the purpose of modeling the unlike interaction between dihydrogen and atomic hydrogen.

#### 5.2.1.3.1 Requirement for a Common Interaction Potential

The force constants associated with application of a given collision interaction potential are unique to that potential and the particle being modeled. Thus, modeling of unlike interactions via common combining rules for force constants (Hirschfelder et al., 1966)

$$\sigma_{H_2-H} = \frac{\sigma_{H_2} + \sigma_H}{2}$$

$$\epsilon_{H_2-H} = \sqrt{\epsilon_{H_2} \cdot \epsilon_H}$$

requires the force constants being combined to have the same underlying interaction potential. As the basic Lennard-Jones 6-12 potential is used for dihydrogen self-interaction, the present work will apply this same potential for modeling the unlike interaction between dihydrogen and atomic hydrogen. It happens that the quantum corrected Lennard-Jones 6-12 model from Boyd (1971) provides a ready means of calculating normalized second virial coefficient with/without quantum corrections. Thus, deploying the Lennard-Jones 6-12 model here is mathematically convenient.

#### 5.2.1.3.2 Recast Atomic Hydrogen Self-Interaction Potential

Kessel'man (1964) relates a method that can describe the second and third virial coefficients and viscosity coefficient for a wide variety of species and across a broad range of temperature. This method employs a Lennard-Jones 6-12 potential in which the force constants - effective collision diameter and characteristic temperature - are both allow to vary with temperature. It is believed that Gorykin (1968) also employed this approach when calculating the dissociating hydrogen properties tabulated in Vargaftik et al. (1996); but this cannot be known for certain, or if the method is exactly the same as from Kessel'man (1964), without recourse to the Gorykin (1968) text. Thus, McDonald (2017, 2018) deployed a qualitatively similar approach in which the force constants corresponding to a standard Lennard-Jones 6-12 potential are allowed to vary with temperature in a manner that simultaneously recreates the atomic hydrogen second virial coefficient discussed in Section 5.2 and the collision integral from statistical mechanics ( $\Omega_{2,2}$ ) on which the viscosity

Revision: Baseline/Revision Level	Document Number: SNP-DOC-0046
Effective Date: 07/01/2024	Page: 27 of 149
Title: Parahydrogen Thermophysical Properties V05 Final Report	

of atomic hydrogen depends (Vanderslice et al., 1962). The details of this method are related in Appendix C. The results are vectors of effective collision diameter and characteristic temperature that vary with temperature. These vectors are then interpolated to obtain needed values for atomic hydrogen second virial coefficient. They are also combined with the dihydrogen force constants already noted to arrive at force constants for modeling the unlike interactions between dihydrogen and atomic hydrogen via the same Lennard-Jones 6-12 potential.

### 5.2.1.3.3 Derivative of Recast Atomic Hydrogen Potential

Deploying the method described in the last section brings up the question of whether, or not, the temperature dependence of force constants should be captured in the constitutive relations that involve derivatives with respect to temperature for calculation of thermodynamic properties. In their usual application in such relations, the effective collision diameter and characteristic temperature force constants are ... constant. This question is addressed here in the following two ways.

First, does inclusion/exclusion of the force constant temperature dependency accurately recreate the derivative of atomic hydrogen second virial coefficient with respect to temperature? This question can be avoided altogether where this derivative is explicit in the relations by simply deploying the quantum corrected Lennard-Jones 6-12 calculations from Boyd (1971) instead of the standard 6-12 potential with temperature varying force constants. But, this derivative is also taken implicitly when taking the derivative with respect to temperature of the unlike interaction parameter - which itself depends on second virial coefficients for dihydrogen and atomic hydrogen self-interactions and their unlike interaction. Verification calculations were conducted in which the derivative with respect to temperature of the atomic hydrogen second virial coefficient was taken for the case operating directly on the quantum corrected calculations of Boyd (1971) and those compared with operating on the second virial coefficient calculated using the 6-12 potential with temperature dependent force constants both with/without inclusion of the force constant temperature dependence. When using the 6-12 potential with temperature varying force constants, failure to capture the force constant temperature dependence results in derivative values that are several orders of magnitude off from either operating directly on the calculations from Boyd (1971) or when accounting for force constant temperature dependence in the derivative. These latter two methods are in excellent agreement with each other.

Second, while executing validation comparisons between the current database results and the Vargaftik et al. (1996) tabulations, it was found that the present enthalpy calculations exhibit a systemic error relative to the Vargaftik values when the present calculations capture temperature dependence of the force constants in the derivatives with respect to temperature. This systemic difference in the enthalpies disappeared when the force constant temperature dependence was excluded from the present methods. This finding implies that Gorykin (1968) may not have included the temperature dependence of the force constants in their calculations - easy to imagine since capturing this dependence in 1968 era computations would be very taxing. This implication isn't certain, by far, since without access to Gorykin (1968) there is no way to understand how similar the approaches are between that work and the approach used in the present work.

Revision: Baseline/Revision Level	Document Number: SNP-DOC-0046
Effective Date: 07/01/2024	Page: 28 of 149
Title: Parahydrogen Thermophysical Properties V05 Final Report	

The present work chooses to capture the force constant temperature dependency in its results, as this properly replicates the first derivative of the second virial coefficient with respect to temperature that appears explicitly and implicitly in the property calculations.

### 5.3 Thermodynamic Property Calculations

This section reviews the mathematical relations used to calculate the properties of interest: dihydrogen mole fraction, mass-density, mass-specific enthalpy, mass-specific entropy, isobaric mass-specific heat, isochoric mass-specific heat, and sound speed. Most of the relations come from Kessel'man (1968). Calculations related to the transport properties, absolute viscosity and thermal conductivity, are related in Section 5.6 along with calculation of frozen isobaric specific heat and frozen thermal conductivity. Both enthalpy and entropy values depend on the chosen reference state. The reference states used for these high temperature calculations are those for the zero-pressure values from Gurvich et al. (1989) used in the present work (see Section 5.1 and Appendix B) – H (enthalpy) = 0 at 0 K and S (entropy) = 0 at 0 K and 1 bar.

The resulting enthalpy and entropy values must be shifted to the REFPROP 10 reference state (Section 5.4) prior to output for the final database, and the molar specific volume and entropy relations must be modified slightly (Section 5.5.2.2 – items 3 and 6, respectively) to enable smooth ‘Bridging’ of these higher temperature results with those from REFPROP 10.

#### 5.3.1 Dihydrogen Mole Fraction

The present calculation scheme does not account for ionization effects, so dihydrogen mole fraction is calculated directly from an algebraic relationship for the single reaction of interest



where the resulting dihydrogen mole fraction relation is

$$x_{H2} = \frac{2 \cdot P + KP - \sqrt{KP \cdot (4 \cdot P + KP)}}{2 \cdot P}$$

where P is pressure and KP is the real-gas equilibrium constant. While the above relation for xH2 is the form that most naturally falls out of the underlying derivation, the presence of terms where KP and P are additive introduces a numerical issue for states where their magnitudes are at opposite extremes (relatively low temperature and high pressure or high temperature and low pressure) resulting in a stair-step behavior in xH2 and dependent property values. Thus, the above xH2 relation is algebraically rearranged such that KP and P only occur in ratio form as follows

$$x_{H2} = 1 - \frac{2}{1 + \sqrt{1 + \frac{4 \cdot P}{KP}}}$$

which effectively eliminates the aforementioned stair-step behavior in the property values. The real-gas equilibrium constant is defined in terms of the ideal gas version, KP0, as follows:

Revision: Baseline/Revision Level	Document Number: SNP-DOC-0046
Effective Date: 07/01/2024	Page: 29 of 149
Title: Parahydrogen Thermophysical Properties V05 Final Report	

$$KP = \frac{KP0}{K\gamma}$$

where  $K\gamma$  accounts for the effect of real-gas behavior on the equilibrium calculation. The following details were nicely related in Lykova (1969a). The  $K\gamma$  correction in terms of activity coefficients,  $\gamma_H$  and  $\gamma_{H2}$ , is

$$\ln(K\gamma) = 2 \cdot \ln(\gamma_H) - 1 \cdot \ln(\gamma_{H2})$$

where H refers to the atomic hydrogen product with a stoichiometric coefficient of 2 and H2 is the dihydrogen reactant with a stoichiometric coefficient of 1. The activity terms can be expressed in terms of the real-gas parts of the virial equations of state for each product as follows:

$$\ln(\gamma_H) = \frac{1}{Ru \cdot T} \cdot (B_{H\_LJappx} \cdot P)$$

where  $B_{H\_LJappx}$  is the second virial coefficient based on the Lennard-Jones approximation where force constants depend on temperature (see 5.2.1.3.2 for discussion and Appendix C for computational details), and

$$\ln(\gamma_{H2}) = \frac{1}{Ru \cdot T} \cdot \left( B_{H2} \cdot P + \frac{(C_{H2} - B_{H2}^2)}{2 \cdot Ru \cdot T} \cdot P^2 \right)$$

where C is the third virial coefficient.

### 5.3.2 Density

The virial equations of state for each product species, presented back in Section 5.2, are cast in terms of molar specific volume, V. The mixture molar specific volume is the weighted sum of the dihydrogen and atomic hydrogen molar specific volumes and an unlike interaction term,  $\Delta V$

$$V_{mix} = x_{H2} \cdot V_{H2} + x_H \cdot V_H + x_{H2} \cdot x_H \cdot \Delta V$$

The unlike interaction term may be expressed as

$$\Delta V = \delta_{H2H} + \frac{(B_{H2} - B_{H\_LJappx})^2}{Ru \cdot T} \cdot P$$

where  $\delta_{H2H}$  is a second virial coefficient grouping for the unlike interaction. The atomic hydrogen second virial coefficient used above does not have to be the Lennard-Jones approximation with temperature dependent force constants - either the quantum corrected model from Boyd (1971) or the Lennard-Jones approximation yield the same values - but the Lennard-Jones approximation was used in the actual Python calculations for the v05 database to allow investigation of the case where force constant temperature dependency was isolated when differentiating with respect to temperature (see Section 5.2.1.3.3 and Appendix C). The unlike interaction second virial coefficient term may be expressed as

Revision: Baseline/Revision Level	Document Number: SNP-DOC-0046
Effective Date: 07/01/2024	Page: 30 of 149
Title: Parahydrogen Thermophysical Properties V05 Final Report	

$$\delta_{H_2H} = 2 \cdot B_{H_2H} - B_{H_2} - B_{H\_LJappx}$$

where H2H refers to the unlike interaction of dihydrogen (H2) with atomic hydrogen (H). This unlike interaction second virial coefficient is calculated via the usual force constant combining rules (see Section 5.2.1.3.1) where the atomic hydrogen force constants are the temperature dependent values discussed in Section 5.2.1.3.2. The force constant combining rules are now where each unlike interaction force constant depends on temperature via the Lennard-Jones 6-12 approximation model for atomic hydrogen from Section 5.2.1.3.2.

$$\sigma_{H_2H}(T) = \frac{\sigma_{H_2} + \sigma_{H\_LJappx}(T)}{2}$$

$$\varepsilon_{H_2H}(T) = \sqrt{\varepsilon_{H_2} \cdot \varepsilon_{H\_LJappx}(T)}$$

Above, one finds all the calculations necessary to arrive at molar specific volume for the dissociation products mixture. Turning this value into mass-specific density requires only the molar mass of the dissociated mixture, which may be calculated as follows

$$MM_{mix} = x_{H_2} \cdot MM_{H_2} + x_H \cdot MM_H = x_{H_2} \cdot MM_{H_2} + (1 - x_{H_2}) \cdot MM_H$$

where the mole fraction of atomic hydrogen may be replaced by (1 - xH2) since only H2 and H products exist. Mass-specific density is then

$$\rho_{mix} = \frac{1}{v_{mix}} = \frac{MM_{mix}}{V_{mix}}$$

where v denotes the mass-specific volume and care should be taken here to correctly account for units, since MM is typically provided in units of gm/mol instead of the Base SI unit of kg/mol.

### 5.3.3 Enthalpy

As the heart of these calculations are carried out in molar terms, the following begins with the desired end result of mass-specific enthalpy and proceeds backwards, if one will, through the detailed molar-based calculation relations.

$$h_{mix} = \frac{H_{mix}}{MM_{mix}}$$

where  $H_{mix}$  is the mixture molar enthalpy. This mixture molar enthalpy is calculated as the weighted sum of product species H's plus an unlike interaction term,  $\Delta H_{H_2H}$ , as follows

$$H_{mix} = x_{H_2} \cdot H_{H_2} + x_H \cdot H_H + x_{H_2} \cdot x_H \cdot \Delta H_{H_2H}$$

Revision: Baseline/Revision Level	Document Number: SNP-DOC-0046
Effective Date: 07/01/2024	Page: 31 of 149
Title: Parahydrogen Thermophysical Properties V05 Final Report	

Variables  $H_{H_2}$  and  $H_H$  are the contributions of dihydrogen and atomic hydrogen interactions with themselves. The unlike interaction between dihydrogen and atomic hydrogen contribution may be expressed as

$$\Delta H_{H_2H} = \left( \delta_{H_2H} - T \cdot \left( \frac{d}{dT} (\delta_{H_2H}) \right) \right) \cdot P + \frac{(B_{H_2} - B_{H-LJappx})}{Ru \cdot T} \cdot P^2 \cdot \left( \left( B_{H_2} - T \cdot \left( \frac{d}{dT} B_{H_2} \right) \right) - \left( B_{H-LJappx} - T \cdot \left( \frac{d}{dT} B_{H-LJappx} \right) \right) \right)$$

The enthalpies associated with each product species are calculated as

$$H_{H_2} = H_{0H_2} + Ru \cdot T \cdot \left( \frac{1}{V_{H_2}} \cdot \left( B_{H_2} - T \cdot \left( \frac{d}{dT} B_{H_2} \right) \right) + \frac{1}{V_{H_2}^2} \cdot \left( C_{H_2} - \frac{T}{2} \cdot \left( \frac{d}{dT} C_{H_2} \right) \right) \right)$$

and

$$H_H = H_{0H} + \Delta H_{form_{H_{0K}}} + Ru \cdot T \cdot \left( \frac{1}{V_H} \cdot \left( B_{H-LJappx} - T \cdot \left( \frac{d}{dT} B_{H-LJappx} \right) \right) \right)$$

where the  $H_0$ 's are the zero-pressure enthalpies (see Section 5.1 and Appendix B). The  $H_0$  values used here correspond to a 0 K reference temperature ( $H_0 = 0$  at  $T = 0$  K). Shifting of these 0 K reference calculations to the REFPROP 10 reference state is the topic of Section 5.4. The enthalpy associated with formation of atomic hydrogen from dihydrogen at 0 K reference temperature,  $\Delta H_{form_{H_{0K}}}$ , is included in the definition of  $H_H$  since all atomic hydrogen present in the products comes from dihydrogen. The atomic hydrogen second virial coefficients in the relations above could be either the quantum corrected model from Boyd (1971) (Section 5.2.1.2) or the Lennard-Jones 6-12 approximation with temperature dependent force constants (Section 5.2.1.3.2); but the latter is chosen here to allow for isolation of the force constant temperature dependence when taking its first derivative with respect to temperature. This isolation of force constant temperature dependence allowed investigation of whether the calculations behind the Vargaftik et al. (1989) dataset might have included/excluded this temperature dependence (see Section 5.2.1.3.3).

### 5.3.4 Entropy

As the heart of these calculations are carried out in molar terms, the following begins with the desired end result of mass-specific entropy and proceeds backwards, if one will, through the detailed molar-based calculation relations.

$$s_{mix} = \frac{S_{mix}}{MM_{mix}}$$

where  $S_{mix}$  is the mixture molar entropy. This mixture molar entropy is calculated as the weighted sum of  $S$ 's for the product species, mixing terms, and an unlike interaction parameter,  $\Delta S_{H_2H}$ , as follows

$$S_{mix} = x_{H_2} \cdot S_{H_2} + x_H \cdot S_H - Ru \cdot x_{H_2} \cdot \ln(x_{H_2}) - Ru \cdot x_H \cdot \ln(x_H) + x_{H_2} \cdot x_H \cdot \Delta S_{H_2H}$$

Revision: Baseline/Revision Level	Document Number: SNP-DOC-0046
Effective Date: 07/01/2024	Page: 32 of 149
Title: Parahydrogen Thermophysical Properties V05 Final Report	

The unlike interaction parameter may be expressed as

$$\Delta S_{H_2H} = -\left(\frac{d}{dT}\delta_{H_2H}\right) \cdot P + \frac{B_{H_2} - B_{H_{LJappx}}}{2 \cdot Ru \cdot T} \cdot P^2 \cdot \left( \left(\frac{B_{H_2}}{T} - 2 \cdot \left(\frac{d}{dT}B_{H_2}\right)\right) - \left(\frac{B_{H_{LJappx}}}{T} - 2 \cdot \left(\frac{d}{dT}B_{H_{LJappx}}\right)\right) \right)$$

The entropies associated with each product species are calculated as:

$$S_{H_2} = S_{0_{H_2}} - Ru \cdot \ln\left(\frac{P}{1 \cdot \text{bar}}\right) - Ru \cdot \left( \frac{T}{V_{H_2}} \cdot \left(\frac{d}{dT}B_{H_2}\right) + \frac{B_{H_2}^2 - C_{H_2}}{2 \cdot V_{H_2}^2} + \frac{T}{2 \cdot V_{H_2}^2} \cdot \left(\frac{d}{dT}C_{H_2}\right) \right)$$

$$S_H = S_{0_H} - Ru \cdot \ln\left(\frac{P}{1 \cdot \text{bar}}\right) - \frac{Ru \cdot T}{V_H} \cdot \left(\frac{d}{dT}B_{H_{LJappx}}\right)$$

where the  $S_0$ 's are the zero-pressure entropies referenced to 0 K and 1 bar (see Section 5.1 and Appendix B). The Shifting of these 0 K reference calculations to the REFPROP 10 reference state is the topic of Section 5.4. In addition to shifting to the REFPROP 10 reference state, for use in the Bridging Region, the above  $S_{H_2}$  relation is modified as discussed in list item 6 of Section 5.5.2.2. The atomic hydrogen second virial coefficients in the relations above could be either the quantum corrected model from Boyd (1971) or the Lennard-Jones 6-12 approximation with temperature dependent force constants; but the latter is chosen here to allow for isolation of the force constant temperature dependence when taking its first derivative with respect to temperature for the same reason noted in Section 5.3.3.

### 5.3.5 Isobaric Specific Heat

Both chemical equilibrium and 'frozen' isobaric mass-specific heat values are provided in the database. The present discussion regards the equilibrium calculations, and the 'frozen' subpart is reviewed in Section 5.6.3.1. As these calculations are carried out in molar terms, the following begins with the desired end result of mass-specific isobaric specific heat and proceeds backwards, if one will, through the detailed molar-based calculation relations. First off, it is noted that:

$$c_{p_{mix}} \neq \frac{C_{p_{mix}}}{MM_{mix}}$$

This relation is the same as that from Kessel'mann et al. (1968) – see immediately below where the subscript CM means mixture - but the above  $C_{p_{mix}}$  and  $MM_{mix}$  have not been expanded.

$$c_{p_{CM}} = \frac{1}{M_{CM}} \left[ \sum_i \left(\frac{\partial H_i}{\partial T}\right)_p x_i + \sum_i H_i \left(\frac{\partial x_i}{\partial T}\right)_p + \sum_{j,i} x_i \left(\frac{\partial x_j}{\partial T}\right)_p \Delta H_{ij} + \sum_{j,i} x_j \left(\frac{\partial x_i}{\partial T}\right)_p \Delta H_{ij} + \sum_{ij} x_i x_j \left(\frac{\partial}{\partial T} \Delta H_{ij}\right) \right] - \frac{H_{CM}}{M_{CM}^2} \sum_i M_i \left(\frac{\partial x_i}{\partial T}\right)_p ;$$

First let us define the mixture isobaric molar specific heat using our earlier definition of isobaric molar specific enthalpy – repeated here for convenience

$$H_{mix} = x_{H_2} \cdot H_{H_2} + x_H \cdot H_H + x_{H_2} \cdot x_H \cdot \Delta H_{H_2H}$$

The isobaric molar specific heat may then be defined as follows

$$C_{p_{mix}} = \left( \frac{\partial}{\partial T} H_{mix} \right)_P$$

Or

$$C_{p_{mix}} = \left[ x_{H_2} \cdot \left( \frac{\partial}{\partial T} H_{H_2} \right)_P + x_H \cdot \left( \frac{\partial}{\partial T} H_H \right)_P + x_{H_2} \cdot x_H \cdot \left( \frac{\partial}{\partial T} \Delta H_{H_2H} \right)_P \right] + \left[ H_{H_2} \cdot \left( \frac{\partial}{\partial T} x_{H_2} \right)_P + H_H \cdot \left( \frac{\partial}{\partial T} x_H \right)_P + x_{H_2} \cdot \left( \frac{\partial}{\partial T} x_H \right)_P \cdot \Delta H_{H_2H} + \left( \frac{\partial}{\partial T} x_{H_2} \right)_P \cdot x_H \cdot \Delta H_{H_2H} \right]$$

where terms in the second set of square brackets represent the ‘reaction’ contribution and those in the first set of square brackets the so-called ‘frozen’. Since the ‘frozen’ isobaric mass-specific heat is to be output in the tabular database, it is convenient to define it as

$$c_{p_{frozen}} = \frac{C_{p_{frozen}}}{MM_{mix}} = \frac{1}{MM_{mix}} \cdot \left( x_{H_2} \cdot \left( \frac{\partial}{\partial T} H_{H_2} \right)_P + x_H \cdot \left( \frac{\partial}{\partial T} H_H \right)_P + x_{H_2} \cdot x_H \cdot \left( \frac{\partial}{\partial T} \Delta H_{H_2H} \right)_P \right)$$

where the variation of  $MM_{mix}$  with temperature need not be considered as the composition is considered to be fixed/‘frozen’. Returning to the question of calculation of  $c_{p_{mix}}$ , the last needed item is to express  $MM_{mix}$  in terms of calculated mole fractions as follows

$$MM_{mix} = x_{H_2} \cdot MM_{H_2} + x_H \cdot MM_H$$

and then

$$\left( \frac{\partial}{\partial T} MM_{mix} \right)_P = MM_{H_2} \cdot \left( \frac{\partial}{\partial T} x_{H_2} \right)_P + MM_H \cdot \left( \frac{\partial}{\partial T} x_H \right)_P$$

Recapitulating the beginning  $c_p$  relation and substituting the expanded relations for  $C_{p_{mix}}$  and the partial derivative of  $MM_{mix}$  just defined

$$C_{p_{reaction}} = \left( H_{H_2} + x_H \cdot \Delta H_{H_2H} - \frac{H_{mix}}{MM_{mix}} \cdot MM_{H_2} \right) \cdot \left( \frac{\partial}{\partial T} x_{H_2} \right)_P + \left( H_H + x_{H_2} \cdot \Delta H_{H_2H} - \frac{H_{mix}}{MM_{mix}} \cdot MM_H \right) \cdot \left( \frac{\partial}{\partial T} x_H \right)_P$$

Revision: Baseline/Revision Level	Document Number: SNP-DOC-0046
Effective Date: 07/01/2024	Page: 34 of 149
Title: Parahydrogen Thermophysical Properties V05 Final Report	

which on close examination is the same as the relation from Kessel'man et al. (1968), but with terms here grouped by 'frozen' and 'reaction' contributions. This relation can be further simplified for computation by grouping reaction terms on the partial derivatives of  $xH_2$  and  $xH$  by substituting  $cp_{frozen}$  to obtain:

$$cp_{mix} = cp_{frozen} + \frac{\left[ \left( H_{H_2} + xH \cdot \Delta H_{H_2H} - H_{mix} \cdot \frac{MM_{H_2}}{MM_{mix}} \right) \cdot \left( \frac{\partial}{\partial T} xH_2 \right)_P + \left( H_H + xH_2 \cdot \Delta H_{H_2H} - H_{mix} \cdot \frac{MM_H}{MM_{mix}} \right) \cdot \left( \frac{\partial}{\partial T} xH \right)_P \right]}{MM_{mix}}$$

### 5.3.6 Isochoric Specific Heat

Isochoric mass-specific heat is provided in the database. Unlike previous property relations, here mass-intensive forms are used and the isochoric specific heat may be calculated as:

$$cv_{mix} = cp_{mix} + T \cdot \frac{\left( \frac{\partial}{\partial T} v_{mix} \right)_P^2}{\left( \frac{\partial}{\partial P} v_{mix} \right)_T}$$

Isochoric specific heat is used in the next section to calculate sound speed. A user may also use isochoric specific heat to calculate the ratio of isobaric-to-isochoric specific heat that is commonly deployed in various approximate relations for sound speed and compressible flow relationships, but such approximations may be avoided with recourse to the present real-gas property database by working directly with relevant conservation relations.

### 5.3.7 Sound Speed

From Kessel'man (1968), the sound speed is expressed as

$$a_{mix} = \sqrt{K \cdot P \cdot v_{mix}}$$

$$K = \frac{\frac{cp_{mix}}{cv_{mix}} \cdot v_{mix}}{\left( \frac{\partial}{\partial P} v_{mix} \right)_T} \cdot P$$

and sound speed becomes

$$a_{mix} = \sqrt{\frac{\frac{cp_{mix}}{cv_{mix}} \cdot v_{mix}^2}{\left( \frac{\partial}{\partial P} v_{mix} \right)_T}}$$

Revision: Baseline/Revision Level	Document Number: SNP-DOC-0046
Effective Date: 07/01/2024	Page: 35 of 149
Title: Parahydrogen Thermophysical Properties V05 Final Report	

The K relation from Kessel'man is just the isentropic bulk modulus for the mixture expressed in terms of  $v_{mix}$  instead of  $\rho_{mix}$ , and divided by pressure. One may substitute the  $cv_{mix}$  relation from Section 5.3.6 into the relation above to obtain the following working relation

$$a_{mix} = \sqrt{\frac{cP_{mix}}{cP_{mix} \cdot \left(\frac{\partial v_{mix}}{\partial P}\right)_T + T \cdot \left(\frac{\partial v_{mix}}{\partial T}\right)_P^2} \cdot v_{mix}^2}$$

which does not incur the numerical inaccuracy related to propagation of error associated with numerical approximation of the partial of  $v_{mix}$  with respect to P, holding T constant, through both  $cv_{mix}$  and  $a_{mix}$  relationships.

#### 5.4 Shifting Enthalpy and Entropy to the REFPROP Reference State

So far, calculated values for enthalpy and entropy correspond to the reference state associated with the zero-pressure enthalpy and entropy 'backbones' on which the calculations are built (see Section 5.1 from earlier in this report). Those backbones correspond to a reference state where enthalpy is zero when both temperature and pressure are 0 and entropy is zero when temperature is 0 and pressure is 1 bar. These high temperature enthalpy and entropy results are to be 'bridged' to the existing lower temperature results from REFPROP 10. The default reference state for parahydrogen in REFPROP 10 is that both enthalpy and entropy equal to 0 for the saturated liquid state at 101325 Pa. Thus, the enthalpy and entropy results calculated as described above must be shifted to match REFPROP's default Normal Boiling Point reference state as follows:

$$H_{mix\_table} = H_{mix} + H0\_H2\_shift\_to\_RP \quad S_{mix\_table} = S_{mix} + S0\_1bar\_H2\_shift\_to\_RP$$

where RP is short for REFPROP. The higher temperature property calculations related in this report have no anchor below the 1500 K lower limit to which the similar (well, believed similar) methods of Gorykin and Kessel'man were deployed. The present approach will only ever use the high temperature methods down to about 700 K - which is well above the REFPROP Normal Boiling Point default reference state. Thus, the high temperature zero-pressure enthalpy is shifted to exactly match its zero-pressure counterpart from REFPROP 10 at 700 K, and the same is done for entropy at 700 K and 1 bar pressure. Details for this process are provided towards the end of Appendix B. Appendix B also relates the construction of the zero-pressure backbones for the present higher temperature enthalpy and entropy calculations, so calculation of the shift to the REFPROP 10 reference state was a natural way to end that appendix. Given that REFPROP 10 and the present methods use fundamentally different pressure-volume-temperature surface (equation of state) models, shifting one to match the other at a single state point for each of enthalpy and entropy will still leave them slightly mis-matched everywhere else. How to handle that is the topic of the next section.

#### 5.5 Bridging High Temperature Thermodynamic Results to REFPROP

The present higher temperature results need to be integrated with the REFPROP results, referred to as bridging in this report, in a manner that smoothly transitions from the REFPROP results to

Revision: Baseline/Revision Level	Document Number: SNP-DOC-0046
Effective Date: 07/01/2024	Page: 36 of 149
Title: Parahydrogen Thermophysical Properties V05 Final Report	

the higher temperature results. Looking back to the figure from Section 3.3.2.3.1, it helps to think of three regions in temperature-space: 1) the REFPROP region where all results come directly from REFPROP 10, 2) the Bridging region, which is the topic of this section, and 3) the Higher Temperature region where the calculation methods related in the subsections of Section 5.3 are applied without modification. First let us consider the interface between the REFPROP and Bridging regions.

### 5.5.1 Bridging Temperature

The underlying models for the REFPROP 10 results do not account for the possibility of dihydrogen dissociation to atomic hydrogen. At the 1000 K upper limit for parahydrogen in REFPROP, the mole fraction of atomic hydrogen is very small - even for pressure as low as 1 Pa - but its impact on isobaric specific heat is non-negligible for pressures as high as 10 kPa. Thus, in this present work, the boundary temperature between the REFPROP and Bridging regions varies with pressure such that the isobaric specific heat reaction component divided by its equilibrium mixture value equals 1.0E-08 - this level being considered negligible for the purposes of the present database. Thus, the Bridging Temperature versus pressure curve from Section 3.3.2.3.1.

### 5.5.2 Modification of PVT Surface to Enable Bridging

Along this curve, the higher temperature model is applied, but modified so as to provide additional degrees of freedom that allow it to 'bend' to match the REFPROP dataset in terms of key thermodynamic parameters at each Bridging Pair (Pressure, Temperature) along the Bridging Temperature curve (hereafter the Bridging Line). These modifications are related in the Bridging Parameters subsection below.

#### 5.5.2.1 Bridging Constraints

Ideally, all of the bridging constraints listed below would be matched along the Bridging Line, but this proves impractical/inadvisable as noted for specific constraints. The primary goal of the bridging process is to ensure continuity and smoothness when transitioning between the REFPROP and current P-V-T surfaces; as well as continuity of properties that depend on the shape of these P-V-T surfaces.

- 1)  $V_{mix}$  mixture molar specific volume – matched exactly
- 2)  $H_{mix}$  mixture molar enthalpy – matched exactly
- 3)  $S_{mix}$  mixture molar entropy – matched exactly but requires use of an additive shift parameter above roughly 10 MPa. Use of this additive shift results in tabulated entropy values not exactly following the real-gas variation term from

$$ds = \frac{c_p}{T} dT - \left( \frac{\partial v}{\partial T} \right)_P dP$$

- 4)  $\left( \frac{\partial}{\partial T} V_{mix} \right)_P$  smoothness of P-V-T surface; important to enthalpy and entropy change along an isobar, and  $(C_p - C_v)$  – matched exactly

Revision: Baseline/Revision Level	Document Number: SNP-DOC-0046
Effective Date: 07/01/2024	Page: 37 of 149
Title: Parahydrogen Thermophysical Properties V05 Final Report	

- 5)  $\left(\frac{\partial}{\partial P} V_{mix}\right)_T$  smoothness of P-V-T surface; important to (Cp - Cv) – matched exactly
- 6)  $\left(\frac{\partial^2}{\partial T^2} V_{mix}\right)_P$  important to pressure dependency of Cp, but this quantity cannot be reliably matched simultaneously with Cp. So, Cp is actually used as a proxy here.
- 7)  $\frac{C_{p_{reaction}}}{C_{p_{mix}}} = 10^{-8}$  minimize impact of dissociation along Bridging Line. Though Bridging Parameters are optimized based on mixture relations; those mixture relations essentially represent dihydrogen only along the Bridging Line.

### 5.5.2.2 Bridging Parameters

The 7 bridging constraints are balanced by 7 model degrees of freedom (Bridging Parameters) as follows (note that the numbering scheme does not imply a direct connection between constraint and degree of freedom):

- 1)  $\sigma_{H_2,bridge}$  - effective collision diameter allowed to vary in the Bridging Region
- 2)  $\left(\frac{\epsilon}{k}\right)_{H_2,bridge}$  - characteristic temperature allowed to vary in the Bridging Region
- 3), 4), 5)  $C0_{bridge}, C1_{bridge}, C2_{bridge}$  see modified dihydrogen virial relation immediately below

$$V_{H2} = C0_{bridge} \cdot \frac{Ru \cdot T}{P} + C1_{bridge} \cdot B_{H2} + C2_{bridge} \cdot \frac{C_{H2} - B_{H2}^2}{Ru \cdot T} \cdot P$$

- 6)  $\Delta S_{bridge}$  additive shift to dihydrogen molar entropy (see Section 5.5.2.1 constraint 3) which is applied as follows

$$S_{mix} = x_{H2} \cdot (S_{H2} + \Delta S_{bridge}) + x_H \cdot S_H - Ru \cdot x_{H2} \cdot \ln(x_{H2}) - Ru \cdot x_H \cdot \ln(x_H) + x_{H2} \cdot x_H \cdot \Delta S_{H2H}$$

- 7)  $T_{bridge}$  vary T to ensure constraint (7) from Section 5.5.2.1 is satisfied. Though not the only Bridging Parameter on which constraint (7) depends; this parameter dominates.

### 5.5.3 Bridging Parameter Variation Along Bridging Boundary

Simultaneous solution of the above 7 constraint - 7 parameter problem results in the following curves of bridging parameter variation with pressure.

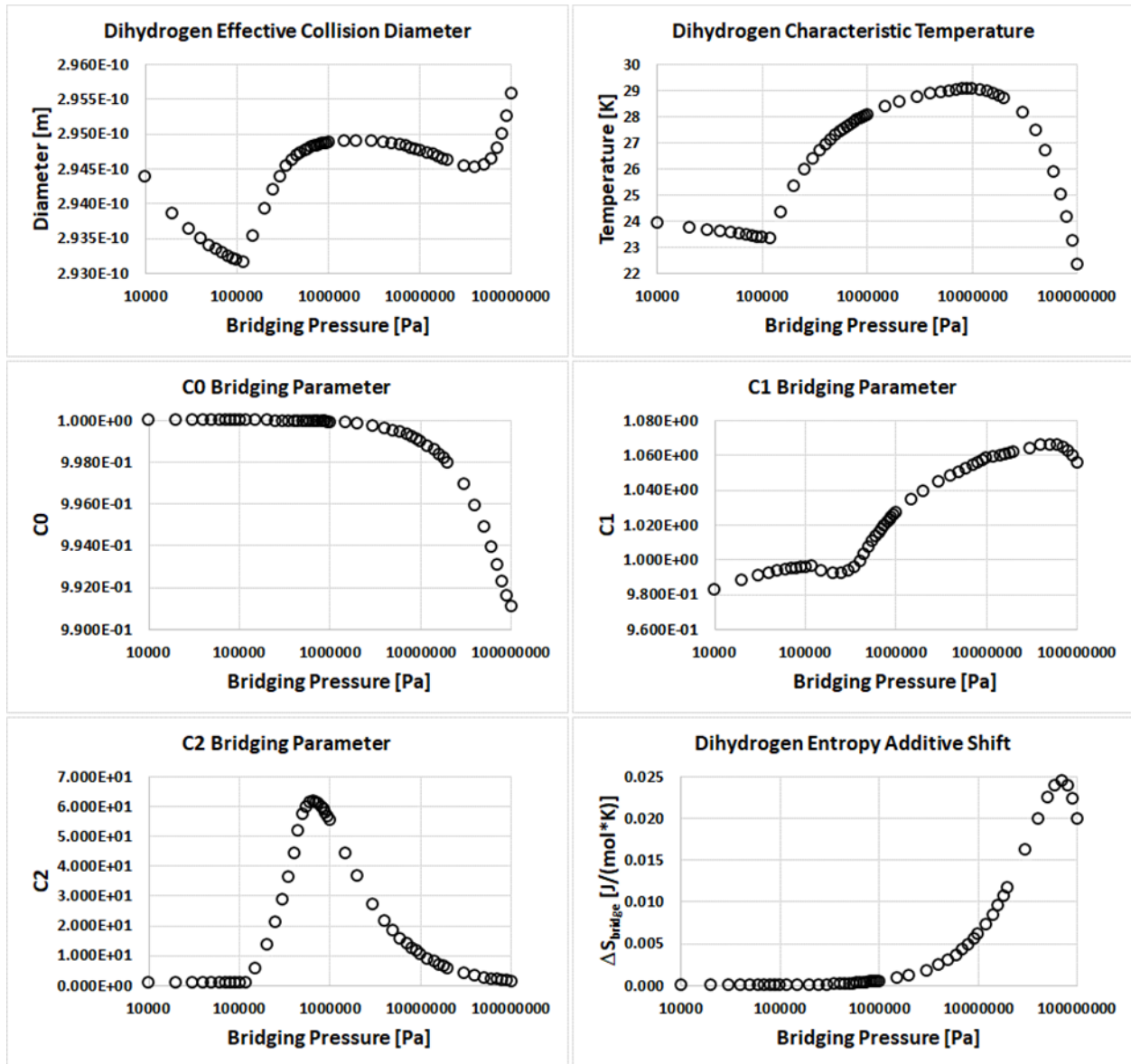


**Figure 5-1. Bridging Parameters between 10 kPa and 100 MPa**

A purposeful discontinuity exists in all of the Bridging Parameters just above 100 kPa, but its impact is not readily apparent in either  $C0$  or  $\Delta S_{\text{bridge}}$  parameters. All Bridging Parameters are held constant at their 10 kPa values for calculations below 10 kPa. Details of the bridging process are related in Appendix I.

#### 5.5.4 Bridging Parameter Variation with Temperature Internal to Bridging Region

For the case of the lowest pressure (1 Pa) tabulated for the present database, the Bridging Temperature is roughly 700 K. The upper limit temperature of the bridging region is taken to be

Revision: Baseline/Revision Level	Document Number: SNP-DOC-0046
Effective Date: 07/01/2024	Page: 39 of 149
Title: Parahydrogen Thermophysical Properties V05 Final Report	

the 1500 K lower limit of the Vargaftik et al. (1996) database. At/above 1500 K, the Bridging Parameter values equal their high-temperature region values as follows:

$$\sigma_{H_2} = 2.934 \text{ Angstrom} \quad (\varepsilon/k)_{H_2} = 34.1 \text{ K} \quad C_0 = C_1 = C_2 = 1.0 \quad \Delta S_{\text{bridge}} = 0$$

Internal to the Bridging region, for each bridging pressure, each bridging parameter is forced to vary according to a cubic relation in temperature whose end slopes are constrained to be 0. Using  $C_0$  as an example:

$$C_{0_{\text{internal}}} = A + B \cdot T_{\text{internal}} + C \cdot T_{\text{internal}}^2 + D \cdot T_{\text{internal}}^3$$

where the constants may be expressed in terms of knowns as follows

$$A = \frac{6750000 \cdot (T_{\text{bridge}} - 500) \cdot (C_0 - C_{0_{\text{bridge}}})}{(T_{\text{bridge}} - 1500)^3} + C_0 \quad B = \frac{9000 \cdot T_{\text{bridge}} \cdot (C_0 - C_{0_{\text{bridge}}})}{(T_{\text{bridge}} - 1500)^3}$$

$$C = \frac{-(3 \cdot (T_{\text{bridge}} + 1500) \cdot (C_0 - C_{0_{\text{bridge}}}))}{(T_{\text{bridge}} - 1500)^3} \quad D = \frac{2 \cdot (C_0 - C_{0_{\text{bridge}}})}{(T_{\text{bridge}} - 1500)^3}$$

or for the case of effective collision diameter, one finds

$$A = \frac{6750000 \cdot (T_{\text{bridge}} - 500) \cdot (\sigma_{H_2} - \sigma_{H_2_{\text{bridge}}})}{(T_{\text{bridge}} - 1500)^3} + \sigma_{H_2} \quad B = \frac{9000 \cdot T_{\text{bridge}} \cdot (\sigma_{H_2} - \sigma_{H_2_{\text{bridge}}})}{(T_{\text{bridge}} - 1500)^3}$$

$$C = \frac{-(3 \cdot (T_{\text{bridge}} + 1500) \cdot (\sigma_{H_2} - \sigma_{H_2_{\text{bridge}}}))}{(T_{\text{bridge}} - 1500)^3} \quad D = \frac{2 \cdot (\sigma_{H_2} - \sigma_{H_2_{\text{bridge}}})}{(T_{\text{bridge}} - 1500)^3}$$

and so on for the other bridging parameters.

#### 5.5.4.1 Exclusion of Bridging Parameter Temperature Variation from Derivatives

The above methodology for variation of bridging parameters internal to the bridging region provides a fairly straightforward means of smoothly transitioning from the Bridging Line, through the bridging region (up to 1500 K), into the high temperature calculation region ( $\Rightarrow$  1500 K). Obviously, the cubic temperature variation defined in the last section is not physical in nature; thus, it is necessary to exclude the temperature dependence introduced by this temperature curve fit when differentiating on the P-V-T surface to calculate properties. In the Python code, this is accomplished by storing bridging parameter values as constants for each P,T pair being calculated instead of calculating them for each use from function calls. A special static variable is also provided as part of the numerical differentiation routine that allows one to pass a parallel independent variable value (possibly temperature) that does not get perturbed when estimating derivatives.

Revision: Baseline/Revision Level	Document Number: SNP-DOC-0046
Effective Date: 07/01/2024	Page: 40 of 149
Title: Parahydrogen Thermophysical Properties V05 Final Report	

## 5.6 Transport Properties

The present database provides values for thermal conductivity and absolute viscosity. These properties are calculated using methods from Vanderslice et al. (1962). Vanderslice et al. (1962) notes that their approach does not account for the effects of ionization, and the reader may refer back to the figure from Section 4.3.1 to get a feel for the importance of ionization. In addition to their chemical equilibrium values, values for thermal conductivity and isobaric specific are provided which exclude the contributions associated with the 'reaction' coordinate - so-called 'frozen' values. While these properties have a mathematical-physics basis in statistical mechanics, far less effort is expended here when 'bridging' their high-temperature values to the lower temperature REFPROP values, since their primary use is for estimation of thermal-hydraulic behaviors as opposed to satisfying primary conservation relations.

### 5.6.1 Thermal Conductivity

Thermal conductivity of the dissociating mixture may be expressed as the sum of frozen and reaction contributions as follows:

$$\lambda_{mix} = \lambda_{frozen} + \lambda_{reaction} = (\lambda_{0_{mix}} + \lambda_{int_{mix}}) + \lambda_{reaction}$$

where the frozen contribution is subdivided into its translational ( $\lambda_0$ ) and internal ( $\lambda_{int}$  - rotational and vibrational) contributions. The use of  $\lambda$  to represent thermal conductivity dominates the theoretical literature, and so it is retained in this work when discussing theory/calculations; but the more common variable name 'k' is used in the database output. Thus,  $k = \lambda_{mix}$  and  $k_{frozen} = \lambda_{frozen}$  where the 'mix' subscript is dropped for the final database output (true for all outputs). The translational contribution for a binary mixture may be expressed as:

$$\lambda_{0_{mix}} = \frac{-4 \cdot \left( \frac{x_1^2}{L_{11}} + \frac{x_2^2}{L_{22}} - 2 \cdot x_1 \cdot x_2 \cdot \frac{L_{12}}{L_{11} \cdot L_{22}} \right)}{1 - \frac{L_{12}^2}{L_{11} \cdot L_{22}}} = \frac{-4 \cdot \left( \frac{x_{H2}^2}{L_{H2}} + \frac{x_H^2}{L_H} - 2 \cdot x_{H2} \cdot x_H \cdot \frac{L_{H2H}}{L_{H2} \cdot L_H} \right)}{1 - \frac{L_{H2H}^2}{L_{H2} \cdot L_H}}$$

where the first form is taken directly from Vanderslice et al. (1962) wherein 1 implies H2 and 2 implies H such that the subscripts 11 and 22 refer to like interactions for H2 and H, respectively, and 12 the unlike interaction of H2 with H; and the second form is the same but expressed in the interaction nomenclature used for the present work where the lone subscripts H2 and H refer to self-interactions and H2H refers to the sole unlike interaction for our dissociating system. For complex multi-component mixtures, the variable L denotes elements in the matrix formulation for calculation of the mixture translational contribution. The various L's relevant here are:

Dihydrogen interaction with itself:

$$L_{H2} = \frac{4 \cdot x_{H2}^2}{\lambda_{0_{H2}}} - \frac{16}{25} \cdot \frac{x_{H2} \cdot x_H}{(MM_{H2} + MM_H)^2} \cdot \frac{T}{P \cdot D_{H2H}} \cdot \left( \frac{15}{2} \cdot MM_{H2}^2 + \frac{25}{4} \cdot MM_H^2 - 3 \cdot MM_H^2 \cdot Bstar_{H2H} + 4 \cdot MM_{H2} \cdot MM_H \cdot Astar_{H2H} \right)$$

Revision: Baseline/Revision Level	Document Number: SNP-DOC-0046
Effective Date: 07/01/2024	Page: 41 of 149
Title: Parahydrogen Thermophysical Properties V05 Final Report	

Atomic interaction with itself:

$$L_H = -\frac{4 \cdot xH^2}{\lambda_{0H}} - \frac{16}{25} \cdot \frac{xH \cdot xH_2}{(MM_H + MM_{H_2})^2} \cdot \frac{T}{P \cdot D_{H_2H}} \cdot \left( \frac{15}{2} \cdot MM_H^2 + \frac{25}{4} \cdot MM_{H_2}^2 - 3 \cdot MM_{H_2}^2 \cdot Bstar_{H_2H} + 4 \cdot MM_H \cdot MM_{H_2} \cdot Astar_{H_2H} \right)$$

Dihydrogen unlike interaction with atomic hydrogen:

$$L_{H_2H} = \frac{16}{25} \cdot \frac{xH_2 \cdot xH \cdot MM_{H_2} \cdot MM_H}{(MM_{H_2} + MM_H)^2} \cdot \frac{T}{P \cdot D_{H_2H}} \cdot \left( \frac{55}{4} - 3 \cdot Bstar_{H_2H} - 4 \cdot Astar_{H_2H} \right)$$

where the  $\lambda_{0s}$  are the translational contributions for self-interactions,  $D_{H_2H}$  is the diffusion coefficient for unlike interaction of dihydrogen with atomic hydrogen, and  $Astar_{H_2H}$  and  $Bstar_{H_2H}$  are collision integral combinations that commonly occur in mixture transport calculations - in the case of  $Bstar$ , not to be confused with the non-dimensional form of the second virial coefficient that appears elsewhere in this work. Both  $Astar_{H_2H}$  and  $Bstar_{H_2H}$  grouping values are used as tabulated in Vanderslice et al. (1962), as these values depend only on the potential energy functions applied in the calculation of their constituent collision integrals. The  $D_{H_2H}$  and  $\lambda_{0s}$  are calculated from first principles as follows:

Unlike interaction diffusion coefficient:

$$D_{H_2H} = \frac{3}{8} \cdot \sqrt{\frac{Ru^3}{\pi \cdot N_{Avogadro}^2}} \cdot \frac{\sqrt{T^3}}{\Omega_{11H_2H}} \cdot \sqrt{\frac{MM_H + MM_{H_2}}{2 \cdot MM_H \cdot MM_{H_2}}}$$

where  $\Omega_{11}$  is used in place of the more common  $\Omega^{(1,1)}$  nomenclature due to equation typesetting limitations, and the  $\Omega_{11H_2H}$  collision integral is used as tabulated in Vanderslice et al. (1962).

Dihydrogen self-interaction translational contribution:

$$\lambda_{0H_2} = \frac{75}{64} \cdot \sqrt{\frac{Ru^3}{\pi \cdot N_{Avogadro}^2}} \cdot \frac{\sqrt{T}}{\Omega_{22H_2}} \cdot \frac{1}{\sqrt{MM_{H_2}}}$$

where the  $\Omega_{22H_2}$  collision integral is used as tabulated in Vanderslice et al. (1962).

Atomic hydrogen self-interaction translational contribution:

$$\lambda_{0H} = \frac{75}{64} \cdot \sqrt{\frac{Ru^3}{\pi \cdot N_{Avogadro}^2}} \cdot \frac{\sqrt{T}}{\Omega_{22H}} \cdot \frac{1}{\sqrt{MM_H}}$$

again with the  $\Omega_{22H}$  collision integral being used as tabulated in Vanderslice et al. (1962).

The internal contribution is due to dihydrogen alone since atomic hydrogen has no internal storage modes absent electronic excitation. Thus, Vanderslice et al. (1962) provide the internal contribution as:

$$\lambda_{int_{mix}} = \frac{P \cdot D_{H2} \cdot \left( C_{p_{H2}} - \frac{5}{2} \cdot Ru \right)}{Ru \cdot T \cdot \left( 1 + \frac{x_H}{x_{H2}} \cdot \frac{D_{H2}}{D_{H2H}} \right)}$$

noting that the parenthetical numerator term represents the internal heat capacity. While this is correct for an ideal gas where  $C_p - C_v = Ru$  such that the term  $5/2 \cdot Ru$  represents the sum of  $3/2 \cdot Ru$  (translational degrees of freedom) and  $C_p - C_v = Ru$ , for a real-gas, one could use the following

$$\lambda_{int_{mix}} = \frac{P \cdot D_{H2} \cdot \left( C_{v_{H2}} - \frac{3}{2} \cdot Ru \right)}{Ru \cdot T \cdot \left( 1 + \frac{x_H}{x_{H2}} \cdot \frac{D_{H2}}{D_{H2H}} \right)}$$

where  $C_{v_{H2}}$  is the real-gas dihydrogen molar isochoric specific heat. Where the  $3/2 \cdot Ru$  translational contribution is the same for both real/ideal gas assumptions. Yet, this requires calculation of  $C_{v_{H2}}$  for this purpose alone. Thus, the 1<sup>st</sup> approximation above is used for the sake of simplicity and it captures the major portion of real-gas effects on thermal conductivity. The dihydrogen diffusion coefficient is

$$D_{H2} = \frac{3}{8} \cdot \sqrt{\frac{Ru^3}{\pi \cdot N_{Avogadro}^2}} \cdot \frac{\sqrt{T^3}}{\Omega_{11_{H2}}} \cdot \frac{1}{\sqrt{MM_{H2}}}$$

where  $\Omega_{11_{H2}}$  is used as tabulated in Vanderslice et al. (1962).

The final contribution to be considered is that associated with the reaction coordinate:

$$\lambda_{rxn_{mix}} = \frac{P \cdot D_{H2H} \cdot \Delta H_{rxn}^2}{Ru^2 \cdot T^3} \cdot \frac{x_{H2} \cdot x_H}{(1 + x_{H2})^2}$$

where  $\Delta H_{rxn}$  is the heat of reaction associated with formation of 2 moles of atomic hydrogen from 1 mole of dihydrogen calculated as follows

$$\Delta H_{rxn} = 2 \cdot H_H - H_{H2}$$

where it is noted that the definition of  $H_H$  used in this work includes the formation enthalpy (see Section 5.3.3). Vanderslice et al. (1962) uses an ideal gas heat of reaction, but this work uses its real-gas counterpart since  $H_H$  and  $H_{H2}$  are readily available. This ideal vs real-gas difference is negligible considering the expected inaccuracy noted by Vanderslice et al. (1962) is as much as 10% for either thermal conductivity or absolute viscosity taken individually.

Revision: Baseline/Revision Level	Document Number: SNP-DOC-0046
Effective Date: 07/01/2024	Page: 43 of 149
Title: Parahydrogen Thermophysical Properties V05 Final Report	

This completes estimation of thermal conductivity for the dissociating mixture in chemical equilibrium. The next section deals with bridging these values to their lower temperature REFPROP counterparts.

### 5.6.1.1 Bridging Dissociating Thermal Conductivity Results to REFPROP Output

This bridging process is far less rigorous than that applied for thermodynamic properties and discussed back in Section 5.5. Here the only goal is to smoothly transition from REFPROP 10 values to the dissociating values. The differences between REFPROP 10 values and dissociating values are large enough that this bridging process occurs between the Bridging Line (Section 5.5.1) and an upper bound Bridging Line at which the reaction contribution to mixture thermal conductivity equals 0.1% of the total value. A simple constant,  $\lambda_{REFPROP\_BP}$ , is defined at each P,T pair along the Bridging Line such that:

$$\lambda_{REFPROP} = \frac{\lambda_{frozen}}{\lambda_{REFPROP\_BP}} + \lambda_{reaction} = \lambda_{mix}$$

thus, since the reaction term is negligibly small along the Bridging Line, forcing the mixture value in this database to match the REFPROP 10 value everywhere along the Bridging Line. The value of  $\lambda_{REFPROP\_BP}$  then varies cubically between the local Bridging Line and the upper bound Bridging Line such that it becomes unity at the upper bound Bridging Line – returning the above relation to its normal form.

### 5.6.2 Absolute Viscosity

Absolute viscosity of the dissociating mixture may be expressed as (Vanderslice et al., 1962)

$$\eta_{mix} = \frac{\frac{x_{H_2}^2}{H_{H_2}} + \frac{x_H^2}{H_H} - \frac{2 \cdot x_{H_2} \cdot x_H \cdot H_{H_2H}}{H_{H_2} \cdot H_H}}{1 - \frac{H_{H_2H}^2}{H_{H_2} \cdot H_H}}$$

where, here, H's are the individual elements of the matrix formulation for complex mixtures – not to be confused with their use to represent molar enthalpy. The present use of H is common in statistical mechanics literature, so it is retained here and should not result in confusion since molar enthalpy has nothing to do with calculation of absolute viscosity. The use of  $\eta$  to represent thermal conductivity dominates the theoretical literature, and so it is retained in this work when discussing theory/calculations; but the more common variable name ' $\mu$ ' is used in the database output. Thus,  $\mu = \eta_{mix}$  and, unlike for thermal conductivity above, there is no frozen/reaction breakdown for viscosity. The various matrix elements, H's, are:

Dihydrogen interaction with itself:

$$\eta_{H_2} = \frac{x_{H_2}^2}{\eta_{H_2}} + \frac{2 \cdot x_{H_2} \cdot x_H}{MM_{H_2} + MM_H} \cdot \frac{Ru \cdot T}{P \cdot D_{H_2H}} \cdot \left( 1 + \frac{3 \cdot MM_H \cdot Astar_{H_2H}}{5 \cdot MM_{H_2}} \right)$$

Atomic interaction with itself:

$$\eta_H = \frac{x_H^2}{\eta_H} + \frac{2 \cdot x_H \cdot x_{H_2}}{MM_H + MM_{H_2}} \cdot \frac{Ru \cdot T}{P \cdot D_{H_2H}} \cdot \left( 1 + \frac{3 \cdot MM_{H_2} \cdot Astar_{H_2H}}{5 \cdot MM_H} \right)$$

Dihydrogen unlike interaction with atomic hydrogen:

$$\eta_{H_2H} = -\frac{2 \cdot x_{H_2} \cdot x_H}{MM_{H_2} + MM_H} \cdot \frac{Ru \cdot T}{P \cdot D_{H_2H}} \cdot \left( 1 - \frac{3}{5} \cdot Astar_{H_2H} \right)$$

where  $D_{H_2H}$  is the same as for thermal conductivity above, and  $Astar_{H_2H}$  is used as tabulated by Vanderslice et al. (1962). This leaves only the self-interaction viscosities to be calculated as:

$$\eta_{H_2} = \frac{5}{16} \cdot \sqrt{\frac{Ru}{\pi \cdot N_{Avogadro}^2}} \cdot \frac{\sqrt{MM_{H_2} \cdot T}}{\Omega_{22H_2}}$$

and

$$\eta_H = \frac{5}{16} \cdot \sqrt{\frac{Ru}{\pi \cdot N_{Avogadro}^2}} \cdot \frac{\sqrt{MM_H \cdot T}}{\Omega_{22H}}$$

where the collision integrals are used as tabulated in Vanderslice et al. (1962), as was the case for thermal conductivity above.

This completes estimation of absolute viscosity for the dissociating mixture in chemical equilibrium. The next section deals with bridging these values to their lower temperature REFPROP counterparts.

### 5.6.2.1 Bridging Dissociating Absolute Viscosity Results to REFPROP Output

This bridging process is far less rigorous than that applied for thermodynamic properties and discussed back in Section 5.5. Here the only goal is to smoothly transition from REFPROP 10 values to the dissociating values. The differences between REFPROP 10 values and dissociating values are large enough that this bridging process occurs between the Bridging Line (Section 5.5.1) and the same upper bound Bridging Line related back in Section 5.6.1.1. A simple constant,  $\eta_{REFPROP\_BP}$ , is defined at each P,T pair along the Bridging Line such that:

$$\eta_{REFPROP} = \frac{\eta_{mix}}{\eta_{REFPROP\_BP}}$$

Revision: Baseline/Revision Level	Document Number: SNP-DOC-0046
Effective Date: 07/01/2024	Page: 45 of 149
Title: Parahydrogen Thermophysical Properties V05 Final Report	

thus, since the reaction term is negligibly small along the Bridging Line, forcing the mixture value in this database to match the REFPROP 10 value everywhere along the Bridging Line. The value of  $\eta_{\text{REFPROP\_BP}}$  then varies cubically between the Bridging Line and its upper bound counterpart, such that it becomes unity at the upper bound Bridging Line – returning the above relation to its normal form.

### 5.6.3 Frozen Transport Properties

So-called 'frozen' values for isobaric specific heat and thermal conductivity are provided in this database. The sections that follow relate how these values are calculated for the present work. Below the bridging temperature, these frozen values are identical to their equilibrium values - since both are just the values output by REFPROP 10. The sections below deal with values for temperatures above the bridging curve related back in Sections 3.3.2.3.1 and 5.5.1.

#### 5.6.3.1 Frozen Isobaric Specific Heat

The frozen isobaric specific heat is very simply based on  $C_{p_{\text{frozen}}}$  as defined back in Section 5.3.5, but converted to a mass basis as follows:

$$c_{p_{\text{frozen}}} = \frac{C_{p_{\text{frozen}}}}{MM_{\text{mix}}}$$

Looking ahead to this output was the reason for breaking out 'frozen' and 'reaction' parts back in Section 5.3.5.

#### 5.6.3.2 Frozen Thermal Conductivity

The frozen thermal conductivity is simply the sum of translational and internal contributions from Section 5.6.1 such that:

$$\lambda_{\text{frozen}} = \lambda_{0_{\text{mix}}} + \lambda_{\text{int}_{\text{mix}}}$$

Revision: Baseline/Revision Level	Document Number: SNP-DOC-0046
Effective Date: 07/01/2024	Page: 46 of 149
Title: Parahydrogen Thermophysical Properties V05 Final Report	

## 6.0 REFERENCES

- [1] Assael, M.J., Assael, J.-A.M., Huber, M.L., Perkins, R.A., and Takata, Y. (2011), "Correlation of the Thermal Conductivity of Normal and Parahydrogen from the Triple Point to 1000 K and up to 100 MPa," J. Phys. Chem. Ref. Data, 40(3), 033101.
- [2] Boyd, M.E. (1970) "Quantum Corrections to the Second Virial Coefficient for the Lennard-Jones (m-6) Potential", JOURNAL OF RESEARCH of the National Bureau of Standards - A. Physics and Chemistry, Vol. 75A, No. 1.
- [3] CEA (2004), Chemical Equilibrium with Applications software application, source code file cea2.f internally dated 5/21/04.
- [4] Chase, M.W., Jr. (1998), NIST-JANAF Thermochemical Tables, Journal of Physical and Chemical Reference Data – Monograph No. 9, Fourth Edition, National Institute of Standards and Technology.
- [5] Farkas, A and Farkas, L (1935), "Experiments on Heavy Hydrogen 0 Part I", Proceedings of the Royal Society of London A144467–480.
- [6] Fegley, B., Jr. (2013), Practical Chemical Thermodynamics for Geoscientists, Academic Press.
- [7] Gorykin, S.F. (1968), Cand. Sci. Dissertation, Lomonosov Odesa Technological Institute.
- [8] Greenwood (2018), series of email exchanges conveying the results of Dr. Michael Greenwood's review of the calculation methods used in McDonald (2018). Dr. Greenwood was employed at the Oak Ridge National Laboratory at the time.
- [9] Gurvich, L.V, Veyts, I.V., and Alcock, C.B. (1989), Thermodynamic Properties of Individual Substances, Fourth Edition, Hemisphere Publishing Corporation, New York.
- [10] Hirschfelder, J.O., Curtis, C.F., and Bird, R.B. (1966), Molecular Theory of Gases and Liquids, John Wiley and Sons.
- [11] Kessel'man, P.M. (1964), "К вопросу расчета теплофизических свойств реальных газов при высоких температурах", TVT, Volume 2, Issue 6, 879–883.
- [12] Kessel'man, P.M., Bestuzhev, A.S., Blank, Y.I., and Shekatolina, S.A. (1966), "Второй вириальный коэффициент для взаимодействий атомов с незаполненными электронными оболочками", TVT, Volume 4, Issue 6, 801–809.
- [13] Kessel'man, P.M., Blank, Y.I., and Mogilevskii, V.I. (1968), "Термодинамические свойства термически диссоциированного водяного пара при температурах 1600–6000° К и давлениях 0,1 ÷ 1000 бар", TVT, Volume 6, Issue 4, 658–664.
- [14] Leachman, J.W., Jacobsen, R.T, Penoncello, S.G., and Lemmon, E.W. (2009), "Fundamental Equations of State for Parahydrogen, Normal Hydrogen, and Orthohydrogen," J. Phys. Chem. Ref. Data, 38(3):721-748.

Revision: Baseline/Revision Level	Document Number: SNP-DOC-0046
Effective Date: 07/01/2024	Page: 47 of 149
Title: Parahydrogen Thermophysical Properties V05 Final Report	

- [15] Lykova, A.V. (1969a), "Heat and Mass Transfer. Volume 7, 1968", AD 698 517, Foreign Technology Division, Wright-Patterson Air Force Base, Ohio, 20 August 1969. Specific sub-article referenced here begins on page 152.
- [16] Lykova, A.V. (1969b), "Heat and Mass Transfer. Volume 7, 1968", AD 698 517, Foreign Technology Division, Wright-Patterson Air Force Base, Ohio, 20 August 1969. Specific sub-article referenced here begins on page 140.
- [17] McCarty, R.D, Hord, J., and Roder, H.M. (1981), Selected Properties of Hydrogen (Engineering Design Data), Monograph 168, National Bureau of Standards.
- [18] McCarty, R.D. and Weber, L.A. (1972), "Thermophysical Properties of Parahydrogen from the Freezing Liquid Line to 5000 R for Pressures to 10,000 psia", Technical Note 617, National Bureau of Standards.
- [19] McDonald (2017), "Re-creation of the Calculations Behind the Dissociating Dihydrogen Thermodynamic Property Tables of Vargaftik et al. (1996)", Jacobs ESSSA Group Report ESSSA-FY17-2355, George C. Marshall Space Flight Center, Science and Engineering Contract NNM12AA41C.
- [20] McDonald (2018), "Reconciling the Dihydrogen Property Calculations of McDonald (2017) to the REFPROP 9.1 Dataset", Jacobs Space Exploration Group Report JPID-FY18-00658, George C. Marshall Space Flight Center, Engineering Services and Science Capability Augmentation Contract 80MSFC18C0011.
- [21] Muzny, C.D., Huber, M.L., and Kazakov, A.F. (2013), "Correlation for the Viscosity of Normal Hydrogen Obtained from Symbolic Regression," J. Chem. Eng. Data, 58:969-979.
- [22] NIST (2018) "REFPROP – Reference Fluid Thermodynamic and Transport Properties", Graphical User Interface to National Institute of Standards and Technology Standard Database 23, DLL Version 10, Applied Chemical and Material Division, U.S. Secretary of Commerce, United States of America.
- [23] Pyper, J.W. and Briggs, C.K. (1977), "The Ortho-Para Forms of Hydrogen Deuterium and Tritium: Radiation and Self-Induced Conversion Kinetics and Equilibria", University of California Livermore Report UCRL-52278, Prepared for U.S. Energy Research & Development Administration under contract No. W-7405-Eng-48.
- [24] Roder, H.M, McCarty, R.D., and Hall, W.J. (1972), "Computer Programs for Thermodynamic and Transport Properties of Hydrogen (Tabcode-II)", Technical Note 625, National Bureau of Standards.
- [25] Tang, K.T. and Wei, P.S.P (1974), "Diffusion coefficient and interaction potential of the (H, H<sub>2</sub>) system", J. Chem. Phys. 60, 2454.
- [26] Vanderslice, J.T., Weissman, S., Mason, E.A., and Fallon, R.J. (1962) "High-Temperature Transport Properties of Dissociating Hydrogen", Phys. Fluids 5, 155–164.

Revision: Baseline/Revision Level	Document Number: SNP-DOC-0046
Effective Date: 07/01/2024	Page: 48 of 149
Title: Parahydrogen Thermophysical Properties V05 Final Report	

- [27] Vargaftik, N.B. and Vasilievskaya, Y.D. (1975), “Transfer Coefficients of Dissociated Hydrogen at Pressures up to 1000 bars and Temperatures up to 10000 K”, *Journal of Engineering Physics*, 28, 719-724.
- [28] Vargaftik, N.B., Vinogradov, Y.K., and Yargin, V.S., Handbook of Physical Properties of Liquids and Gases - Pure Substances and Mixtures, Third Augmented and Revised Edition, Begell House, New York.
- [29] Woolley, H.W., Scott, R.B., and Brickwedde, F.G (1948), “Compilation of Thermal Properties of Hydrogen in Its Various Isotopic and Ortho-Para Modifications”, Research Paper RP1932, Volume 41, National Bureau of Standards.

Revision: Baseline/Revision Level	Document Number: SNP-DOC-0046
Effective Date: 07/01/2024	Page: 49 of 149
Title: Parahydrogen Thermophysical Properties V05 Final Report	

## **APPENDIX A.**

### **SYSTEMIC ENTROPY ERROR IN NBS-168 PARAHYDROGEN TABULATIONS**

This appendix consists of two main parts:

#### **RATIONALE FOR EXCLUSION OF NBS-168 DATA FROM VALIDATION EFFORTS**

which reviews the observed error and its apparent source, and

#### **IDEALIZED THRUST CHAMBER CALCULATIONS USING NBS-168 DATA**

which provides a quantitative assessment of the observed error's impact on a common thrust chamber throat sizing task.

### **Rationale for Exclusion of NBS-168 Data from Validation Efforts**

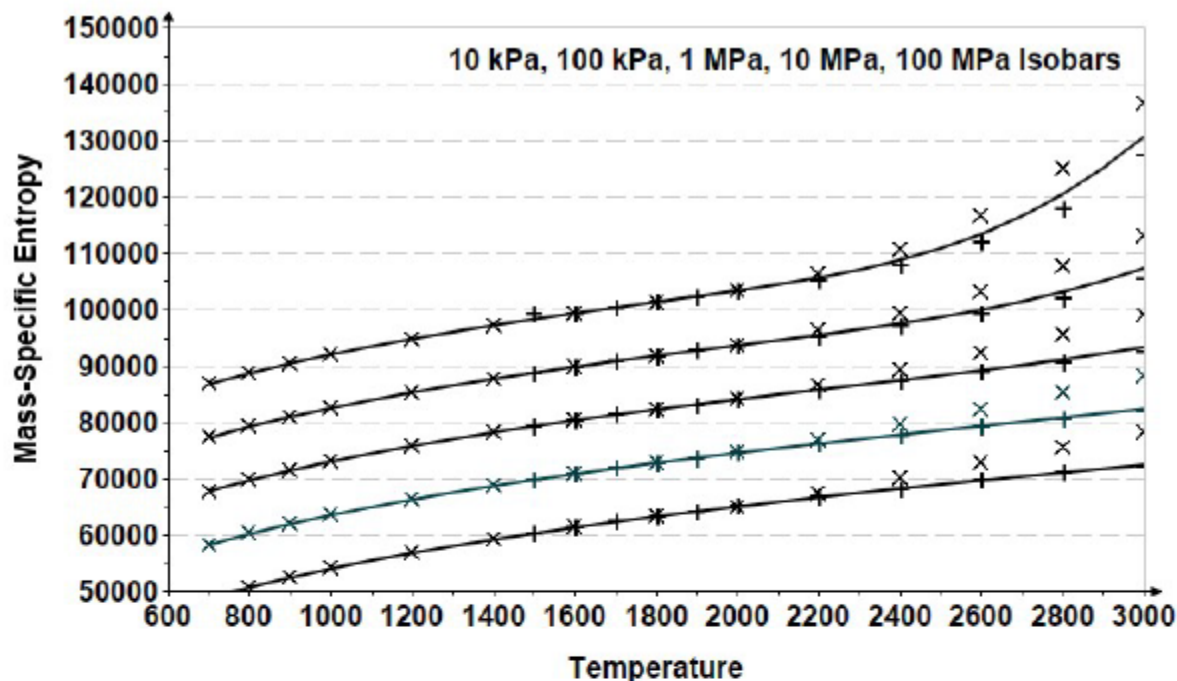
The present effort to create a working database for parahydrogen thermo-physical properties uses existing parahydrogen property sources to validate the current work. For various reasons, these existing sources were deemed inadequate to support the current Space Nuclear Propulsion efforts, but they still serve as the basis for validating (checking for errors in methods and/or their implementation) results from the present effort. The other data sources against which to validate the present results are: 1) the Chemical Equilibrium with Applications tool (CEA, 2004), 2) tabulations from National Bureau of Standards Publication 168 (NBS-168, McCarty et al., 1981), and 3) "Handbook of Physical Properties of Liquids and Gases" (Vargaftik et al., 1996).

Validation efforts for the current release of this parahydrogen database - v03b, documented in McDonald (2018), relied primarily on CEA. Though CEA treats products as an ideal gas mixture, it has a long history of extensive use and the non-ideal nature of the present results deviate from CEA results in manners both knowable and consistent. McDonald (2018) did not validate the v03b results directly against either NBS-168 or Vargaftik et al. (1996); but a predecessor publication (McDonald, 2017) did validate the methods behind v03b against the Vargaftik et al. (1996) database. The main reason v03b was never validated against NBS-168 lay in some obvious sound speed errors found in NBS-168 (see McDonald, 2018) and regular disagreement between NBS-168 versus either CEA or Vargaftik in values for entropy at all pressures. Entropy values from NBS-168 agree very closely with either CEA or Vargaftik until one gets close to the highest temperature of 3000 K tabulated in NBS-168, where NBS-168 entropy values rise steadily above the other sources. Without an understanding of why the NBS-168 entropy values behaved differently, the present author chose the two heavily-documented sources in good agreement (CEA and Vargaftik) over the single, scarcely documented source of NBS-168.

Validation efforts for the current database required revisiting both Vargaftik et al. (1996) and NBS-168 sources on several occasions, and the reason for the deviation of NBS-168 entropy became apparent while reviewing these earlier sources for the present validation work. That reason is the topic of this Appendix. All units are Base SI, unless otherwise noted.

#### **Entropy Behavior - NBS-168 Versus Other Sources**

The plot on the next page depicts isobars of entropy for 10kPa, 100kPa (1 bar), 1 MPa, 10 MPa, and 100 MPa as tabulated by NBS-168 and Vargaftik et al. (1996), and as calculated by CEA. Note that the low end of the temperature range is 700 K, above which all nuclear spin-state forms of dihydrogen exhibit the same specific heat capacity, and the high end is the 3000 K maximum of the NBS-168 tabulations. Note that one may readily identify isobar groupings knowing that entropy increases as pressure decreases. The solid lines represent CEA results with the underlying ideal-gas behavior assumption of that tool. The Plus signs represent that tabulations of Vargaftik et al. (1996) which apply real-gas effects to not only mixture properties but also to mixture composition. The Xs represent data from NBS-168 which assume ideal gas behavior for composition but account for real-gas effects on mixture properties. All sources exhibit excellent agreement up to 2000 K. The CEA and Vargaftik results are in excellent agreement at higher pressures where dissociation is minimal, but the Vargaftik results fall below those of CEA as dihydrogen dissociates to atomic hydrogen.



The entropy calculation methods of NBS-168 are not discussed in that document, but the section discussing entropy provides a generic reference to four supporting references, of which, NBS-Technical Note-617 (McCarty and Weber, 1972) is the only one to deal with the temperatures of present interest. NBS-TN-617 states that all highest temperature properties are based on extrapolation of an equation of state for parahydrogen to temperatures as high as 3000 K - which is only possibly realistic for the highest pressure considered (100 MPa) where dissociation is almost completely suppressed even at 3000 K. NBS-TN-617 does note in a separate paragraph that dissociation is important near 3000 K and refers the reader to an "In Preparation" 1972 NBS Technical Note to be entitled "Approximate Computer Programs for Thermodynamic and Transport Properties of Hydrogen" for details on how dissociation effects are accounted for in NBS-TN-617 and, thus presumably, NBS-168 by extension. No such NBS-TN appears to have ever been published. Thus, all references from the entropy section of NBS-168 result in Dead-Ends as regards the methods used to create entropy entries in that tabulation. The actual tabulations of NBS-168 are in its Chapter 6 and Table 1, Chapter 6 states that all of the Chapter 6 tabulated results were calculated using a program named "H2 Gen", but no further reference information for this program is provided in Table 1 - nor anywhere else in NBS-168 (this author looked very carefully everywhere in NBS-168 and on the internet to no avail). NBS-168 does reference another computer program report by the same three authors as the "In Preparation" 1972 TN and dealing with a program to calculate parahydrogen properties that itself was published as NBS-TN-625 (Roder, et al., 1972). It's unclear whether TN-625 is intended to be the same as the missing TN for the H2 Gen program, particularly since Table 1 makes a separate reference to TN-625. Nevertheless, TN-625 does seem to be the code used to generate the parahydrogen tabulations of NBS-168 based on it being on the exact topic, written by the exact same authors, and in the same 1972 year of the promised "H2 Gen" TN. Thus, NBS-TN-625 was reviewed very thoroughly as a possible source for a more complete understanding of the methods behind the

parahydrogen entropy tabulations of NBS-168. Results from that review are discussed in the next section.

### Methods Behind NBS-168 Tabulations (Presuming They are Related in TN-625)

Reviewing TN-625 carefully for references to 2000 K, or 3600 R, temperatures reveals the source of the erroneous entropy behavior in NBS-168. TN-625 uses ideal gas property data from Woolley et al. (1948) - NBS Research Paper 1932 - as its zero-pressure/ideal-gas backbone on which to calculate real-gas values for enthalpy and entropy. The authors of TN-625 note that RP-1932 "... discontinues entries for parahydrogen but continues entries for normal hydrogen ..." to 5000 K. And, furthermore, that normal hydrogen properties were used for both para and equilibrium spin-states above 3000 K. The 'discontinuance' of parahydrogen tabulation in RP-1932 was not so much a matter of lacking results to tabulate, but rather of not tabulating values that could be readily derived from the normal hydrogen values that were tabulated above 2000 K. Since the zero-pressure values for isobaric specific heat cease to differ among the various spin-states above 700 K, the missing parahydrogen values for entropy aren't really missing at all; but it is left for the reader to fill them in by adding the differences in the continued normal hydrogen tabulation. Instead, the authors of TN-625 simply replace the 'missing' parahydrogen values with ones for normal hydrogen - using a "higher order interpolation" method to ensure smoothness. Such a substitution is defended by the statements "It becomes necessary to switch to the normal mixture at some point because the dissociation calculations ... are based on normal hydrogen." Yet, dissociation is negligibly impacted by nuclear spin-state. Mathematically, yes, but to an extent so small it would be difficult to account for it if one tried to do so.

Thus, the erroneous behavior of entropy observed in NBS-168 appears to be the result of erroneous use of, otherwise good, ideal gas (zero-pressure) entropy data from its RP-1932 source publication. The table in question from RP-1932 is reproduced immediately below.

TABLE 4. *Thermodynamic functions for H<sub>2</sub> in the ideal gaseous state*

Values for  $S^\circ$  and  $-(F^\circ - F_0^\circ)/T$  include nuclear spin

Temperature	$S^\circ$ , cal mole <sup>-1</sup> deg <sup>-1</sup>			$H^\circ - F_0^\circ$ , cal mole <sup>-1</sup>			$-\frac{F^\circ - F_0^\circ}{T}$ , cal mole <sup>-1</sup> deg <sup>-1</sup>			$C_p^\circ$ cal mole <sup>-1</sup> deg <sup>-1</sup>		
	<i>p</i> -H <sub>2</sub>	<i>o</i> -H <sub>2</sub>	<i>n</i> -H <sub>2</sub>	<i>p</i> -H <sub>2</sub>	<i>o</i> -H <sub>2</sub>	<i>n</i> -H <sub>2</sub>	<i>p</i> -H <sub>2</sub>	<i>o</i> -H <sub>2</sub>	<i>n</i> -H <sub>2</sub>	<i>p</i> -H <sub>2</sub>	<i>o</i> -H <sub>2</sub>	<i>n</i> -H <sub>2</sub>
<sup>o</sup> K												
10	11.215	15.581	15.607	49.6785	388.327	303.665	6.247	-23.252	-14.760	4.968	4.968	4.968
20	14.658	19.024	19.050	99.357	438.006	353.344	9.690	-2.876	1.382	4.968	4.968	4.968
20.39	14.754	19.120	19.146	101.295	439.943	355.281	9.786	-2.457	1.721	4.968	4.968	4.968
30	16.672	21.039	21.064	149.036	487.684	403.022	11.705	4.783	7.630	4.968	4.968	4.968
33.1	17.161	21.527	21.553	164.437	503.085	418.423	12.193	6.328	8.911	4.968	4.968	4.968
40	18.102	22.468	22.494	198.729	537.363	452.705	13.134	9.034	11.176	4.973	4.968	4.969
50	19.214	23.576	23.603	248.581	587.041	502.426	14.243	11.836	13.554	5.007	4.968	4.978
60	20.135	24.492	24.513	299.106	636.722	552.318	15.150	13.870	15.307	5.115	4.969	5.005
70	20.938	25.248	25.288	351.222	686.422	602.622	15.921	15.442	16.679	5.330	4.972	5.061
80	21.669	25.913	25.969	406.015	736.179	653.638	16.594	16.710	17.799	5.646	5.982	5.148
90	22.356	26.500	26.581	464.385	786.085	705.660	17.197	17.766	18.741	6.036	5.003	5.261
100	23.014	27.029	27.142	526.837	836.277	758.916	17.745	18.667	19.554	6.455	5.039	5.393
120	24.259	27.959	28.151	663.752	938.227	869.609	18.729	20.140	20.904	7.204	5.170	5.678
150	25.945	29.143	29.461	890.605	1,097.78	1,045.99	20.007	21.825	22.488	7.807	5.487	6.067
200	28.202	30.808	31.275	1,282.70	1,387.90	1,361.61	21.788	23.869	24.466	7.742	6.110	6.518
250	29.889	32.225	32.758	1,660.49	1,705.80	1,694.47	23.246	25.402	25.981	7.380	6.565	6.770
298.16	31.168	33.404	33.963	2,009.99	2,028.34	2,023.75	24.426	26.602	27.175	7.158	6.803	6.891
300	31.212	33.446	34.005	2,023.16	2,040.87	2,036.44	24.468	26.643	27.217	7.152	6.809	6.894

Revision: Baseline/Revision Level	Document Number: SNP-DOC-0046
Effective Date: 07/01/2024	Page: 53 of 149
Title: Parahydrogen Thermophysical Properties V05 Final Report	

350.....	32.306	34.505	35.073	2,377.84	2,384.39	2,382.75	25.512	27.693	28.265	7.049	6.917	6.951
400.....	33.244	35.432	36.003	2,729.19	2,731.54	2,730.95	26.421	28.603	29.175	7.010	6.963	6.975
500.....	34.806	36.990	37.561	3,429.24	3,429.53	3,429.46	27.948	30.131	30.702	6.998	6.992	6.993
600.....	36.083	38.266	38.838	4,129.48	4,129.52	4,129.51	29.200	31.383	31.955	7.010	7.009	7.009
700.....	37.165	39.348	39.920	4,831.65	4,831.66	4,831.66	30.263	32.446	33.018	7.037	7.036	7.036
1,000.....	39.701	41.884	42.455	-----	-----	6,966.23	32.735	34.918	35.490	-----	-----	7.219
1,500.....	42.720	44.903	45.475	-----	-----	10,697.20	35.589	37.770	38.343	-----	-----	7.720
2,000.....	45.007	47.190	47.762	-----	-----	14,679.2	37.668	39.851	40.422	-----	-----	8.195
3,000.....	-----	-----	51.221	-----	-----	23,230.9	-----	-----	43.478	-----	-----	8.859
4,000.....	-----	-----	53.839	-----	-----	32,345.	-----	-----	45.753	-----	-----	9.342
5,000.....	-----	-----	55.969	-----	-----	41,895.	-----	-----	47.590	-----	-----	9.748

As a final check to ensure that this entropy error in NBS-168 is understood, one may use data from both NBS-168 and Vargaftik et al. (1996) at 100 MPa to see if the resulting entropy differences between 2000 K and 3000 K correspond to the differences in the para- and normal spin-state data tabulated in Table 4 of RP-1932. The 100 MPa isobar is used as dissociation is minimal at this pressure across the 2000 K to 3000 K temperature range of interest - assuming the equations of state produce similar real gas contributions to entropy, these differences should be primarily due to the ideal gas entropy values used as backbones for the real gas property calculations. The entropy values for para- and normal spin-states at 2000 K from Table 4 of RP-1932 are:

$$s_{normal\_2000K} := 47.762 \cdot \frac{tcal}{mol \cdot K} \qquad s_{para\_2000K} := 45.007 \cdot \frac{tcal}{mol \cdot K}$$

where tcal is the thermochemical calorie = 4.184 Joules, and the desired difference is

$$s_{normal\_2000K} - s_{para\_2000K} = 11.527 \frac{J}{mol \cdot K}$$

or on a mass-specific basis

$$\frac{s_{normal\_2000K} - s_{para\_2000K}}{2.016 \cdot \frac{gm}{mol}} = 5718 \frac{J}{kg \cdot K}$$

At 2000 K, this difference will not be manifest in the entropy difference between NBS-168 and Vargaftik et al. (1996) values, but their difference should grow to equal - roughly so - this value at 3000 K. It would be a bonus to be able to deduce the "higher order interpolation" means used in TN-625 - but that is not likely since the real gas equations of state used by NBS-168 and Vargaftik et al. (1996) are unlikely to be in exact agreement at 100 MPa. Before plotting the desired differences, let us get right to the punchline and calculate the difference at 3000 K

$$\left( s_{100MPa\_NBS168_{13}} - s_{100MPa\_Vrgftk_{10}} \right) \cdot 2.016 \cdot \frac{gm}{mol} = 11.723 \frac{J}{mol \cdot K}$$

that is a very convincing result differing from the expected difference by only 1.7%.

Now on to plot the differences in the real gas curves between 2000 K and 3000 K. First, create cubic spline models for the supporting 100 MPa isobars to facilitate generation of a continuous difference curve.

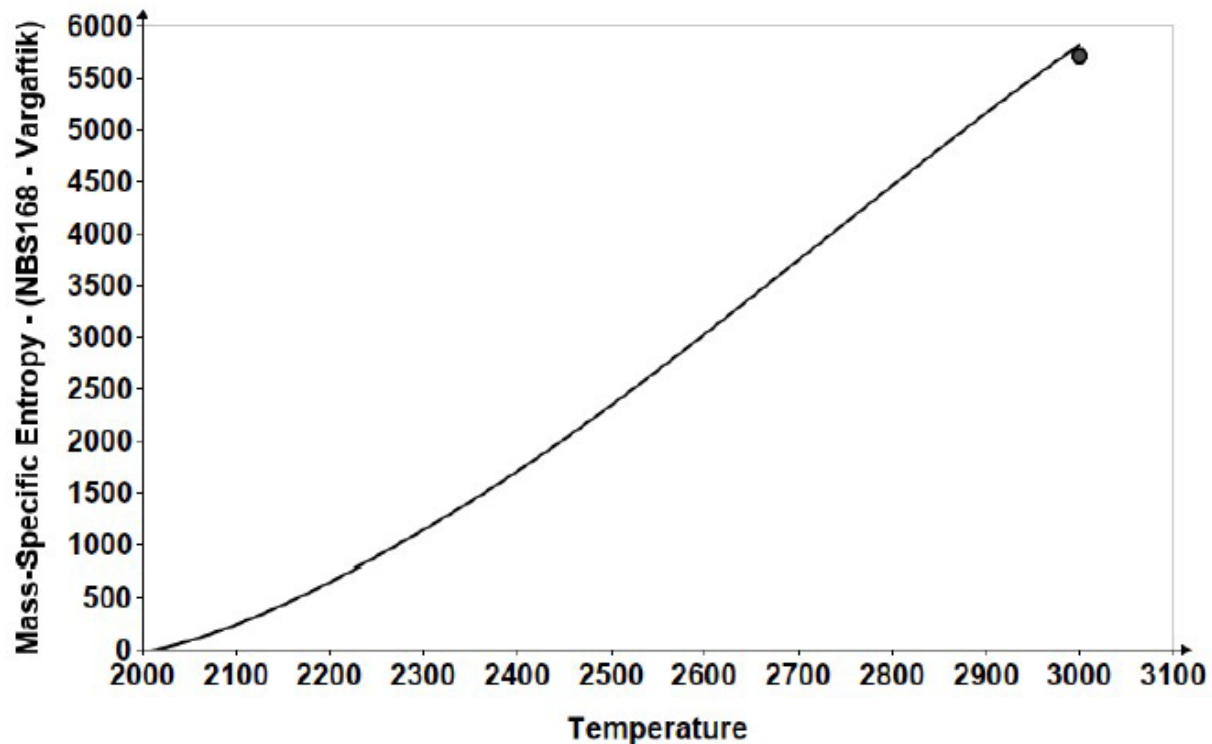
Revision: Baseline/Revision Level	Document Number: SNP-DOC-0046
Effective Date: 07/01/2024	Page: 54 of 149
Title: Parahydrogen Thermophysical Properties V05 Final Report	

$s_{NBS168\_spline}(T) := \text{interp}(\text{cspline}(T_{NBS168}, s_{100MPa\_NBS168}), T_{NBS168}, s_{100MPa\_NBS168}, T)$

$s_{Vrgftk\_spline}(T) := \text{interp}(\text{cspline}(T_{Vrgftk}, s_{100MPa\_Vrgftk}), T_{Vrgftk}, s_{100MPa\_Vrgftk}, T)$

and create a fairly dense T vector for plotting the difference

$$idifplot := 0 .. 100 \quad T_{diffplot}_{idifplot} := 2000 \cdot K + \frac{3000 \cdot K - 2000 \cdot K}{100} \cdot idifplot$$



The resulting difference curve does seem to indicate application of some form of smoothing curve between the 2000 K parahydrogen point and the 3000 K normal hydrogen point from RP-1932 Table 4. It does appear that NBS-168 tabulations apply the interpretation/use described in TN-625 of the zero-pressure entropy data from RP-1932. Such interpretation/use is simply incorrect. As such, while this only impacts entropy data between 2000 K and 3000 K, present validation needs are for existing, trusted, sources of parahydrogen data in the temperature range 1500 K to 6000 K. Given the error found in the underlying methods, and the relatively sparse supporting documentation, the present author has chosen not to rely on NBS-168 in the validation of the current database results. Rather, validation will rely on CEA and Vargaftik et al. (1996) sources.

The next section considers the impact of this entropy error in NBS-168 on a fundamental nuclear thermal rocket task.

Revision: Baseline/Revision Level	Document Number: SNP-DOC-0046
Effective Date: 07/01/2024	Page: 55 of 149
Title: Parahydrogen Thermophysical Properties V05 Final Report	

### Idealized Thrust Chamber Calculations using NBS-168 Data

A common deployed idealized model of thrust chamber performance assumes the presence of some 'reservoir' conditions - total temperature and total pressure - entering the throat of the converging-diverging nozzle. These total conditions serve as the reference state for calculation of throat conditions assuming the flow accelerates isentropically to a sonic (Mach Number = 1) state at the throat station. Furthermore, the same total conditions serve as the reference state for calculation of static flow states in the supersonic expansion downstream of the nozzle throat station - ultimately arriving at the supersonic nozzle exit plane.

The great advantage of real-gas tabulations of working fluid properties is that they readily enable direct solution of the underlying governing relations without recourse to calorically/thermally-perfect approximate relations. Such approximate relations can be quite inaccurate when expansions occur over large area ratios - and, thus, large variations in static conditions within the problem. The simple one-dimensional relations to be solved are:

mass conservation:  $\rho_{throat} \cdot c_{throat} \cdot A_{throat} = \rho \cdot V \cdot A$  at any other flow station

where  $\rho$  is the static density,  $c$  is sound speed, and  $A$  is flow area

momentum conservation: herein handled by assuming entropy,  $s$ , is constant throughout the thrust chamber, and equal to its value at the provided total conditions  
 $s(P_{total}, T_{total}) = \text{constant}$

energy conservation:  $h(T_{total}, P_{total}) = h_{throat} + \frac{c_{throat}^2}{2} = h + \frac{V^2}{2}$  at any station

For our example calculation, to avoid having to interpolate in the NBS-168 tabulation to obtain the needed total conditions, assume the following:

$$T_{total} := 2800 \cdot K \quad P_{total} := 7000000 \cdot Pa \quad \text{which, from NBS-168, yields}$$

$$h_{total} := 45736900 \cdot \frac{J}{kg}$$

$$s_{total} := 86716 \cdot \frac{J}{kg \cdot K}$$

at the throat station one has

$$s_{throat}(P_{throat}, T_{throat}) = s_{total} \quad h_{throat}(P_{throat}, T_{throat}) + \frac{c_{throat}(P_{throat}, T_{throat})^2}{2} = h_{total}$$

and one may guess at a value for  $P_{throat}$  to gain entry to the solution process - the total to static pressure ratio for sonic flow may be approximated by assuming calorically perfect, isentropic flow yielding, for a diatomic molecule:

Revision: Baseline/Revision Level	Document Number: SNP-DOC-0046
Effective Date: 07/01/2024	Page: 56 of 149
Title: Parahydrogen Thermophysical Properties V05 Final Report	

$$P_{throat} := \frac{P_{total}}{\left(1 + \frac{1.4-1}{2} \cdot 1^2\right)^{\frac{1.4}{1.4-1}}} \quad P_{throat} = (3.698 \cdot 10^6) \text{ Pa}$$

very close to the table value of 3500000 Pa, so use 3500000 Pa as the first guess.

Thus, for

$$P_{throat} := 3500000 \cdot \text{Pa} \quad \text{and} \quad s_{throat} := s_{total} \quad s_{throat} = 86716 \frac{\text{J}}{\text{kg} \cdot \text{K}}$$

NBS-168 yields the following when linearly interpolating using the know entropy

Entropy (J/(kg*K))	Sound Speed (m/s)	Enthalpy (J/kg)
86713	3698	41718800
86716	$c_{throat} := 3698.1 \cdot \frac{\text{m}}{\text{s}}$	$h_{throat} := 41723184.93 \cdot \frac{\text{J}}{\text{kg}}$
89758	3806	46169500

now apply the interpolated sound speed and enthalpy to the energy relation

$$h_{throat} + \frac{c_{throat}^2}{2} = 48561157 \frac{\text{J}}{\text{kg}} \quad \text{compared to} \quad h_{total} = 45736900 \frac{\text{J}}{\text{kg}}$$

which implies the guess of 3500000 Pa is too high, so try the next lower NBS-168 table value of 3000000 Pa.

$$P_{throat} := 3000000 \cdot \text{Pa} \quad \text{and} \quad s_{throat} := s_{total} \quad s_{throat} = 86716 \frac{\text{J}}{\text{kg} \cdot \text{K}}$$

NBS-168 yields the following when linearly interpolating using the know entropy

Entropy (J/(kg*K))	Sound Speed (m/s)	Enthalpy (J/kg)
84461	3578	37750000
86716	$c_{throat} := 3667.0 \cdot \frac{\text{m}}{\text{s}}$	$h_{throat} := 40864810.68 \cdot \frac{\text{J}}{\text{kg}}$
87374	3693	41773700

now apply the interpolated sound speed and enthalpy to the energy relation

$$h_{throat} + \frac{c_{throat}^2}{2} = 47588255 \frac{J}{kg} \quad \text{compared to} \quad h_{total} = 45736900 \frac{J}{kg}$$

which implies the guess of 3000000 Pa is still too high, so try the next lower NBS-168 table value of 2500000 Pa.

$$P_{throat} := 2500000 \cdot Pa \quad \text{and} \quad s_{throat} := s_{total} \quad s_{throat} = 86716 \frac{J}{kg \cdot K}$$

NBS-168 yields the following when linearly interpolating using the know entropy

Entropy (J/(kg*K))	Sound Speed (m/s)	Enthalpy (J/kg)
85227	3574	37777100
86716	$c_{throat} := 3631.9 \cdot \frac{m}{s}$	$h_{throat} := 39844122.59 \cdot \frac{J}{kg}$
88158	3688	41845900

now apply the interpolated sound speed and enthalpy to the energy relation

$$h_{throat} + \frac{c_{throat}^2}{2} = 46439471 \frac{J}{kg} \quad \text{compared to} \quad h_{total} = 45736900 \frac{J}{kg}$$

which implies the guess of 2500000 Pa is still too high, so try the next lower NBS-168 table value of 2000000 Pa.

$$P_{throat} := 2000000 \cdot Pa \quad \text{and} \quad s_{throat} := s_{total} \quad s_{throat} = 86716 \frac{J}{kg \cdot K}$$

NBS-168 yields the following when linearly interpolating using the know entropy

Entropy (J/(kg*K))	Sound Speed (m/s)	Enthalpy (J/kg)
85227	3569	37815500
86716	$c_{throat} := 3590.0 \cdot \frac{m}{s}$	$h_{throat} := 38582632.28 \cdot \frac{J}{kg}$
88158	3682	41944600

now apply the interpolated sound speed and enthalpy to the energy relation

Revision: Baseline/Revision Level	Document Number: SNP-DOC-0046
Effective Date: 07/01/2024	Page: 58 of 149
Title: Parahydrogen Thermophysical Properties V05 Final Report	

$$h_{throat} + \frac{c_{throat}^2}{2} = 45026682 \frac{J}{kg} \quad \text{compared to} \quad h_{total} = 45736900 \frac{J}{kg}$$

which implies the guess of 2000000 Pa is too low, so the desired solution is bounded by

$$2000000 \text{ Pa} < P_{throat} < 2500000 \text{ Pa}$$

gather the state variables for the bounding pressure solutions and interpolate in  $P_{throat}$  space to arrive at an estimate of the throat static state

$P_{throat}$	$h_{throat} + \frac{c_{throat}^2}{2}$	$c_{throat}$	$\rho_{throat}$
2000000	45026682	3590.0	0.198376
$P_{throat} := 2251353 \cdot Pa$	$h_{total} = 45736900 \frac{J}{kg}$	$c_{throat} := 3611.1 \cdot \frac{m}{s}$	$\rho_{throat} := 0.220068 \cdot \frac{kg}{m^3}$
2500000	46439471	3631.9	0.241527

Recapitulate the throat conditions found from use of the NBS-168 table values and estimate the resulting mass flux that would be used to size a nozzle throat area for a given thrust level.

$$P_{throat} = 2251353 \text{ Pa} \quad c_{throat} = 3611 \frac{m}{s} \quad \rho_{throat} = 0.2201 \frac{kg}{m^3} \quad \rho_{throat} \cdot c_{throat} = 794.7 \frac{kg}{m^2 \cdot s}$$

for the purpose of comparison, estimation of the same parameters using the Chemical Equilibrium with Applications tool and its Rocket problem yields

$P_{throat}$	$c_{throat}$	$\rho_{throat}$	$\rho_{throat} \cdot c_{throat}$
$38.426 \cdot bar = 3842600 \text{ Pa}$	$3617 \cdot \frac{m}{s}$	$0.3758 \cdot \frac{kg}{m^3}$	$0.3758 \cdot \frac{kg}{m^3} \cdot 3617 \cdot \frac{m}{s} = 1359 \frac{kg}{m^2 \cdot s}$

were NBS-168 used to execute a basic throat sizing problem, it would overpredict the throat area by roughly

$$\frac{0.3758 \cdot \frac{kg}{m^3} \cdot 3617 \cdot \frac{m}{s}}{\rho_{throat} \cdot c_{throat}} = 1.71 \quad \text{times}$$

Revision: Baseline/Revision Level	Document Number: SNP-DOC-0046
Effective Date: 07/01/2024	Page: 59 of 149
Title: Parahydrogen Thermophysical Properties V05 Final Report	

## **APPENDIX B.**

### **DERIVATION OF ZERO-PRESSURE BACKBONES FOR NEW DATABASE AND ENTHALPY AND ENTROPY SHIFTS TO THE REFPROP 10 STANDARD REFERENCE STATE**

This appendix is in a landscape orientation to better accommodate lengthy equations.

Revision: Baseline/Revision Level	Document Number: SNP-DOC-0046
Effective Date: 07/01/2024	Page: 60 of 149
Title: Parahydrogen Thermophysical Properties V05 Final Report	

### **Bridging Zero-Pressure Properties**

McDonald (2018) 'bridged' the REFPROP and higher temperature methods detailed in McDonald (2017, 2018) at the 1000 K upper bound of the REFPROP parahydrogen dataset. While working on the present update to the parahydrogen properties dataset, it occurred to the author that much of the trouble with bridging these datasets was the result of finite chemical contributions that exist at 1000 K for lower pressures. The methods behind REFPROP ignore these effects and, thus, the two methods were at odds with each other for combinations of 1000 K and lower pressures. While the small amounts of dissociation at/below 1000 K for lower pressures (< roughly 100 kPa) are of little practical interest due to the associated large chemical characteristic times (>> seconds) compared to typical residence times in practical systems (<< seconds), it must be considered for an equilibrium database.

The zero-pressure isobaric specific heat backbone will be taken directly from REFPROP at/below 1000 K, taken directly from Gurvich et al. (1989) at/above 1500 K, and bridged between 1000 K and 1500 K. The zero-pressure values for enthalpy and entropy extracted from this new isobaric specific heat backbone will extend down to 700 K to accommodate the lowest imaginable bridging temperature for the lowest pressure, 1 Pa, considered in the present database.

Calculation of real gas isobaric specific heat is done by differentiation of the relations for real gas enthalpy and, thus, this calculation depends on how accurately one can extract zero-pressure isobaric specific heat from differentiation of the chosen zero-pressure enthalpy model. The next section addresses this issue for the case of using tabulated values for zero-pressure enthalpy.

### **Accuracy Associated with Direct Use of Zero-Pressure Tabulations**

The property calculations of McDonald (2017, 2018) use only zero-pressure enthalpy ( $H_0$ ) and entropy ( $S_{0,1\text{bar}}$  - entropy must be referenced to a pressure) values. Extraction of zero-pressure isobaric specific heat ( $C_{p0}$ ) occurs implicitly in the calculation of real gas isobaric specific via differentiation of a cubic spline model of the zero-pressure enthalpy data. In this section, we test the accuracy of this process to ensure it is suitable for the main database. The needed values for  $C_{p0}$  and  $H_0$  are taken from Gurvich et al. (1989). The NIST-JANNAF Thermochemical Tables (Chase 1998) represent a source with a newer publication date, but the needed data for dihydrogen from that source were calculated using a "program" borrowed from the National Bureau of Standards and informally referenced by Chase (1998). Thus, the underlying methods are unknown and the data itself no newer than 1988 when the NBS changed its name to NIST. Gurvich et al. (1989) extensively discusses their methods internal to that publication.

Units in this work are Molar Base SI.

Revision: Baseline/Revision Level	Document Number: SNP-DOC-0046
Effective Date: 07/01/2024	Page: 61 of 149
Title: Parahydrogen Thermophysical Properties V05 Final Report	

*T\_H2\_Grvch*    *Cp0\_H2\_Grvch*    *H0\_H2\_Grvch*    *S0\_1bar\_H2\_Grvch*

100	28.155	2999	100.725
200	27.447	5693	119.410
298.15	28.836	8468	130.679
300	28.849	8521	130.856
400	29.181	11426	139.213
500	29.260	14350	145.735
600	29.327	17278	151.075
700	29.440	20216	155.603
800	29.623	23169	159.546
900	29.880	26143	163.049
1000	30.204	29147	166.213
1100	30.580	32186	169.109
1200	30.991	35263	171.787
1300	31.422	38385	174.285
1400	31.860	41548	176.629
1500	32.296	44757	178.843
1600	32.724	48008	180.941
1700	33.138	51301	182.937
1800	33.535	54634	184.842
1900	33.915	58007	186.666
2000	34.277	61418	188.415

Revision: Baseline/Revision Level	Document Number: SNP-DOC-0046
Effective Date: 07/01/2024	Page: 62 of 149
Title: Parahydrogen Thermophysical Properties V05 Final Report	

2100	34.622	64863	190.096
2200	34.949	68341	191.714
2300	35.259	71850	193.274
2400	35.555	75391	194.781
2500	35.837	78960	196.238
2600	36.106	82558	197.649
2700	36.363	86184	199.017
2800	36.610	89832	200.344
2900	36.847	93505	201.633
3000	37.076	97200	202.885
3100	37.298	100920	204.105
3200	37.513	104659	205.292
3300	37.723	108421	206.450
3400	37.928	112203	207.579
3500	38.129	116008	208.682
3600	38.326	119829	209.758
3700	38.520	123673	210.811
3800	38.711	127535	211.841
3900	38.899	131414	212.849
4000	39.085	135312	213.836
4100	39.269	139232	214.804
4200	39.450	143165	215.752
4300	39.629	147120	216.682

Revision: Baseline/Revision Level	Document Number: SNP-DOC-0046
Effective Date: 07/01/2024	Page: 63 of 149
Title: Parahydrogen Thermophysical Properties V05 Final Report	

4400	39.806	151091	217.595
4500	39.980	155083	218.492
4600	40.151	159091	219.373
4700	40.318	163113	220.238
4800	40.482	167150	221.088
4900	40.641	171211	221.925
5000	40.796	175280	222.747
5100	40.945	179367	223.557
5200	41.088	183466	224.353
5300	41.226	187583	225.137
5400	41.357	191716	225.909
5500	41.480	195855	226.669
5600	41.596	200010	227.417
5700	41.703	204180	228.155
5800	41.803	208353	228.881
5900	41.893	212536	229.596
6000	41.974	216726	230.301
6200	42.107	225141	231.680
6400	42.200	233568	233.018

Model the zero-pressure enthalpy with a cubic spline,

$$H0\_H2\_spline(T) := \text{interp}(\text{cspline}(T\_H2\_Grvch, H0\_H2\_Grvch), T\_H2\_Grvch, H0\_H2\_Grvch, T)$$

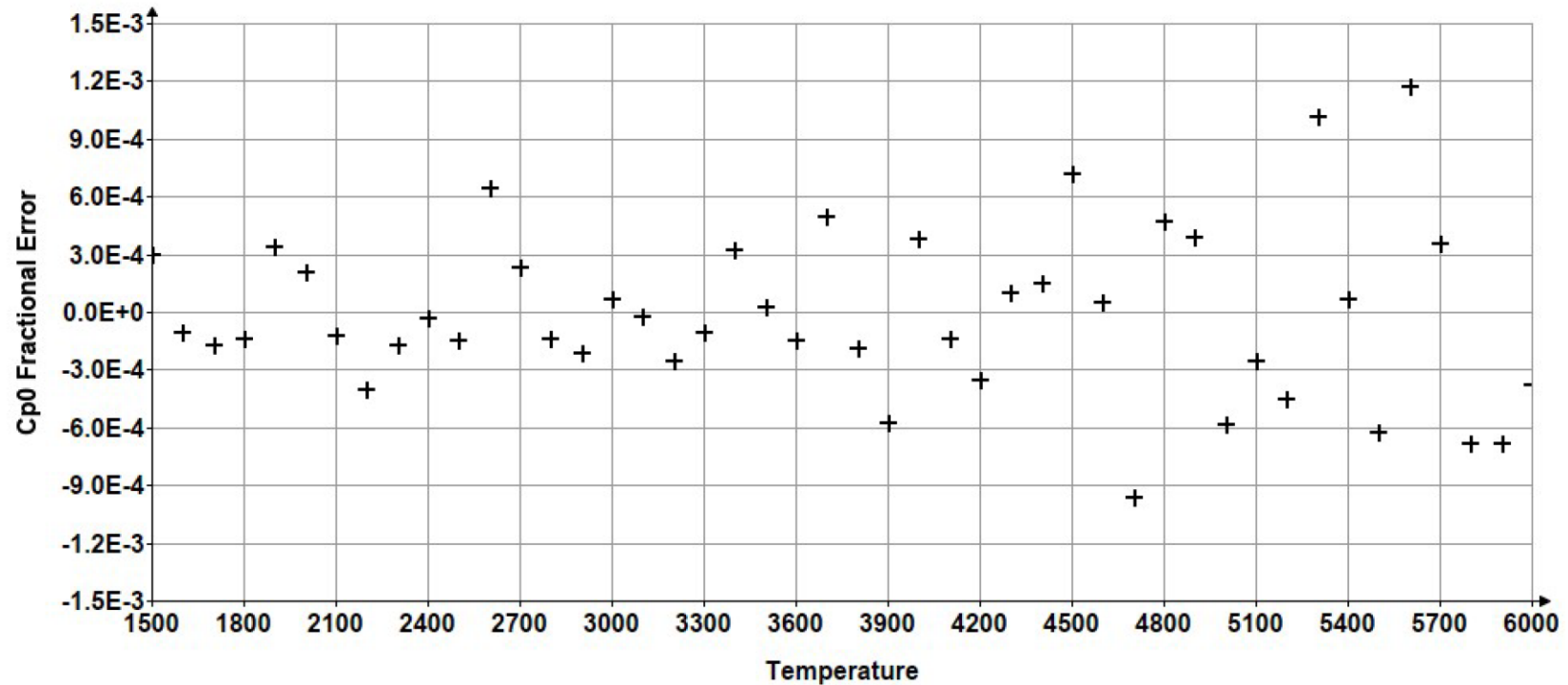
extract the estimate of zero-pressure isobaric specific heat,

$$Cp0\_H2\_spline(T) := \frac{d}{dT} H0\_H2\_spline(T)$$

and define the error as follows

$$Error\_Cp0\_spline := \frac{Cp0\_H2\_spline(T\_H2\_Grvch) - Cp0\_H2\_Grvch}{Cp0\_H2\_Grvch}$$

The resulting error is plotted immediately below and all points are within roughly 0.001, which is not really very good.



While it will not improve actual accuracy of the Gurvich et al. (1989) tabulated values, a mathematical model is needed that will reproduce those results without the issue of numerical inaccuracy when  $Cp0$  is implicitly extracted from  $H0$  in the calculations.

### Establish a Mathematical Model for Zero-Pressure Properties

The task here is to recreate available Cp0 values using a mathematical model that may be analytically integrated to obtain expressions for H0 and S0\_1bar. The model used by REFPROP 10 is provided by Leachman et al. (2009) and has the form. This model will be used here to obtain point and slope values at 600 K. The new model will apply at/above 700 K and must match the REFPROP point and slope values at 700 K. Define the REFPROP model and test for correct definition.

$$Ru\_REFPROP := 8.3144598$$

$$u := \begin{bmatrix} 4.30256 \\ 13.0289 \\ -47.7365 \\ 50.0013 \\ -18.6261 \\ 0.993973 \\ 0.536078 \end{bmatrix} \quad v := \begin{bmatrix} 499 \\ 826.5 \\ 970.8 \\ 1166.2 \\ 1341.4 \\ 5395 \\ 10185 \end{bmatrix} \quad Cp0\_H2\_RP\_model(T) := \left( 2.5 + \sum_{i=0}^{\text{last}(u)} u_i \cdot \left(\frac{v_i}{T}\right)^2 \cdot \frac{\exp\left(\frac{v_i}{T}\right)}{\left(\exp\left(\frac{v_i}{T}\right) - 1\right)^2} \right) \cdot Ru\_REFPROP$$

Compare the definition above with a few values of interest from REFPROP 10 itself

$T\_H2\_RP$	$Cp0\_H2\_RP$	
700	29.4383378883998	$\overrightarrow{Cp0\_H2\_RP\_model(T\_H2\_RP) - Cp0\_H2\_RP} = \begin{bmatrix} 1.8 \cdot 10^{-14} \\ -7.1 \cdot 10^{-15} \\ -2.8 \cdot 10^{-14} \\ 2.1 \cdot 10^{-14} \end{bmatrix}$
800	29.6266337675153	
900	29.8940185079240	
1000	30.2276277658247	

Definition of the REFPROP model appears correct.

Revision: Baseline/Revision Level	Document Number: SNP-DOC-0046
Effective Date: 07/01/2024	Page: 66 of 149
Title: Parahydrogen Thermophysical Properties V05 Final Report	

Necessary brief aside on origin of Ru\_REFPROP used in this work.

Note that Leachman et al. (2009) reports a value of 8.314472 and REFPROP 10 itself outputs a value of 8.31451 when the user requests the molar gas constant from its Excel interface tool via the command recommended for such in that tool (=REFPROP("R",,"Molar Base SI")). Yet, the same Excel command may be made for specific fluids in the REFPROP database in the form (=REFPROP("R","Fluid Name","TP","Molar Base SI","User Input T","User Input P")) and different values result depending only on the specified fluid name. The value used in this work is the value output for the fluid "parahydrogen". As seen above, it accurately recreates Cp0 values from the model of Leachman et al. (2009).

Point and slope values at 700 K needed for use as constraints on the model to be applied at/above 700 K. The REFPROP value for point is:

$$Cp0\_H2\_RP\_700K := Cp0\_H2\_RP\_model(700) \quad Cp0\_H2\_RP\_700K = 2.94383378883998 \cdot 10$$

and define the slope function as:  $dCp0dT\_H2\_RP(T) := \frac{d}{dT} Cp0\_H2\_RP\_model(T)$

$$dCp0dT\_H2\_RP\_700K := dCp0dT\_H2\_RP(700) \quad dCp0dT\_H2\_RP\_700K = 1.47459581380849 \cdot 10^{-3}$$

The next Cp0 model will join the REFPROP point at 700 K to the tabulation of Gurvich et al. (1989). The REFPROP 10 software uses a molar gas constant value defined above, but the value used to calculate the Cp0 values tabulated in Gurvich et al. (1989) is not known. The direct summation method used to calculate Cp0 ultimately makes use of a molar gas constant multiplier to arrive at the tabulated results - thus, the results themselves are directly proportional to the applied gas constant. Typically, gas constant values change very little as they are updated, but they do vary. The listing to the right is based on references from the NIST webpage (<https://physics.nist.gov/cuu/Constants/index.html>) - where the % error uses the 2014 value which is the same as that used by REFPROP 10 for parahydrogen.

Year	Value	% Deviation
1969	8.3143435	1.4E-03
1973	8.3144126	5.7E-04
1986	8.3145107	-6.1E-04
1998	8.31447215	-1.5E-04
2010	8.314462175	-2.8E-05
2014	8.314459848	0.0E+00
2018	8.314462618	-3.3E-05

Revision: Baseline/Revision Level	Document Number: SNP-DOC-0046
Effective Date: 07/01/2024	Page: 67 of 149
Title: Parahydrogen Thermophysical Properties V05 Final Report	

Given that the Gurvich et al. (1989) data had to be generated before its publication, its values likely apply one of the R values from 1969, 1973, or 1986. It cannot be assumed that the values in Gurvich et al. (1989) were recalculated specifically for that publication and they, therefore, may not be based on the most recent value preceding the 1989 publication date. The largest value of Cp0 of interest is 41.974 at 6000 K, and this value would become 41.973 if corrected from a 1969 molar gas constant to the 2014 value used by REFPROP 10. Given this fact, the Cp0 values from Gurvich et al. (1989) will be used as-is. The H0 and S0\_1bar values will also be used as-is, but there is a chance that they would have been altered slightly by correction from even the 1973 value (reported to 6 figures for the higher temperatures). That possibility is here acknowledged, but there is nothing to do about it without knowledge of the molar gas constant actually used by Gurvich et al. (1989).

### Weighted Average Points Between 1000 K and 1500 K

The parahydrogen data from REFPROP is valid up to 1000 K, but REFPROP will continue to provide values up to 1500 K. Rather than abruptly changing from REFPROP to Gurvich et al. (1989) supporting data 1000 K, the region between 1000 K and 1500 K is used to more smoothly transition between these two - slightly different - datasets. Since Gurvich et al. (1989) only provided values every 100 K, this bridging region will only include points for the following temperatures:

$$T_{bridge} := \begin{bmatrix} 1000 \\ 1100 \\ 1200 \\ 1300 \\ 1400 \\ 1500 \end{bmatrix} \quad \begin{aligned} & PolyWeight(T, C0, C1, C2, C3) := C0 + C1 \cdot T + C2 \cdot T^2 + C3 \cdot T^3 \\ & dPolyWeight(T, C1, C2, C3) := C1 + 2 \cdot C2 \cdot T + 3 \cdot C3 \cdot T^2 \end{aligned}$$

### Define the Solve Block

Guess Values	$\begin{bmatrix} C0 \\ C1 \\ C2 \\ C3 \end{bmatrix} := \begin{bmatrix} 0 \\ 0 \\ 0 \\ 0 \end{bmatrix}$
Constraints	$PolyWeight(1000, C0, C1, C2, C3) = 1 \quad PolyWeight(1500, C0, C1, C2, C3) = 0$ $dPolyWeight(1000, C1, C2, C3) = 0 \quad dPolyWeight(1500, C1, C2, C3) = 0$
Solver	$\begin{bmatrix} C0 \\ C1 \\ C2 \\ C3 \end{bmatrix} := \text{minerr}(C0, C1, C2, C3)$

$$\begin{bmatrix} C0 \\ C1 \\ C2 \\ C3 \end{bmatrix} = \begin{bmatrix} -27 \\ 0.072 \\ -6 \cdot 10^{-5} \\ 1.6 \cdot 10^{-8} \end{bmatrix} \quad PolyWeight \left( \begin{bmatrix} 1000 \\ 1100 \\ 1200 \\ 1300 \\ 1400 \\ 1500 \end{bmatrix}, C0, C1, C2, C3 \right) = \begin{bmatrix} 9.99999999999977 \cdot 10^{-1} \\ 8.95999999999979 \cdot 10^{-1} \\ 6.48 \cdot 10^{-1} \\ 3.5200000000000004 \cdot 10^{-1} \\ 1.039999999999999 \cdot 10^{-1} \\ 0 \end{bmatrix} \quad Weight := \begin{bmatrix} 0.896 \\ 0.648 \\ 0.352 \\ 0.104 \end{bmatrix}$$

The REFPROP and Gurvich et al. (1989) datasets have the following shared temperature values in this region:

$$T_{bridge} := \begin{bmatrix} 1100 \\ 1200 \\ 1300 \\ 1400 \end{bmatrix} \quad Cp0\_H2\_RP\_bridge := \begin{bmatrix} 30.6095746987412 \\ 31.0225909579166 \\ 31.4523687268219 \\ 31.8879784814083 \end{bmatrix} \quad Cp0\_H2\_Gurvch\_bridge := \begin{bmatrix} 30.580 \\ 30.991 \\ 31.422 \\ 31.860 \end{bmatrix}$$

Revision: Baseline/Revision Level	Document Number: SNP-DOC-0046
Effective Date: 07/01/2024	Page: 69 of 149
Title: Parahydrogen Thermophysical Properties V05 Final Report	

$$Cp0\_H2\_bridge := \overline{Cp0\_H2\_RP\_bridge \cdot Weight + Cp0\_H2\_Grvch\_bridge \cdot (1 - Weight)}$$

All of the data to support creation of a Cp0 model is now available. Join the data into one set for use in model creation, and plot that dataset here to help ensure it is correct/suitable. Now, create a single set of data vectors that support model definition.

Cp0 will be fit from 700 K to 6400 K using supporting constraints as follows:

- 1) Match point (to at least the accuracy of Gurvich et al. (1989) tabulations) and slope (roughly, but not so critical) at 700 K
- 2) Match values from Leachman et al. (2009) (REFPROP 10) in the range 700 K < T <= 1000 K with a density of points sufficient to keep the model well-behaved in between the supporting points. Desired accuracy is, again, to exactly match to the three decimal places of the Gurvich et al. (1989) tabulations.
- 3) Match the 'bridge' values immediately above, but apply a separate weighting factor for this region since it is a sort of No-Person's Land between the Leachman/REFPROP and Gurvich regions.
- 4) Match Gurvich et al. (1989) values for 1500 K < T < 6000 K - supporting fit data will extend to 6400 K to help ensure the model is well-behaved at least up to the desired 6000 K upper bound.

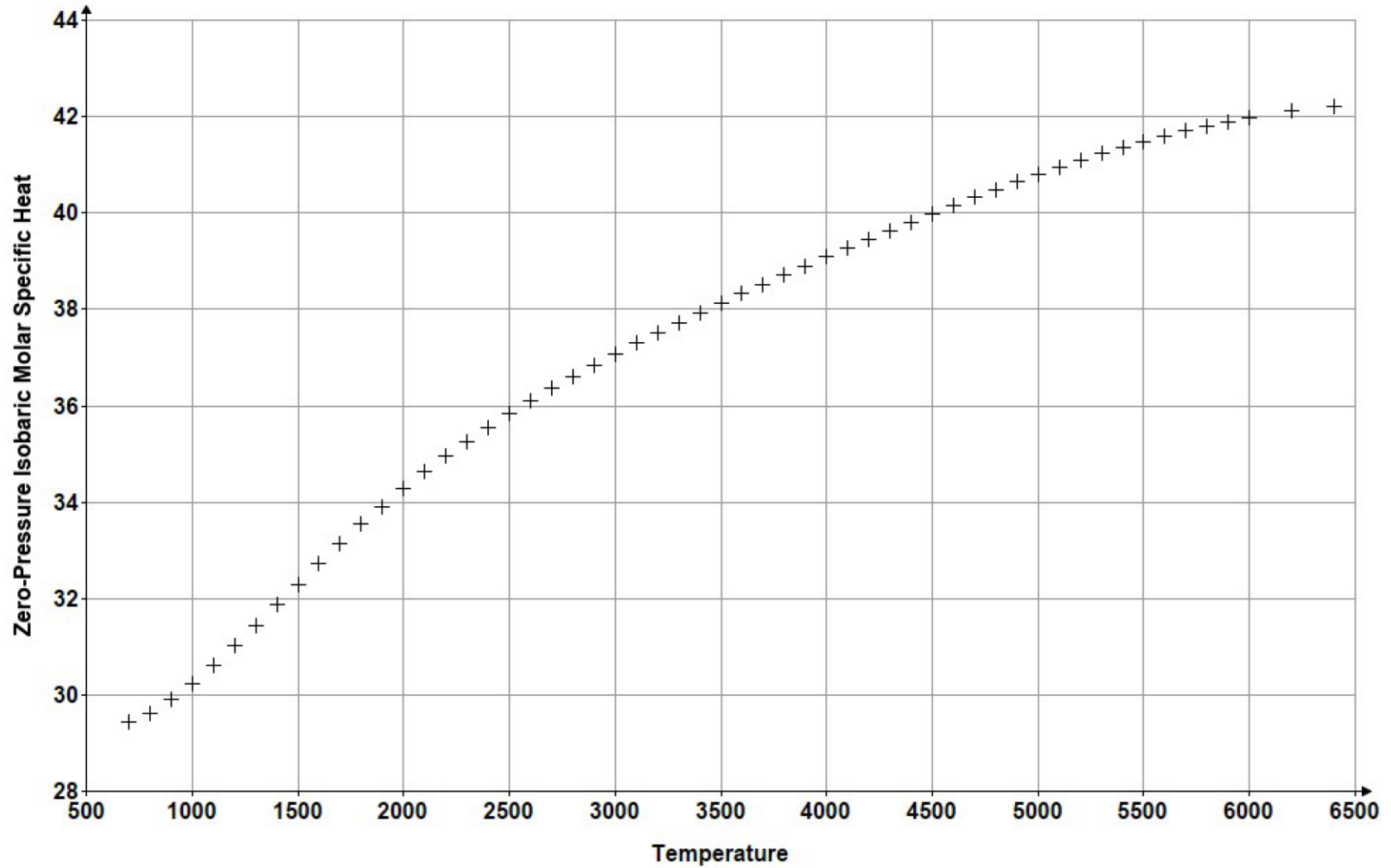
The same mathematical model will leverage H0 and S0\_1bar data from Gurvich et al. (1989) to determine fit constants. Thus, the desired H0 and S0\_1bar models with a 0 K reference state will just fall out of the process. These models should generally match Gurvich et al. (1989) values within 5 significant figures and produce the same differences as REFPROP between 700 K and 1000 K.

Trim down the vectors from Gurvich et al. (1989) to include only the 1500 K <= T <= 6400 K range to be used in fitting:

$$T\_H2\_Grvch := \text{submatrix}(T\_H2\_Grvch, 15, 62, 0, 0) \quad T\_H2\_Grvch_0 = 1500 \quad T\_H2\_Grvch_{\text{last}(T\_H2\_Grvch)} = 6400$$

$$Cp0\_H2\_Grvch := \text{submatrix}(Cp0\_H2\_Grvch, 15, 62, 0, 0) \quad H0\_H2\_Grvch := \text{submatrix}(H0\_H2\_Grvch, 15, 62, 0, 0)$$

$$S0\_1bar\_H2\_Grvch := \text{submatrix}(S0\_1bar\_H2\_Grvch, 15, 62, 0, 0)$$



The desired Cp0 dataset appears correct, so proceed with creation of the models for temperatures above 1000 K.

Revision: Baseline/Revision Level	Document Number: SNP-DOC-0046
Effective Date: 07/01/2024	Page: 71 of 149
Title: Parahydrogen Thermophysical Properties V05 Final Report	

## Mathematical Model for Zero-Pressure Properties

The model form to be applied at/above 700 K is based on the models used to represent the same properties in the computer program Chemical Equilibrium with Applications (CEA). The present model extends that model by adding both negative and positive power of temperature terms as needed for the present needs. Many of the relations below do not fit within the page width when presented in Mathcad functional form, so abbreviated non-working forms are presented here with the working forms hidden off-page.

The Cp0 model is:

$$Cp0\_H2 = am6 \cdot T^{-6} + am5 \cdot T^{-5} + am4 \cdot T^{-4} + am3 \cdot T^{-3} + am2 \cdot T^{-2} + am1 \cdot T^{-1} + a0 + a1 \cdot T + a2 \cdot T^2 + a3 \cdot T^3 + a4 \cdot T^4 + a5 \cdot T^5 + a$$

where the pattern repeats off-page up to a ninth power term  $a9 \cdot T^9$

Define the derivative of Cp0 with respect to T, as this derivative is needed to match REFPROP results at 700 K and to ascertain whether the new Cp0 model over-fits the supporting data - does it exhibit waviness between the supporting data points.

$$dCp0dT\_H2 = -6 \cdot am6 \cdot T^{-7} + -5 \cdot am5 \cdot T^{-6} + -4 \cdot am4 \cdot T^{-5} + -3 \cdot am3 \cdot T^{-4} + -2 \cdot am2 \cdot T^{-3} + -am1 \cdot T^{-2} + a1 + 2 \cdot a2 \cdot T + 3 \cdot a3 \cdot T$$

where the off-page terms are  $3 \cdot a3 \cdot T^2 + 4 \cdot a4 \cdot T^3 + 5 \cdot a5 \cdot T^4 + 6 \cdot a6 \cdot T^5 + 7 \cdot a7 \cdot T^6 + 8 \cdot a8 \cdot T^7 + 9 \cdot a9 \cdot T^8$

Integration of the Cp0 model with respect to T yields the H0 model:

$$H0\_H2 = -\frac{am6}{5} \cdot T^{-5} + -\frac{am5}{4} \cdot T^{-4} + -\frac{am4}{3} \cdot T^{-3} + -\frac{am3}{2} \cdot T^{-2} + -am2 \cdot T^{-1} + am1 \cdot \ln(T) + a0 \cdot T + \frac{a1}{2} \cdot T^2 + \frac{a2}{3} \cdot T^3 + \frac{a3}{4} \cdot T^4$$

where the off-page terms are  $\frac{a3}{4} \cdot T^4 + \frac{a4}{5} \cdot T^5 + \frac{a5}{6} \cdot T^6 + \frac{a6}{7} \cdot T^7 + \frac{a7}{8} \cdot T^8 + \frac{a8}{9} \cdot T^9 + \frac{a9}{10} \cdot T^{10} + b1$

b1 is the resulting integration constant.

Revision: Baseline/Revision Level	Document Number: SNP-DOC-0046
Effective Date: 07/01/2024	Page: 72 of 149
Title: Parahydrogen Thermophysical Properties V05 Final Report	

Integration of the Cp0 model divided by T with respect to T yields the S0 at 1 bar model:

$$S0_{1bar\_H2} = -\frac{am6}{6} \cdot T^{-6} + -\frac{am5}{5} \cdot T^{-5} + -\frac{am4}{4} \cdot T^{-4} + -\frac{am3}{3} \cdot T^{-3} + -\frac{am2}{2} \cdot T^{-2} + -am1 \cdot T^{-1} + a0 \cdot \ln(T) + a1 \cdot T + \frac{a2}{2} \cdot T^2 + \frac{a3}{3} \cdot T^3$$

where the off-page terms are  $\frac{a2}{2} \cdot T^2 + \frac{a3}{3} \cdot T^3 + \frac{a4}{4} \cdot T^4 + \frac{a5}{5} \cdot T^5 + \frac{a6}{6} \cdot T^6 + \frac{a7}{7} \cdot T^7 + \frac{a8}{8} \cdot T^8 + \frac{a9}{9} \cdot T^9 + b2$

b2 is the resulting integration constant.

Define normalized solution constraints for Cp0, H0, and S0\_1bar to be applied in the range of Gurvich supporting data.

$$Cp0\_H2\_resid = \frac{Cp0\_H2(T\_H2\_Grvch, am6, am5, am4, am3, am2, am1, a0, a1, a2, a3, a4, a5, a6, a7, a8, a9)}{Cp0\_H2\_Grvch} - 1$$

$$H0\_H2\_resid = \frac{H0\_H2(T\_H2\_Grvch, am6, am5, am4, am3, am2, am1, a0, a1, a2, a3, a4, a5, a6, a7, a8, a9, b1)}{H0\_H2\_Grvch} - 1$$

$$S0_{1bar\_H2\_resid} = \frac{S0_{1bar\_H2}(T\_H2\_Grvch, am6, am5, am4, am3, am2, am1, a0, a1, a2, a3, a4, a5, a6, a7, a8, a9, b2)}{S0_{1bar\_H2\_Grvch}} - 1$$

noting here, again, that the above relations are abbreviated to fit the page and not working Mathcad relations.

Revision: Baseline/Revision Level	Document Number: SNP-DOC-0046
Effective Date: 07/01/2024	Page: 73 of 149
Title: Parahydrogen Thermophysical Properties V05 Final Report	

A trial solution of this non-linear system already revealed that the 100 K spacing in the REFPROP data region is not adequate, so define Cp0 values from REFPROP at 50 K intervals.

$T_{H2\_RP}$	$Cp0_{H2\_RP}$
750	29.52222495
800	29.62663377
850	29.75103311
900	29.89401851
950	30.05363053
1000	30.22762777

Define the normalized residual to be minimized for the REFPROP data region.

$$Cp0_{H2\_RP\_resid} = \frac{Cp0_{H2}(T_{H2\_RP}, am6, am5, am4, am3, am2, am1, a0, a1, a2, a3, a4, a5, a6, a7, a8, a9)}{Cp0_{H2\_RP}} - 1$$

Recapitulate the bridging region temperature and Cp0 vectors and define their associated normalized residual.

$$T_{bridge} = \begin{bmatrix} 1100 \\ 1200 \\ 1300 \\ 1400 \end{bmatrix} \quad Cp0_{H2\_bridge} = \begin{bmatrix} 30.606498930072100 \\ 31.011470940730000 \\ 31.432689791841300 \\ 31.862909762066500 \end{bmatrix}$$

$$Cp0\_bridge\_resid = \frac{Cp0\_H2(T\_bridge, am6, am5, am4, am3, am2, am1, a0, a1, a2, a3, a4, a5, a6, a7, a8, a9)}{Cp0\_H2\_bridge} - 1$$

Solve the resulting system to find best fit constants.

Guess Values	<i>am6</i>	10000000000	Initial guess at constants. The solver does not engage <i>am6</i> through <i>am4</i> when their initial guess is 0, so supply guess values that force the solver to perturb these as well.
	<i>am5</i>	10000000000	
	<i>am4</i>	10000000000	
	<i>am3</i>	0	
	<i>am2</i>	0	
	<i>am1</i>	0	
	<i>a0</i>	0	
	<i>a1</i>	0	
	<i>a2</i>	0	
	<i>a3</i>	0	
	<i>a4</i>	0	
	<i>a5</i>	0	
	<i>a6</i>	0	
	<i>a7</i>	0	
	<i>a8</i>	0	
	<i>a9</i>	0	
<i>b1</i>	0		
<i>b2</i>	0		

Match point and slope to their REFPROP values at 700 K. Weight to match point to at least 5 significant figures, but slope is far less important.

$$\left( \frac{Cp0\_H2(700, am6, am5, am4, am3, am2, am1, a0, a1, a2, a3, a4, a5, a6, a7, a8, a9)}{Cp0\_H2\_RP\_700K} - 1 \right) \cdot 50 = 0$$

$$\left( \frac{dCp0dT\_H2(700, am6, am5, am4, am3, am2, am1, a1, a2, a3, a4, a5, a6, a7, a8, a9)}{dCp0dT\_H2\_RP\_700K} - 1 \right) \cdot 0.01 = 0$$

Match REFPROP points up to 1000 K to at least 5 significant figures.

$$Cp0\_H2\_RP\_resid(am6, am5, am4, am3, am2, am1, a0, a1, a2, a3, a4, a5, a6, a7, a8, a9) \cdot 47 = 0$$

Match points between 1000 K and 1500 K, but leave weighting factor alone as these don't have to be so close.

$$Cp0\_bridge\_resid(am6, am5, am4, am3, am2, am1, a0, a1, a2, a3, a4, a5, a6, a7, a8, a9) \cdot 1 = 0$$

Match Cp0 values from Gurvich et al. (1989) and leverage values for H0 and S0\_1bar to help guide the model in the region at/above 1500 K.

$$Cp0\_H2\_resid(am6, am5, am4, am3, am2, am1, a0, a1, a2, a3, a4, a5, a6, a7, a8, a9) \cdot 3 = 0$$

$$H0\_H2\_resid(am6, am5, am4, am3, am2, am1, a0, a1, a2, a3, a4, a5, a6, a7, a8, a9, b1) \cdot 1 = 0$$

$$S0\_1bar\_H2\_resid(am6, am5, am4, am3, am2, am1, a0, a1, a2, a3, a4, a5, a6, a7, a8, a9, b2) \cdot 1 = 0$$

Solver

$$\begin{bmatrix} am6 \\ am5 \\ am4 \\ am3 \\ am2 \\ am1 \\ a0 \\ a1 \\ a2 \\ a3 \\ a4 \\ a5 \\ a6 \\ a7 \\ a8 \\ a9 \\ b1 \\ b2 \end{bmatrix} := \text{minerr} (am6, am5, am4, am3, am2, am1, a0, a1, a2, a3, a4, a5, a6, a7, a8, a9, b1, b2)$$

Revision: Baseline/Revision Level	Document Number: SNP-DOC-0046
Effective Date: 07/01/2024	Page: 77 of 149
Title: Parahydrogen Thermophysical Properties V05 Final Report	

List the resulting fit constants.

$$\begin{bmatrix} am6 \\ am5 \\ am4 \\ am3 \\ am2 \\ am1 \\ a0 \\ a1 \\ a2 \\ a3 \\ a4 \\ a5 \\ a6 \\ a7 \\ a8 \\ a9 \\ b1 \\ b2 \end{bmatrix} = \begin{bmatrix} 3.098724099059950 \cdot 10^{18} \\ 1.766811303039880 \cdot 10^{16} \\ -2.719981238965310 \cdot 10^{14} \\ 1.166011154687590 \cdot 10^{12} \\ -2.706133966564940 \cdot 10^9 \\ 3.983548759821220 \cdot 10^6 \\ -3.950508326558500 \cdot 10^3 \\ 2.786818187327030 \\ -1.390134045001550 \cdot 10^{-3} \\ 5.008283136105820 \cdot 10^{-7} \\ -1.303004558960640 \cdot 10^{-10} \\ 2.419797018983610 \cdot 10^{-14} \\ -3.120833614748410 \cdot 10^{-18} \\ 2.650442609803220 \cdot 10^{-22} \\ -1.330924056482820 \cdot 10^{-26} \\ 2.990871164837520 \cdot 10^{-31} \\ -2.677928803615390 \cdot 10^7 \\ 2.818007870817000 \cdot 10^4 \end{bmatrix}$$

Create single vectors for temperature, Cp0, H0, and S0\_1bar spanning the range 700 K to 6000 K, so the model results can be compared to its supporting data. Both supporting data and model results will be rounded to the desired level of accuracy, and the differences in these rounded values output so that one may readily visually tell when the results agree, slightly disagree, or disagree by, possibly, unacceptable amounts.

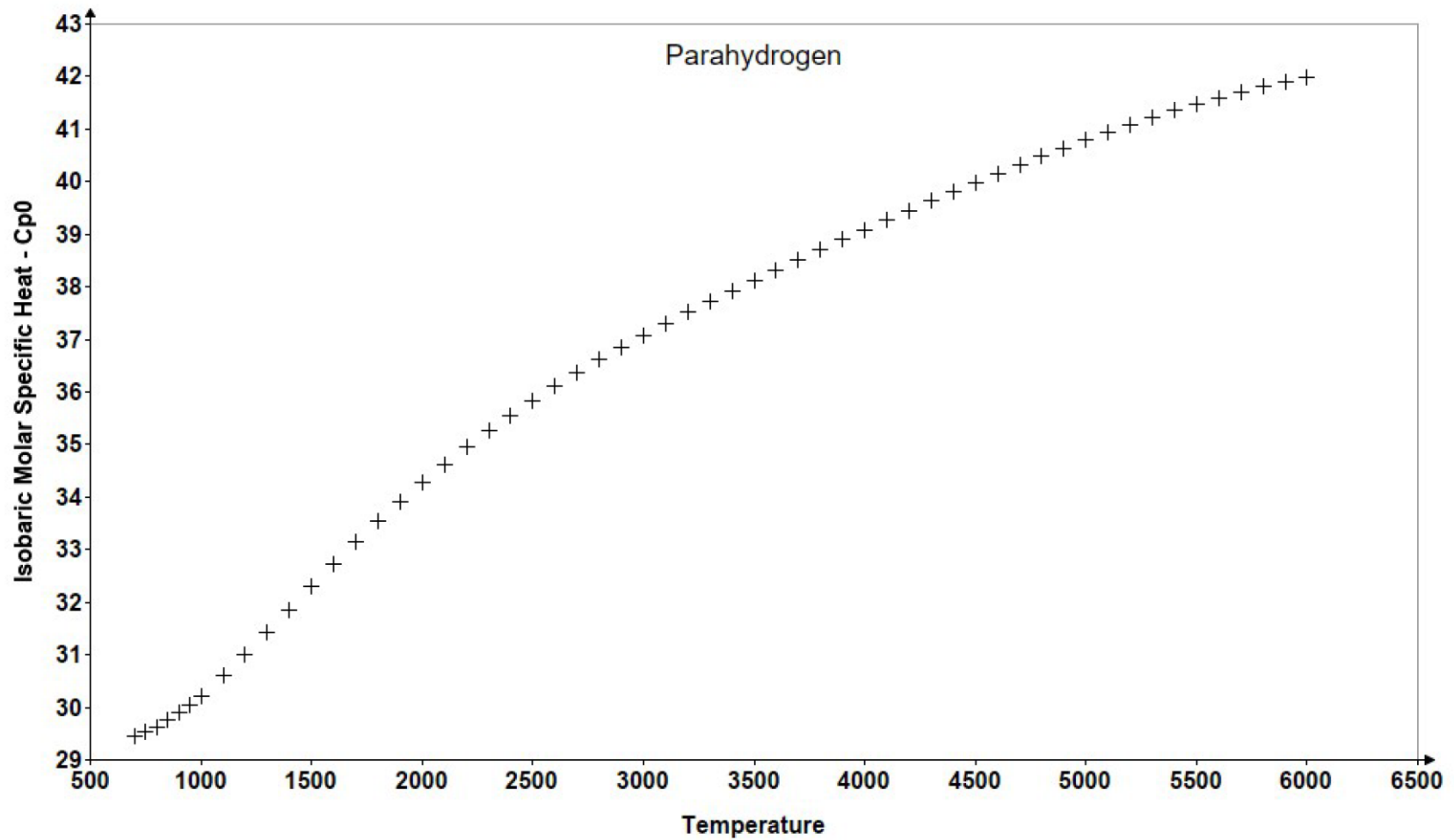
$T\_H2\_chck\_Cp0 := stack(700, T\_H2\_RP, T\_bridge, submatrix(T\_H2\_Grvch, 0, 45, 0, 0))$

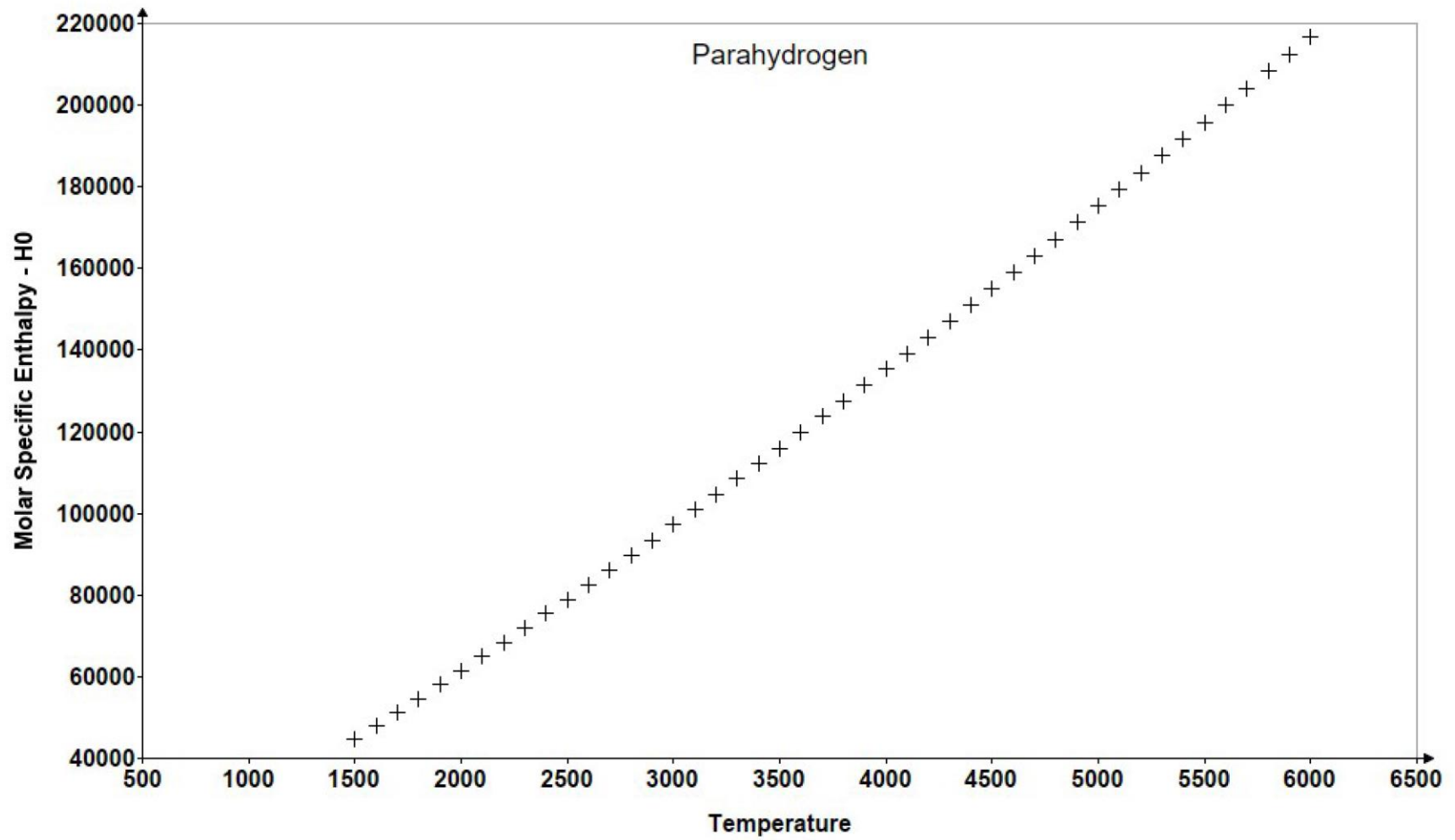
$Cp0\_H2\_chck := stack(Cp0\_H2\_RP\_700K, Cp0\_H2\_RP, Cp0\_H2\_bridge, submatrix(Cp0\_H2\_Grvch, 0, 45, 0, 0))$

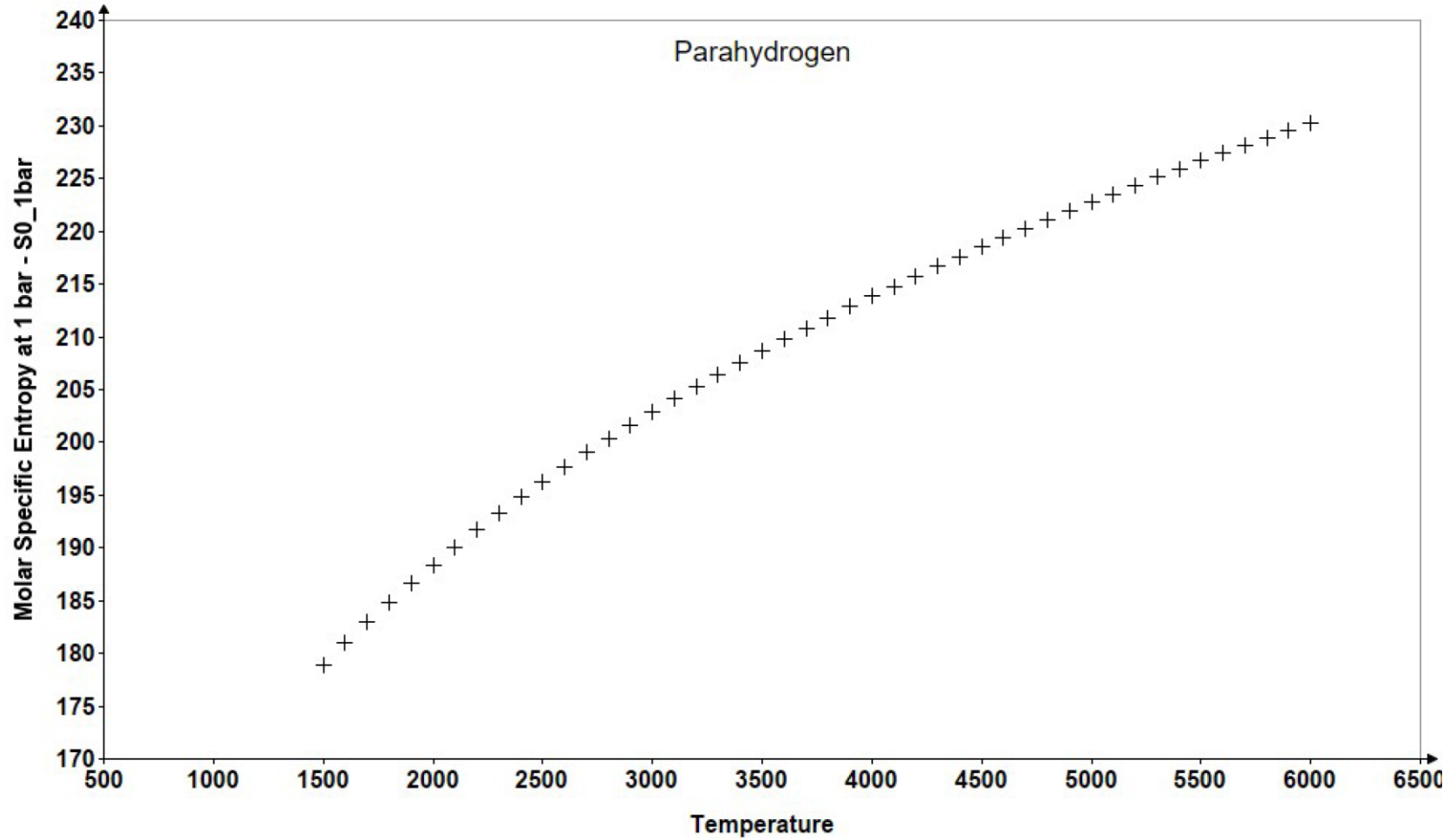
$T\_H2\_chck\_H0S0 := submatrix(T\_H2\_Grvch, 0, 45, 0, 0)$

$H0\_H2\_chck := submatrix(H0\_H2\_Grvch, 0, 45, 0, 0)$        $S0\_1bar\_H2\_chck := submatrix(S0\_1bar\_H2\_Grvch, 0, 45, 0, 0)$

Plot these check data vectors to help ensure they are correct.







All of the supporting data vectors appear to have been properly defined.

Revision: Baseline/Revision Level	Document Number: SNP-DOC-0046
Effective Date: 07/01/2024	Page: 81 of 149
Title: Parahydrogen Thermophysical Properties V05 Final Report	

Create the rounded vectors whose difference will provide a quick check on model accuracy.

$$Cp0\_H2\_mdl\_rnd := \overline{\text{round}(Cp0\_H2(T\_H2\_chck\_Cp0, am6, am5, am4, am3, am2, am1, a0, a1, a2, a3, a4, a5, a6, a7, a8, a9), 3)}$$

$$Cp0\_H2\_data\_rnd := \overline{\text{round}(Cp0\_H2\_chck, 3)} \quad Cp0\_H2\_diff := Cp0\_H2\_mdl\_rnd - Cp0\_H2\_data\_rnd$$

$$H0\_H2\_mdl\_rnd := \overline{\text{round}(H0\_H2(T\_H2\_chck\_H0S0, am6, am5, am4, am3, am2, am1, a0, a1, a2, a3, a4, a5, a6, a7, a8, a9, b1), 0)}$$

$$H0\_H2\_data\_rnd := \overline{\text{round}(H0\_H2\_chck, 0)} \quad H0\_H2\_diff := H0\_H2\_mdl\_rnd - H0\_H2\_data\_rnd$$

$$S0\_1bar\_H2\_mdl\_rnd := \overline{\text{round}(S0\_1bar\_H2(T\_H2\_chck\_H0S0, am6, am5, am4, am3, am2, am1, a0, a1, a2, a3, a4, a5, a6, a7, a8, a9, b2), 3)}$$

$$S0\_1bar\_H2\_data\_rnd := \overline{\text{round}(S0\_1bar\_H2\_chck, 3)} \quad S0\_1bar\_H2\_diff := S0\_1bar\_H2\_mdl\_rnd - S0\_1bar\_H2\_data\_rnd$$

	700	0		
	750	0		
	800	0		
	850	0		
	900	0		
	950	0		
	1000	0		
	1100	0		
	1200	0.003		
	1300	0.005		
	1400	0.006		
	1500	0.003		
	1600	-0.001	0	0
	1700	-0.002	0	0
	1800	-0.001	0	0
	1900	-0.001	0	0
	2000	0	0	0
	2100	0	-1	0
	2200	0.001	-1	0
	2300	0.001	0	0
	2400	0.001	1	0
	2500	0	1	0
	2600	0	2	0
	2700	-0.001	1	0
	2800	-0.001	-1	0
	2900	0	-1	0
	3000	0	-1	-0.001
	3100	0	0	0
$T_{H2\_chck\_Cp0} =$	3200	0	-1	0
	3300	0	1	0
$Cp0\_H2\_diff =$				

3400	0		1	0
3500	0		1	0
3600	0		-1	0
3700	0		1	0
3800	0	$H0\_H2\_diff =$	-1	0
3900	0		-1	0
4000	0		0	0
4100	0		2	0
4200	0		-1	0
4300	0		2	0
4400	0		1	0
4500	0		2	0
4600	0		-1	0
4700	0		-2	0
4800	0		-1	0
4900	0		2	0
5000	0		-2	0
5100	0		0	0
5200	0.001		1	0
5300	0		3	0
5400	0		2	0
5500	0		-2	0
5600	0		1	0
5700	0		0	0
5800	0		-5	0
5900	0		-3	0
6000	0		-1	0
			3	0

These results appear excellent. Errors in Cp0 are clustered near the bridging region and all are less than 0.003 outside of the bridging region. Errors in H0 are all less than 5 in the sixth significant figure and only 1 S0\_1bar value fails to match.

Revision: Baseline/Revision Level	Document Number: SNP-DOC-0046
Effective Date: 07/01/2024	Page: 84 of 149
Title: Parahydrogen Thermophysical Properties V05 Final Report	

The last validation item is to check to see how well the H0 and S0\_1bar models reproduce local differences in these values in the region at/below 1000 K where no H0 or S0\_1bar supporting data from REFPROP was used to guide the fit. Given the excellent match in Cp0 in this temperature range, difference in H0 and S0\_1bar should also match REFPROP differences.

First off, confirm that model results for the local derivative of Cp0\_H2 with respect to T at 600 K agree with those from Leachman et al. (2009)/REFPROP.

$$\left( \frac{dCp0dT\_H2(700, am6, am5, am4, am3, am2, am1, a1, a2, a3, a4, a5, a6, a7, a8, a9)}{dCp0dT\_H2\_RP\_700K} - 1 \right) = -0.023$$

This represents a normalized error of 2.3% - not as good as what is demanded from Cp0, H0, or S0\_1bar but this derivative is just a qualitative measure of how well the model matches REFPROP at 700 K so this value seems fine.

The difference checks for H0 and S0\_1bar will be made on the basis of REFPROP output values corresponding to temperature values from T\_H2\_RP\_chk defined just below.

$$T\_H2\_RP\_chk := \begin{bmatrix} 700 \\ 800 \\ 900 \\ 1000 \end{bmatrix} \quad H0\_H2\_RP\_chk := \begin{bmatrix} 2.07317395495550 \cdot 10^4 \\ 2.36843047321679 \cdot 10^4 \\ 2.66597181156566 \cdot 10^4 \\ 2.96653209596519 \cdot 10^4 \end{bmatrix} \quad S0\_1bar\_RP\_chk := \begin{bmatrix} 1.39504554816422 \cdot 10^2 \\ 1.43446877064317 \cdot 10^2 \\ 1.46951100296602 \cdot 10^2 \\ 1.50117510299018 \cdot 10^2 \end{bmatrix}$$

Note that correct values for S0 in REFPROP cannot be obtained by simply specifying T and P, since REFPROP actually calculates on the basis of density and temperature and the density REFPROP feeds the problem is a real gas density. This interface error in REFPROP can be overcome by calculating a D0 as P/T/R\_REFPROP and executing a D,T call using this D0 for density.

Revision: Baseline/Revision Level	Document Number: SNP-DOC-0046
Effective Date: 07/01/2024	Page: 85 of 149
Title: Parahydrogen Thermophysical Properties V05 Final Report	

Condense the H0 and S0\_1bar functions, now that fit constants are known.

$$H0\_H2\_cnd(T) := H0\_H2(T, am6, am5, am4, am3, am2, am1, a0, a1, a2, a3, a4, a5, a6, a7, a8, a9, b1)$$

$$S0\_1bar\_H2\_cnd(T) := S0\_1bar\_H2(T, am6, am5, am4, am3, am2, am1, a0, a1, a2, a3, a4, a5, a6, a7, a8, a9, b2)$$

700 to 800

$$H0\_H2\_RP\_chk_1 - H0\_H2\_RP\_chk_0 = 2952.6$$

$$S0\_1bar\_RP\_chk_1 - S0\_1bar\_RP\_chk_0 = 3.9423$$

$$H0\_H2\_cnd(800) - H0\_H2\_cnd(700) = 2952.6$$

$$S0\_1bar\_H2\_cnd(800) - S0\_1bar\_H2\_cnd(700) = 3.9423$$

800 to 900

$$H0\_H2\_RP\_chk_2 - H0\_H2\_RP\_chk_1 = 2975.4$$

$$S0\_1bar\_RP\_chk_2 - S0\_1bar\_RP\_chk_1 = 3.5042$$

$$H0\_H2\_cnd(900) - H0\_H2\_cnd(800) = 2975.4$$

$$S0\_1bar\_H2\_cnd(900) - S0\_1bar\_H2\_cnd(800) = 3.5042$$

900 to 1000

$$H0\_H2\_RP\_chk_3 - H0\_H2\_RP\_chk_2 = 3005.6$$

$$S0\_1bar\_RP\_chk_3 - S0\_1bar\_RP\_chk_2 = 3.1664$$

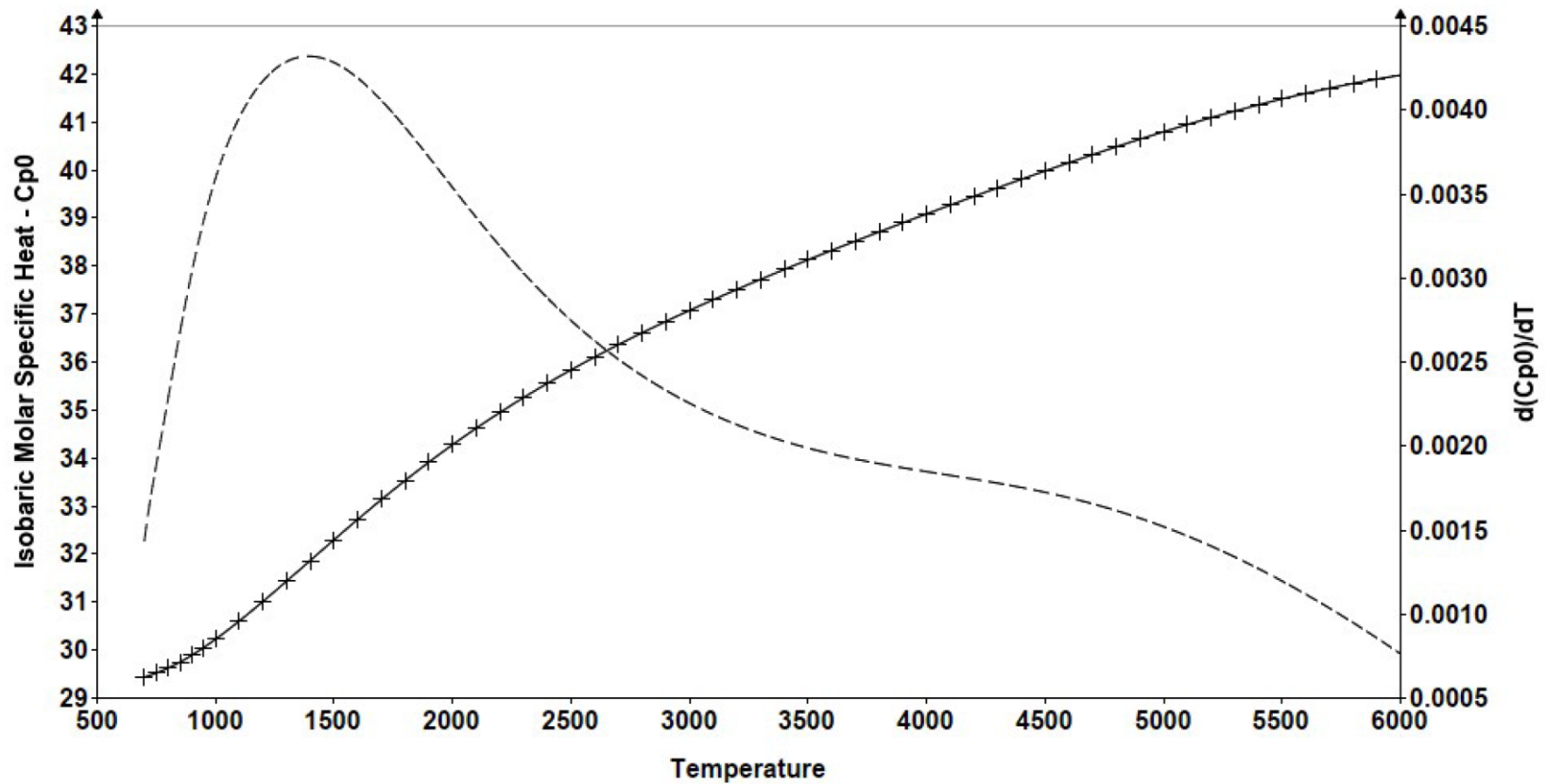
$$H0\_H2\_cnd(1000) - H0\_H2\_cnd(900) = 3005.6$$

$$S0\_1bar\_H2\_cnd(1000) - S0\_1bar\_H2\_cnd(900) = 3.1664$$

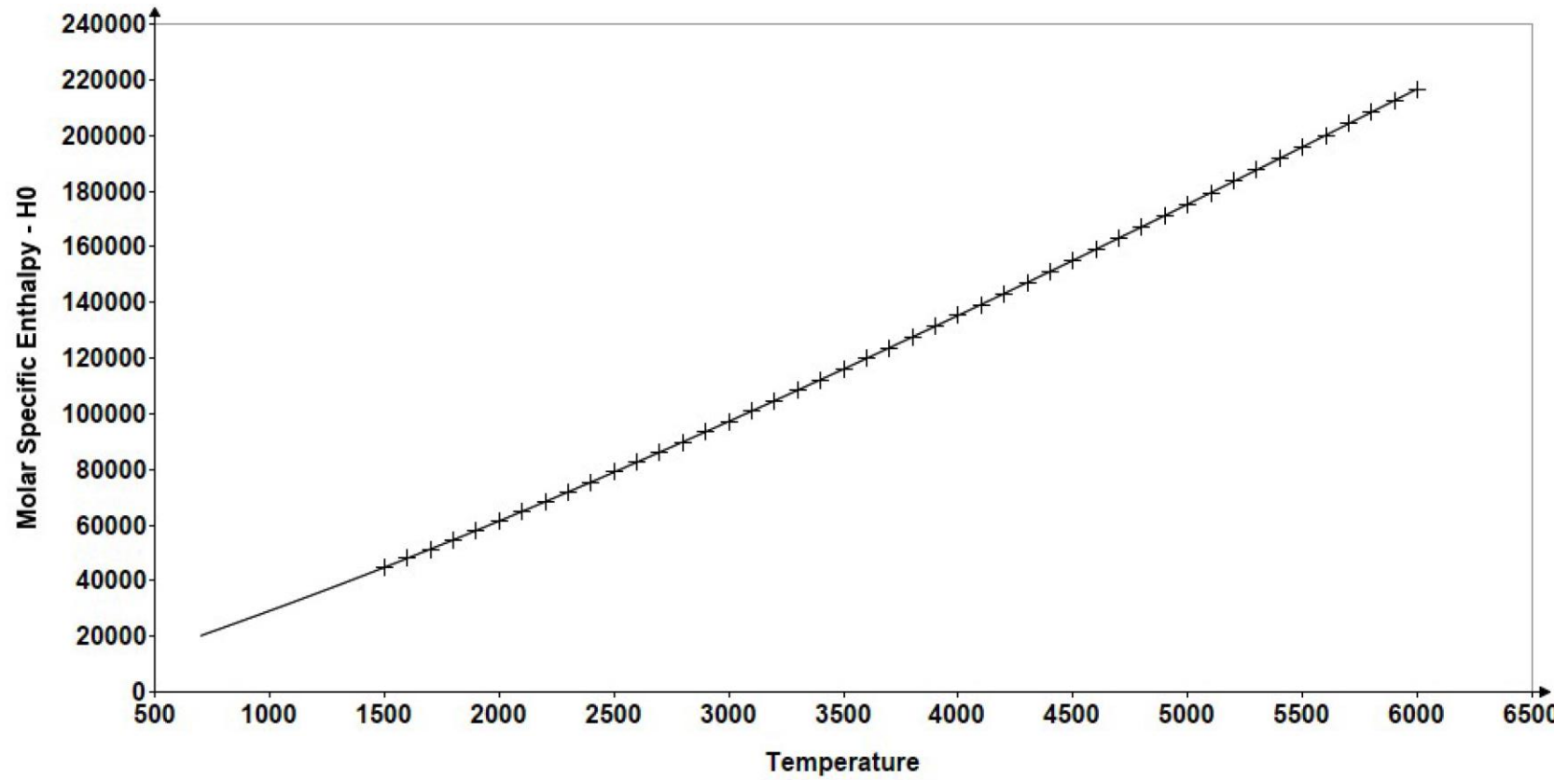
All of these differences are the same to at least 5 significant figures.

Plot the parahydrogen models for Cp0, H0, and S0\_1bar along with their supporting data. Also plot the derivative of the Cp0 model with respect to temperature to discern if it might be over-fitting the supporting dataset. First create a dense temperature vector for plotting purposes.

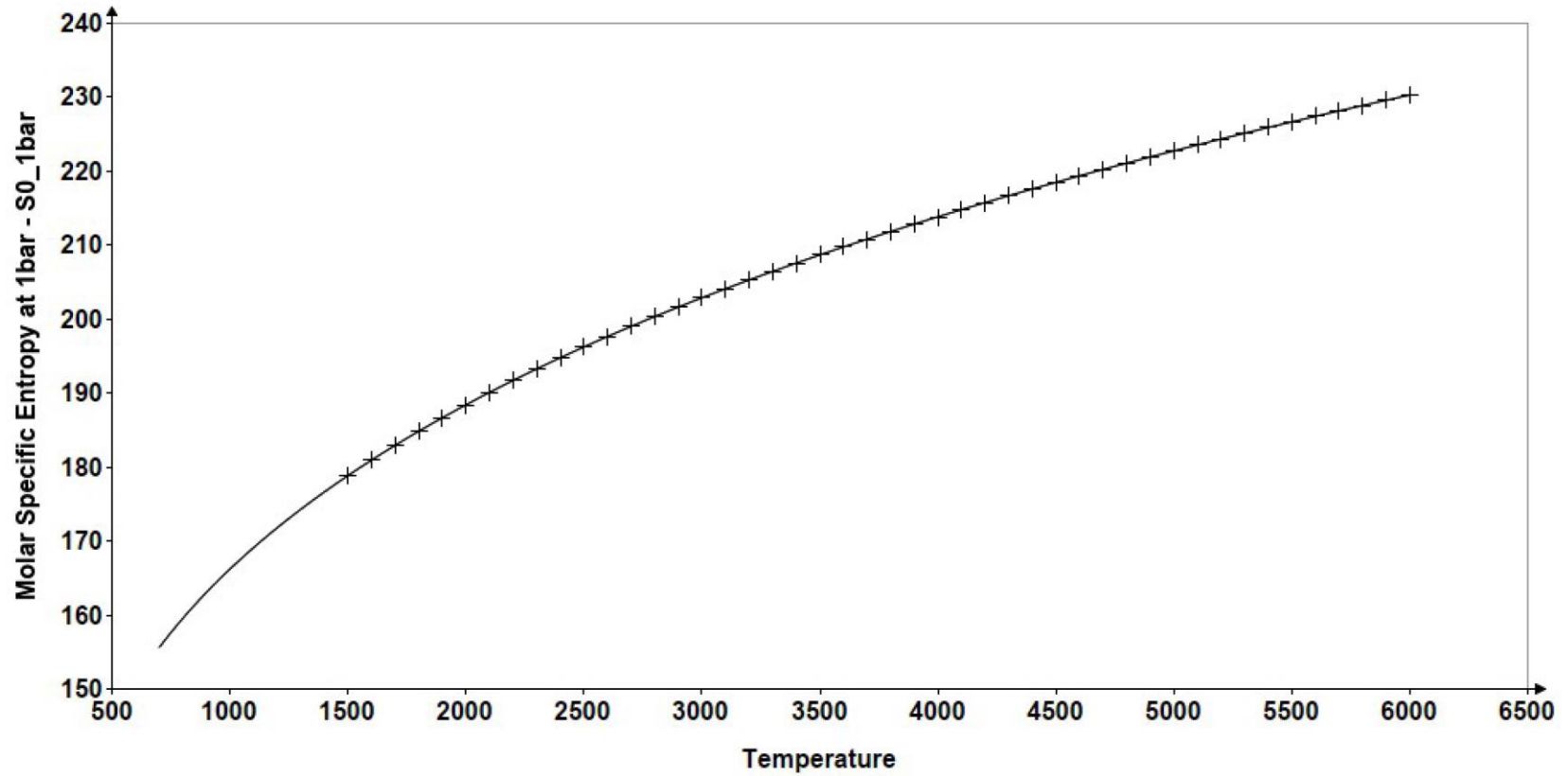
$$npoints := 1000000 \quad i\_plot := 0 .. npoints \quad T\_plot_{i\_plot} := 700 + \frac{6000 - 700}{npoints} \cdot i\_plot$$



The model results appear correct and the derivative is everywhere smooth with no apparent small-scale waviness that might indicate the model over-fitting Cp0.



The zero-pressure enthalpy model also looks to be well-behaved.



The zero-pressure entropy model also looks to be well-behaved.

### Molar Enthalpy and Entropy at 1 bar for Atomic Hydrogen

The main body of work above deals with the parahydrogen spin state of dihydrogen, but similar models are also needed for atomic hydrogen as well. The supporting data for these models is taken solely from Gurvich et al. (1989) and defined below only for the range 700 K to 6000 K of interest here.

$T_{H\_Gurvch}$	$Cp0_{H\_Gurvch} := 20.786$	$H0_{H\_Gurvch}$	$S0_{1bar\_H\_Gurvch}$
	for all temperatures in the range of interest		
700		14550	132.456
800		16629	135.232
900		18707	137.680
1000		20786	139.870
1100		22865	141.851
1200		24943	143.660
1300		27022	145.324
1400		29100	146.864
1500		31179	148.298
1600		33258	149.640
1700		35336	150.900
1800		37415	152.088
1900		39493	153.212
2000		41572	154.278
2100		43651	155.292
2200		45729	156.259
2300		47808	157.183

Revision: Baseline/Revision Level	Document Number: SNP-DOC-0046
Effective Date: 07/01/2024	Page: 90 of 149
Title: Parahydrogen Thermophysical Properties V05 Final Report	

2400	49886	158.068
2500	51965	158.916
2600	54044	159.731
2700	56122	160.516
2800	58201	161.272
2900	60279	162.001
3000	62358	162.706
3100	64437	163.388
3200	66515	164.047
3300	68594	164.687
3400	70672	165.308
3500	72751	165.910
3600	74830	166.496
3700	76908	167.065
3800	78987	167.620
3900	81065	168.159
4000	83144	168.686
4100	85223	169.199
4200	87301	169.700
4300	89380	170.189
4400	91458	170.667
4500	93537	171.134
4600	95616	171.591
4700	97694	172.028

Revision: Baseline/Revision Level	Document Number: SNP-DOC-0046
Effective Date: 07/01/2024	Page: 91 of 149
Title: Parahydrogen Thermophysical Properties V05 Final Report	

<del>4700</del>	<del>97094</del>	<del>172.058</del>
4800	99773	172.475
4900	101852	172.904
5000	103930	173.324
5100	106009	173.736
5200	108087	174.139
5300	110166	174.535
5400	112245	174.924
5500	114323	175.305
5600	116402	175.680
5700	118480	176.048
5800	120559	176.409
5900	122638	176.764
6000	124716	177.114

Creation of these models would appear to require one to only use Cp0 since it is a constant, but it is also important to retain the 0 K reference for both H0 and S0\_1bar. Thus, the present model will be created much like that for parahydrogen above. The models themselves are much simpler, though.

H0 will be a simple slope-intercept form, where the slope is Cp0 value, and the intercept must be solved for a value that best fits the supporting data above. The intercept is not 0 because Cp0 is not constant very close to 0 K.

$$H0\_H(T, H0\_H\_intercept) := Cp0\_H\_Grvch \cdot T + H0\_H\_intercept$$

Revision: Baseline/Revision Level	Document Number: SNP-DOC-0046
Effective Date: 07/01/2024	Page: 92 of 149
Title: Parahydrogen Thermophysical Properties V05 Final Report	

The  $S0\_1bar$  model has the form

$$S0\_1bar\_H(T, S0\_H\_1bar\_intercept) := Cp0\_H\_Grvch \cdot \ln(T) + S0\_H\_1bar\_intercept$$

Unlike for parahydrogen, there is no needed to simultaneously fit  $Cp0$ ,  $H0$  and  $S0\_1bar$  because  $Cp0$  is a known constant value.

Define a residual functions for fitting  $H0\_H$  and  $S0\_H\_1bar$

$$H0\_H\_resid(H0\_H\_intercept) := \frac{H0\_H(T\_H\_Grvch, H0\_H\_intercept)}{H0\_H\_Grvch} - 1$$

$$S0\_1bar\_H\_resid(S0\_H\_1bar\_intercept) := \frac{S0\_1bar\_H(T\_H\_Grvch, S0\_H\_1bar\_intercept)}{S0\_1bar\_H\_Grvch} - 1$$

Guess Values	$H0\_H\_intercept := 0$
Constraints	$H0\_H\_resid(H0\_H\_intercept) = 0$
Solver	$H0\_H\_intercept := \text{minerr}(H0\_H\_intercept)$

$$H0\_H\_intercept = -2.168049523648170 \cdot 10^{-2}$$

Guess Values

$$S0\_H\_1bar\_intercept := 0$$

Constraints

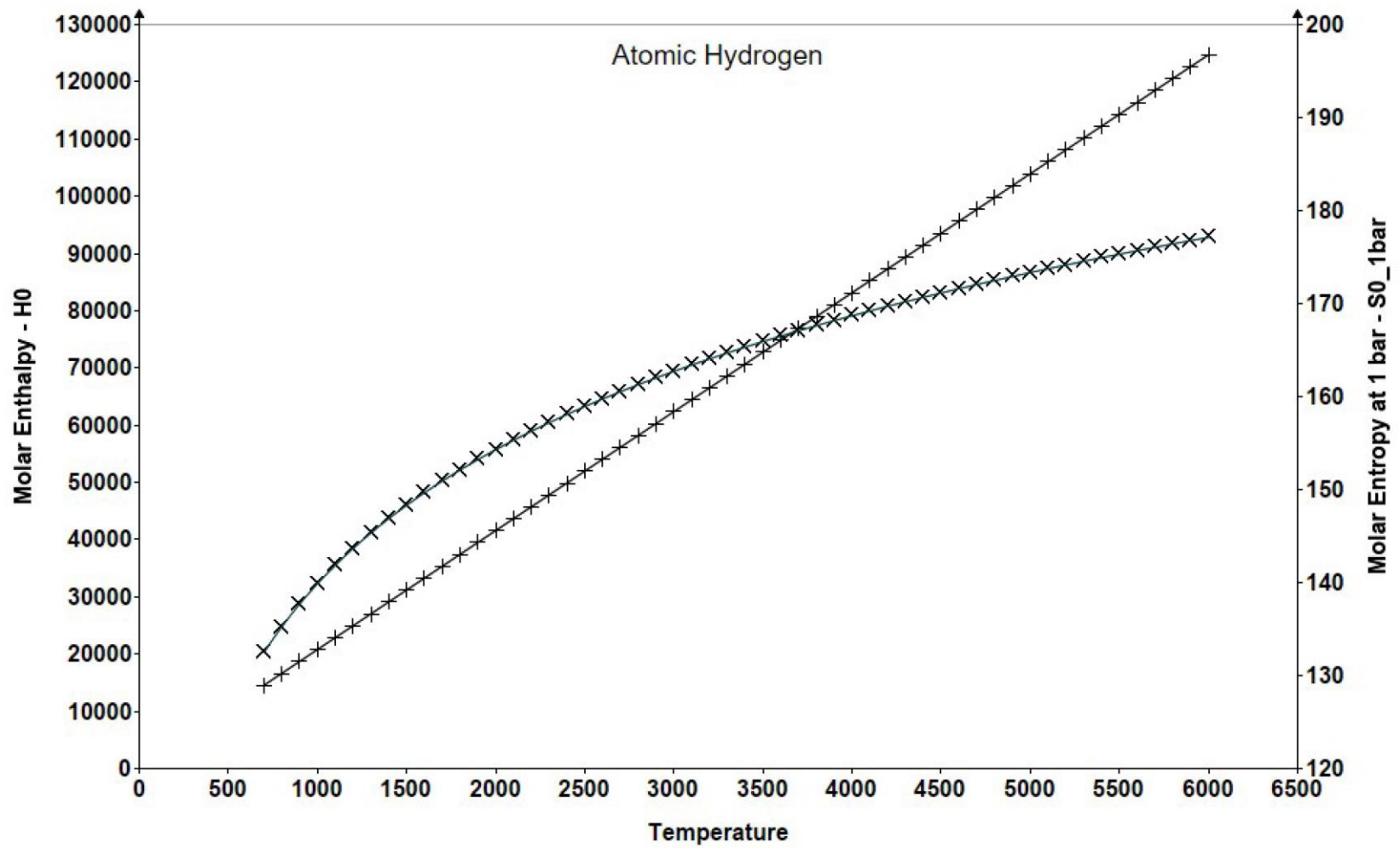
$$S0\_1bar\_H\_resid(S0\_H\_1bar\_intercept) = 0$$

Solver

$$S0\_H\_1bar\_intercept := \text{minerr}(S0\_H\_1bar\_intercept)$$

$$S0\_H\_1bar\_intercept = -3.714389051971060$$

Now, test these models by plotting them against their supporting data.



No obvious issues above.

$$H0\_H\_mdl\_rnd := \overrightarrow{\text{round}(H0\_H(T\_H\_Grvch, H0\_H\_intercept), 0)}$$

$$H0\_H\_data\_rnd := \overrightarrow{\text{round}(H0\_H\_Grvch, 0)} \quad H0\_H\_diff := H0\_H\_mdl\_rnd - H0\_H\_data\_rnd$$

$$S0\_1bar\_H\_mdl\_rnd := \overrightarrow{\text{round}(S0\_1bar\_H(T\_H\_Grvch, S0\_H\_1bar\_intercept), 3)}$$

$$S0\_1bar\_H\_data\_rnd := \overrightarrow{\text{round}(S0\_1bar\_H\_Grvch, 3)} \quad S0\_1bar\_H\_diff := S0\_1bar\_H\_mdl\_rnd - S0\_1bar\_H\_data\_rnd$$

700	0	0.000
800	0	0.000
900	0	0.000
1000	0	0.000
1100	0	0.000
1200	0	0.000
1300	0	0.000
1400	0	0.000
1500	0	0.000
1600	0	0.000
1700	0	0.000
1800	0	0.000
1900	0	0.000
2000	0	0.000
2100	0	0.000
2200	0	0.000
2300	0	0.000
2400	0	0.000
2500	0	0.000
2600	0	0.000

<i>T_H_Grvch</i> =	2700	0	0.000
	2800	0	0.000
	2900	0	0.000
	3000	0	0.000
	3100	0	0.000
	3200	0	0.000
	3300	0	0.000
	3400	0	0.000
	3500	0	0.000
	3600	0	0.000
	3700	0	0.000
	3800	0	0.000
	3900	0	0.000
	4000	0	0.000
	4100	0	0.000
	4200	0	0.000
	4300	0	0.000
	4400	0	0.000
	4500	0	0.000
	4600	0	0.000
	4700	0	0.000
	4800	0	0.000
	4900	-1	0.000
	5000	0	0.000
	5100	0	0.000
	5200	0	0.000
	5300	0	0.000
	5400	-1	0.000
	5500	0	0.000
	5600	0	0.000
	5700	0	0.000
	5800	0	0.000
	5900	-1	0.000

Revision: Baseline/Revision Level	Document Number: SNP-DOC-0046
Effective Date: 07/01/2024	Page: 97 of 149
Title: Parahydrogen Thermophysical Properties V05 Final Report	

[ 6000 ]

[ 0 ]

[ 0.000 ]

The models appear to recreate the supporting data perfectly.

One now has all that is needed to calculate the real gas database in a 0 K reference state for both enthalpy and entropy. Using this 0 K reference state, the formation enthalpy value to be used in the real gas calculations is that for a 0 K reference state:

$$216035 \cdot \frac{J}{mol}$$

Revision: Baseline/Revision Level	Document Number: SNP-DOC-0046
Effective Date: 07/01/2024	Page: 98 of 149
Title: Parahydrogen Thermophysical Properties V05 Final Report	

### Calculate Constants Needed to Shift Solution into REFPROP 10 Reference State

The last items needed are the shifts in H0 and S0\_1bar from the 0 K reference state to the REFPROP 10 Normal Boiling Point reference state. This is done by simply adding a constant shift to each of H0 and S0\_1bar that shifts the present values to exactly match the corresponding REFPROP values at 700 K. At 700 K, truly negligible H atom is present, so the shift is based on parahydrogen only. The needed REFPROP values at 700 K were already used above:

$$T_{H2\_RP\_chk}_0 = 700 \quad H0_{H2\_RP\_chk}_0 = 2.073173954955500 \cdot 10^4 \quad S0_{1bar\_RP\_chk}_0 = 1.395045548164220 \cdot 10^2$$

Values from the new parahydrogen model are:

$$H0_{H2\_cnd}(700) = 2.020459652899580 \cdot 10^4 \quad S0_{1bar\_H2\_cnd}(700) = 1.555928095446510 \cdot 10^2$$

The shift will be defined as the value that, when added to the 0 K reference state values, results in the REFPROP values.

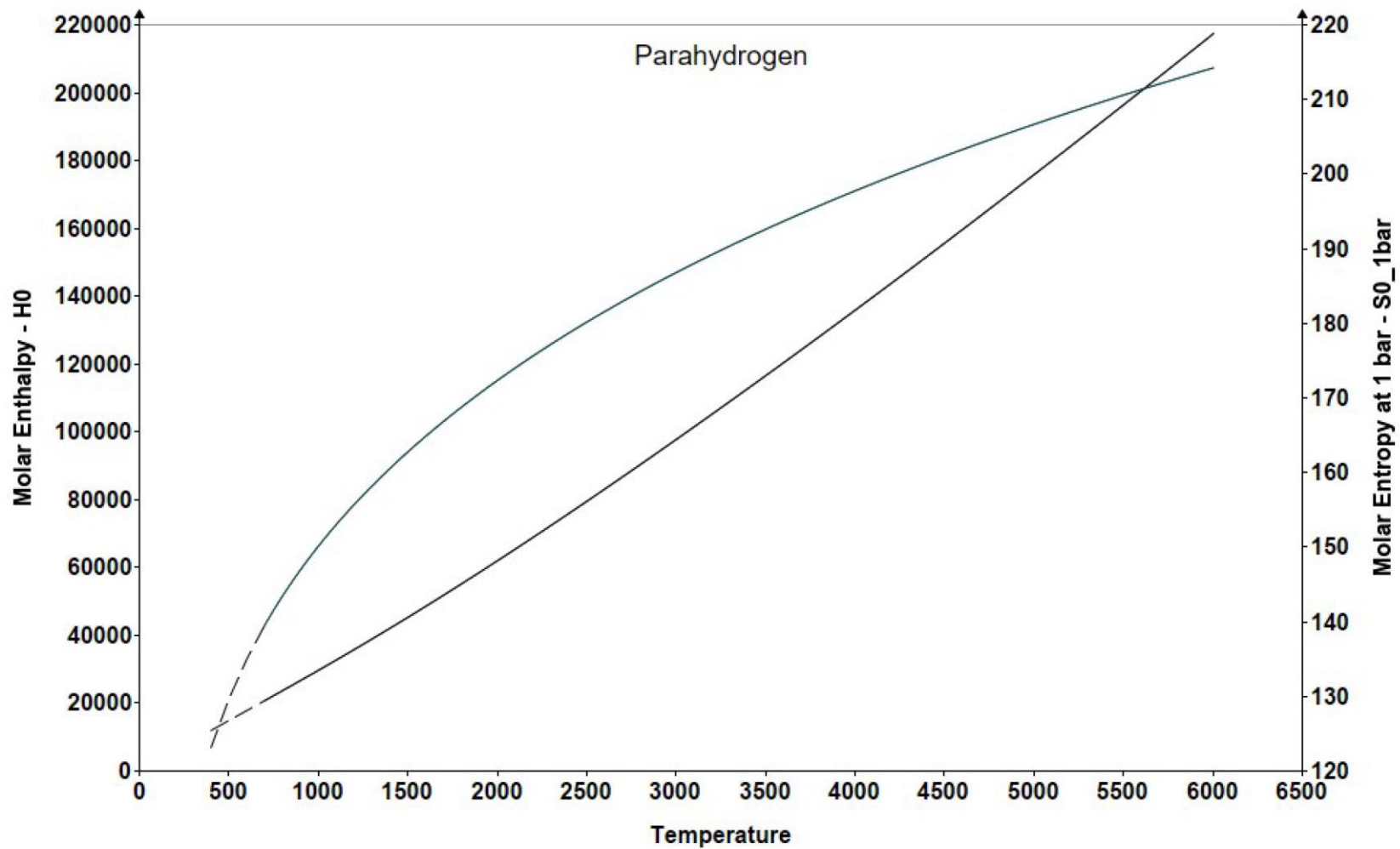
$$H0_{H2\_RP} = H0_{H2\_0K} + H0_{H2\_shift\_to\_RP} \quad S0_{1bar\_H2\_RP} = S0_{1bar\_H2\_0K} + S0_{1bar\_H2\_shift\_to\_RP}$$

$$H0_{H2\_shift\_to\_RP} := H0_{H2\_RP\_chk}_0 - H0_{H2\_cnd}(700) \quad H0_{H2\_shift\_to\_RP} = 5.271430205592190 \cdot 10^2$$

$$S0_{1bar\_H2\_shift\_to\_RP} := S0_{1bar\_RP\_chk}_0 - S0_{1bar\_H2\_cnd}(700) \quad S0_{1bar\_H2\_shift\_to\_RP} = -1.608825472822870 \cdot 10$$

As a final check that all is good with this part of the world, define some REFPROP values below 700 K and plot alongside the shifted parahydrogen models.

$$T_{H2\_RP\_low} := \begin{bmatrix} 400 \\ 500 \\ 600 \\ 700 \end{bmatrix} \quad H0_{H2\_RP\_low} := \begin{bmatrix} 11934.88934876 \\ 14863.9976951749 \\ 17794.0049556242 \\ 20731.739549555 \end{bmatrix} \quad S0_{1bar\_RP\_low} := \begin{bmatrix} 123.098024599863 \\ 129.634328155229 \\ 134.976233309719 \\ 139.504554816422 \end{bmatrix}$$



This final check appears to confirm that the shifts to the REFPROP 10 references state were handled correctly.

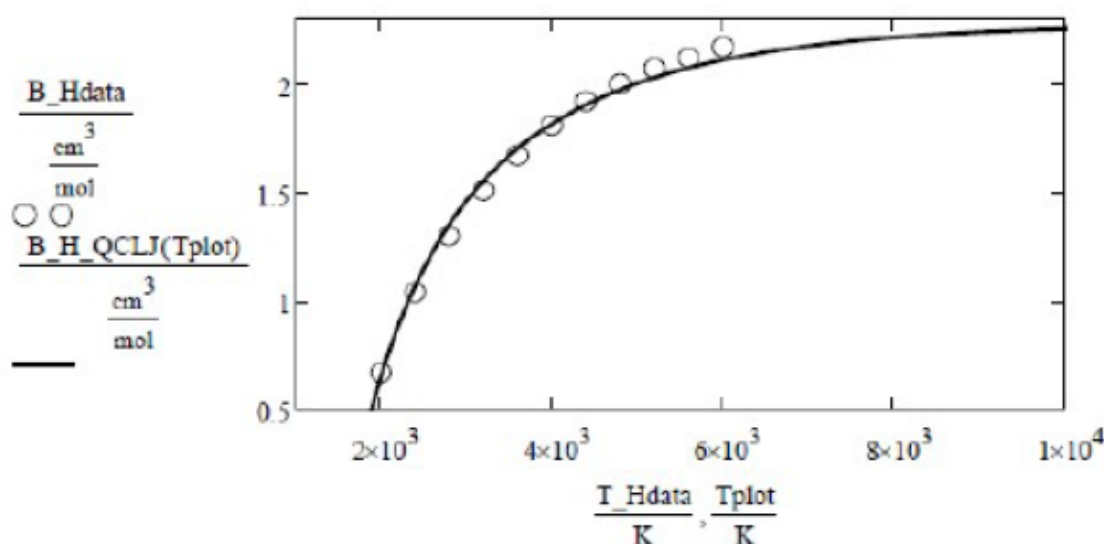
Revision: Baseline/Revision Level	Document Number: SNP-DOC-0046
Effective Date: 07/01/2024	Page: 100 of 149
Title: Parahydrogen Thermophysical Properties V05 Final Report	

## **APPENDIX C.**

### **DERIVATION OF H-ATOM TEMPERATURE-VARYING FORCE CONSTANTS**

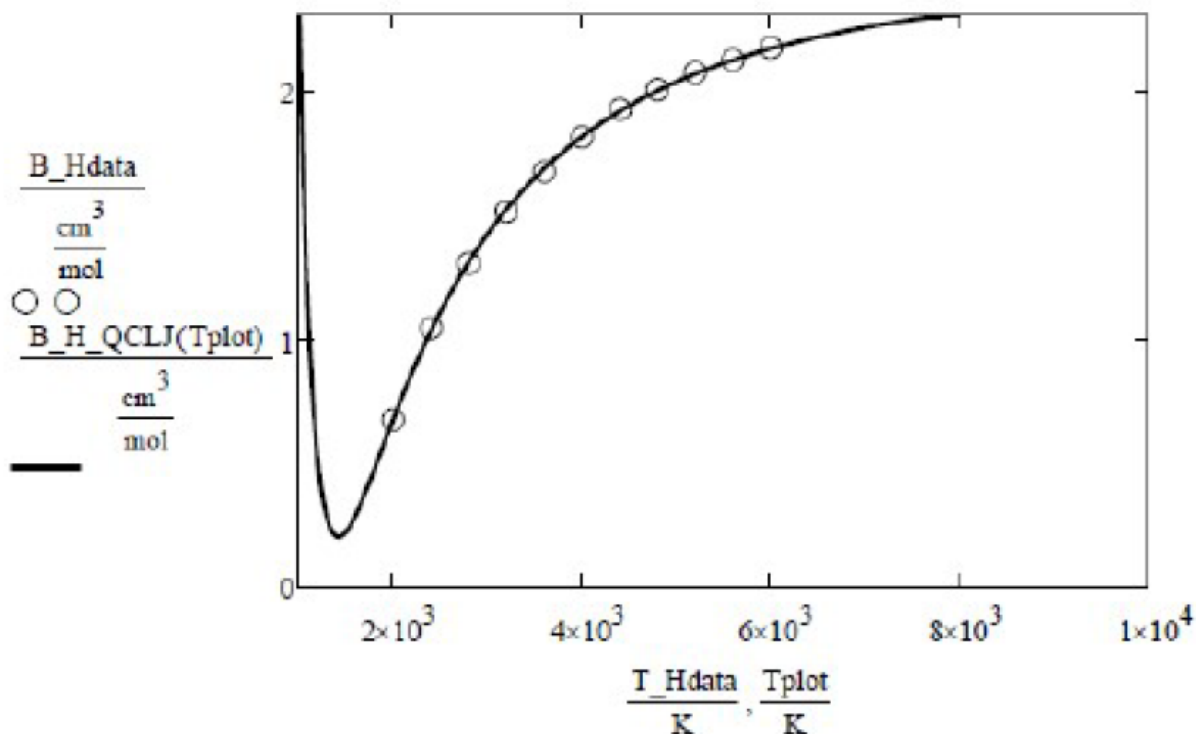
## Derivation of H-Atom Temperature-Varying Force Constants

The dissociating hydrogen property tabulations of Vargaftik et al. (1996) are based on methods related in an unavailable work by Gorykin (1968). Gorykin worked in the same research group as Kessel'man from a specific paper from Lykova (1969b) entitled "Transport Coefficient of Water Vapor and Air at  $T = 1000-6000$  K with Account of Their Thermal Dissociation". This Kessel'man work tabulates variation of the second virial coefficient for atomic hydrogen self-interaction with temperature, along with force constants that also vary with temperature such that they recreate the tabulated second virial coefficient values for atomic hydrogen when applied to a standard Lennard-Jones 6-12 collision interaction potential. Thus, it is believed that Gorykin (1968) used the atomic hydrogen methods from Lykova (1969b). The calculation scheme for estimation of the tabulated second virial coefficient values is not presented in the noted Kessel'man et alia work from Lykova (1969b), but the reader is referred to Kessel'man's doctoral dissertation for the calculation details. The Kessel'man doctoral dissertation could not be obtained via the Redstone Scientific Information Center (RSIC) at Redstone Arsenal prior to its closure, nor from any online source (2017 timeframe). Thus, the works of McDonald (2017 and 2018) proceeded on the basis of the tabulated values for the atomic hydrogen second virial coefficient from Lykova (1969b), knowledge that accurate calculation for atomic hydrogen second virial coefficient requires quantum corrections (various sources), and a presumption that the potential used in the Kessel'man dissertation was a quantum corrected Lennard-Jones 6-12 collision potential. Yet, McDonald (2017) found a quantum corrected Lennard-Jones 6-12 potential to not adequately recreate the second virial coefficient values tabulated in Lykova (1969b) - see figure immediately below.



So, the approach taken by McDonald (2017) was to use the quantum corrected Lennard-Jones 6-12 potential as the basis for curve-fitting the data from Lykova (1969b), but no longer requiring some of the underlying physics relationships to hold. The resulting method did an excellent job of representing the data - see figure immediately below - in the temperature range

of the data itself; but the curve-fit behaved in a physically non-sensical manner below roughly 1500 K in that the second virial coefficient went through a relative minimum and turned abruptly upward. This behavior was viewed to have no meaningful impact on results from McDonald (2017, 2018) because very little atomic hydrogen exists below 1500 K except for very low pressures.



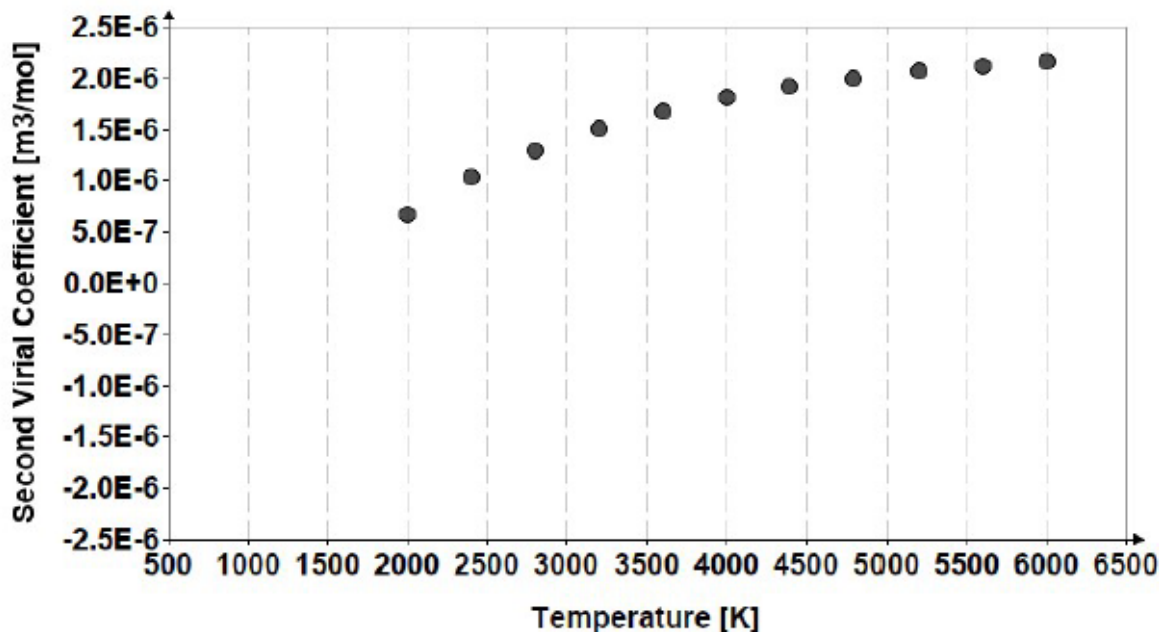
The present work intends to use the methods set forth in McDonald (2017, 2018), and originally attributable to Lykova/Kessel'man down to temperatures as low as 700 K and pressure as low as 1 Pa. Thus, a better behaved model is desired for atomic hydrogen second virial coefficient; one that both recreates 2000 K and up tabulation from Lykova (1969b) and is well-behaved down to 700 K.

### The Parent Data for Second Virial Coefficient and OMEGA22 Collision Integral

The second virial coefficient data from Lykova (1969b) is:

$$\begin{array}{l}
 \left[ \begin{array}{c} 2000 \\ 2400 \\ 2800 \\ 3200 \\ 3600 \\ 4000 \\ 4400 \\ 4800 \\ 5200 \\ 5600 \\ 6000 \end{array} \right] \cdot K \quad B\_Hdata := \left[ \begin{array}{c} 0.67 \\ 1.04 \\ 1.30 \\ 1.51 \\ 1.67 \\ 1.81 \\ 1.92 \\ 2.00 \\ 2.07 \\ 2.12 \\ 2.17 \end{array} \right] \cdot \frac{cm^3}{mol}
 \end{array}$$

The plot below depicts the above data, and leaves room in the lower left for one to visualize how the curve might extrapolate below its 2000 K lowest data pair. Within its temperature range, a cubic spline fit should enable excellent interpolation; but some means is needed by which to extrapolate below 2000 K. Since the works of McDonald (2017, 2018), translation and review of Kessel'man et al. (1966) reveals possible interaction potentials to represent atomic hydrogen - none of which are the Lennard-Jones 6-12 form. Though it is known that a quantum corrected Lennard-Jones 6-12 potential was not the basis, it might suit as a basis for extrapolation below 2000 K where the goal is to not be grossly wrong since atomic hydrogen should have a minimal impact on properties below 2000 K for most pressures. The basis for such a fit will be the model of Boyd (1971) that was also used in McDonald (2017).



Revision: Baseline/Revision Level	Document Number: SNP-DOC-0046
Effective Date: 07/01/2024	Page: 104 of 149
Title: Parahydrogen Thermophysical Properties V05 Final Report	

## Quantum Corrected Second Virial Coefficient from Boyd (1971)

The specific sub-model chosen from Boyd (1971) is that for the Lennard-Jones 6-12 potential (note that Boyd refers to the potential as the 12-6 instead of 6-12). The relations were described in some detail in Appendix C of McDonald (2017), but they are set forth here with minimal explanation.

First gather some constants/parameters that are required for the Boyd calculations.

$$\text{Avogadro's Number} \quad N_{Avogadro} := 6.022140857 \cdot 10^{23} \cdot \frac{1}{\text{mol}}$$

$$\text{Molar gas constant} \quad Ru := 8.3144598 \cdot \frac{J}{\text{mol} \cdot K}$$

$$\text{Planck constant} \quad h := 6.62607004081 \cdot 10^{-34} \cdot J \cdot s$$

Note that the above 2014 CODATA values are used on purpose, instead of the more up to date 2018 CODATA values, since REFPROP 10.0 is based on the 2014 CODATA values.

$$\text{Dihydrogen} \quad MM_{H2} := 2.01588 \cdot \frac{gm}{mol} \quad \text{and atomic hydrogen} \quad MM_H := \frac{MM_{H2}}{2}$$

the above molar mass is that provided in REFPROP 10.0 for parahydrogen.

Define normalizing parameters since the Boyd model is normalized.

$$\text{Classical hard-sphere second virial coefficient,} \\ \text{where } \sigma \text{ is the effective collision diameter} \quad b0(\sigma) := \frac{2}{3} \cdot \pi \cdot N_{Avogadro} \cdot \sigma^3$$

$$\text{Reduced temperature, where } \varepsilon \text{ is the characteristic} \\ \text{energy and k is Boltzman's constant} \quad Tstar(\varepsilon_{ovr\_k}, T) := \frac{T}{\varepsilon_{ovr\_k}}$$

Define the Boyd model calculations (allowed to run off page and not fully reported here).

$$p\_prime(p) := 3 - 2 \cdot p$$

$$Jtp(m, p, t) := \text{if}\left(p = 0, 1, \text{if}\left(p = 1, \frac{((m-6) \cdot 6 \cdot t - (m-1))}{12}, \text{if}\left(p = 2, \frac{(21 \cdot (m-6)^2 \cdot 6^2 \cdot t^2 +}{12}\right.\right.\right.$$

Revision: Baseline/Revision Level	Document Number: SNP-DOC-0046
Effective Date: 07/01/2024	Page: 105 of 149
Title: Parahydrogen Thermophysical Properties V05 Final Report	

$$Bstar\_p(m, p, Tstar) := \frac{(-1)^{p+1} \cdot 3}{(2 \cdot \pi)^{2 \cdot p}} \cdot \sum_{t=0}^{100} \left( Tstar^{\left( \left( \frac{6}{m} - 1 \right) \cdot t - p - \frac{p \text{ prime}(p)}{m} \right)} \cdot \left( \Gamma \left( \frac{6 \cdot t - p \text{ prime}(p)}{m} \right) \right) \right)$$

Normalized second virial coefficient for Lennard-Jones 6-12 model (m=12 in Jtp and Bstar\_p formulas above) including the first three quantum correction terms per Boyd (1971).

$$Bstar(Astar, Tstar) := Bstar\_p(12, 0, Tstar) + Astar^2 \cdot Bstar\_p(12, 1, Tstar) + Astar^4 \cdot Bstar\_p(12, 2, Tstar)$$

The quantum correction parameter, Lstar, can be related to the force constants as follows (Boyd 1971):

requires definition of atomic hydrogen reduced mass

$$\text{atomic hydrogen mass} \quad m_H := \frac{MM\_H}{N_{Avogadro}}$$

$$\text{atomic hydrogen reduced mass} \quad \mu_H := \frac{m_H \cdot m_H}{m_H + m_H}$$

$$\text{and the Boltzmann constant} \quad k := \frac{Ru}{N_{Avogadro}}$$

$$Astar(\sigma, \varepsilon\_ovr\_k) := \frac{h}{\sigma \cdot \sqrt{2 \cdot \mu_H \cdot \varepsilon\_ovr\_k \cdot k}}$$

Applying b0 and Tstar definitions, the second virial coefficient directly in terms of force constants and temperature is

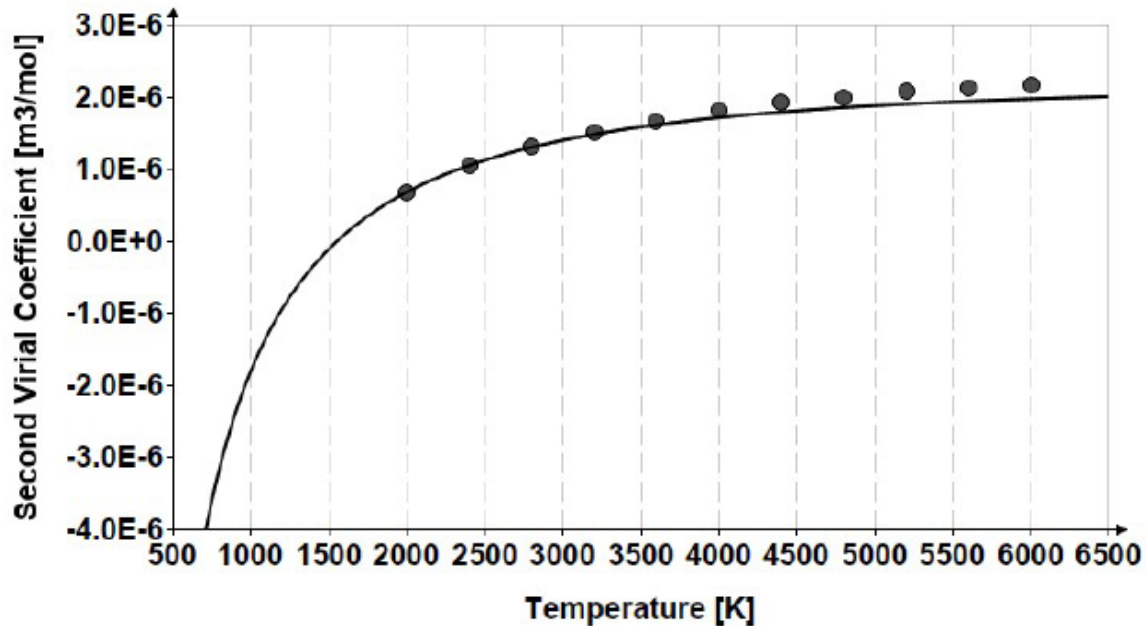
$$B(\sigma, \varepsilon\_ovr\_k, T) := b0(\sigma) \cdot Bstar(Astar(\sigma, \varepsilon\_ovr\_k), Tstar(\varepsilon\_ovr\_k, T))$$

One may now find the force constant values that exactly match the two lowest temperature data pairs from Lykova (1969b).

Guess Values	$\sigma_{H\_extrap} := 1.5 \cdot \text{Angstrom}$ $\varepsilon_{ovr\_k\_H\_extrap} := 500 \cdot K$
Constraints	$B(\sigma_{H\_extrap}, \varepsilon_{ovr\_k\_H\_extrap}, 2000 \cdot K) = 0.67 \cdot \frac{\text{cm}^3}{\text{mol}}$
Constraints	$B(\sigma_{H\_extrap}, \varepsilon_{ovr\_k\_H\_extrap}, 2400 \cdot K) = 1.04 \cdot \frac{\text{cm}^3}{\text{mol}}$
Solver	$\begin{bmatrix} \sigma_{H\_extrap} \\ \varepsilon_{ovr\_k\_H\_extrap} \end{bmatrix} := \text{find}(\sigma_{H\_extrap}, \varepsilon_{ovr\_k\_H\_extrap})$

$$\sigma_{H\_extrap} = 1.458159 \text{ Angstrom} \quad \varepsilon_{ovr\_k\_H\_extrap} = 499.834392 K$$

Next, the original data and the extrapolation curve will be plotted together to confirm that the results appear suitable.



The plotted results suggest the extrapolation scheme to be suitable. It recreates the two lowest temperature points from Lykova (1969b) and exhibits qualitatively typical behavior with decreasing temperature wherein the coefficient slope becomes increasingly more positive and the value itself becomes negative.

Before addressing at which temperatures to extrapolate below 2000 K and/or at which to tabulate the temperature varying force constants that are the ultimate goal here, it is best to move on to the other atomic hydrogen property that will serve as the other major constraint on determination of the temperature varying force constants - the OMEGA22 collision integral.

### OMEGA22 Collision Integral

The OMEGA22 collision integral is used to estimate absolute viscosity and thermal conductivity for the dissociating parahydrogen system under consideration. The specific source for the atomic hydrogen values used in the present work is Vanderslice et al. (1962) which estimates these transport properties for dissociating hydrogen using an ideal gas dissociation model. The data from Vanderslice et al. is:

$$T_{\Omega 22 H} := \begin{bmatrix} 1000 \\ 1500 \\ 2000 \\ 2500 \\ 3000 \\ 3500 \\ 4000 \\ 4500 \\ 5000 \\ 5500 \\ 6000 \\ 6500 \end{bmatrix} \cdot K \quad \Omega 22\_H\_Vanderslice := \begin{bmatrix} 5.954 \\ 5.222 \\ 4.743 \\ 4.392 \\ 4.118 \\ 3.895 \\ 3.742 \\ 3.614 \\ 3.500 \\ 3.392 \\ 3.281 \\ 3.167 \end{bmatrix} \cdot \text{Angstrom}^2$$

Overall, a power law curve does an excellent job fitting the OMEGA22 data, so the small needed extrapolation from 1000 K down to 700 K will be effected via a power law curve through only the lowest two temperature points -  $OMEGA22 = 55.644 \cdot T^{-0.32354}$ .

$$OMEGA22\_700K := 55.644 \cdot \left( \frac{700 \cdot K}{K} \right)^{-0.32354} \cdot \text{Angstrom}^2$$

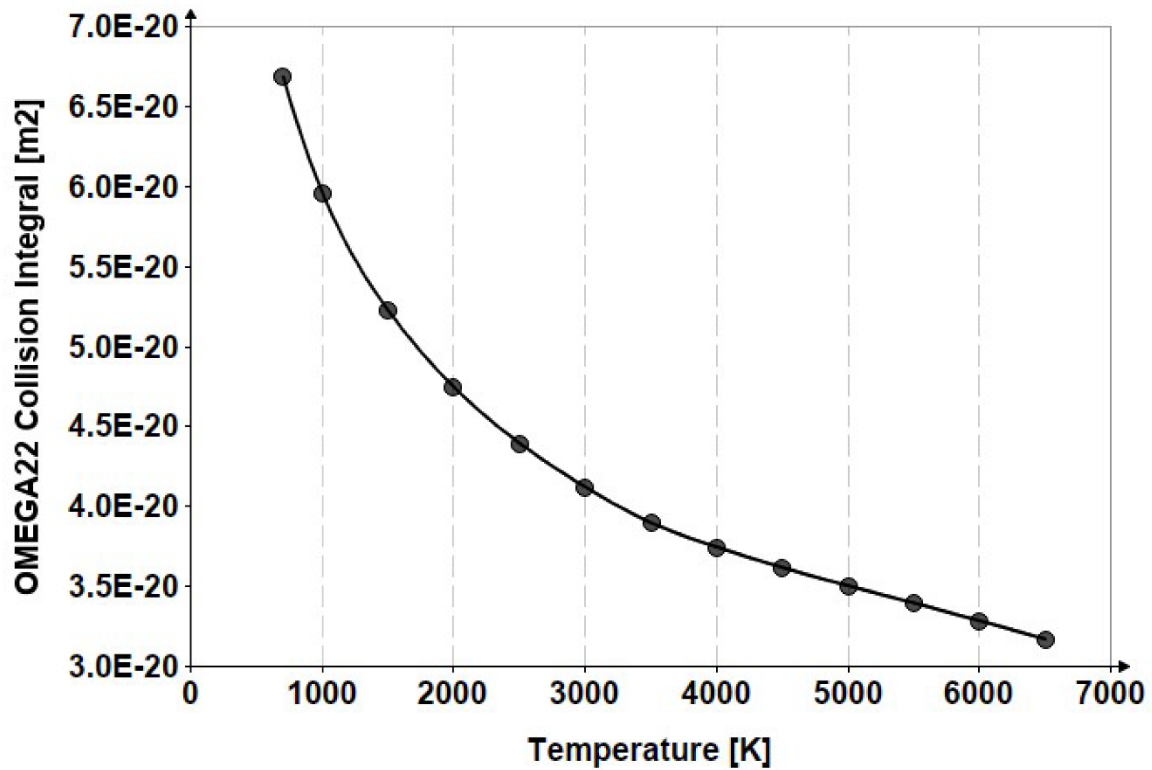
$$OMEGA22\_700K = (6.682 \cdot 10^{-20}) \text{ m}^2$$

$$T_{\Omega 22 H} := \text{stack}(700 \cdot K, T_{\Omega 22 H})$$

$$\Omega 22\_H := \text{stack}(OMEGA22\_700K, \Omega 22\_H\_Vanderslice)$$

Define a cubic spline fit to this OMEGA integral constraint data, so that values can be generated for pairing with the second virial coefficient constraint data.

$$\Omega_{22\_H\_spline}(T) := \text{interp}(\text{cspline}(T_{\Omega_{22\_H}}, \Omega_{22\_H}), T_{\Omega_{22\_H}}, \Omega_{22\_H}, T)$$

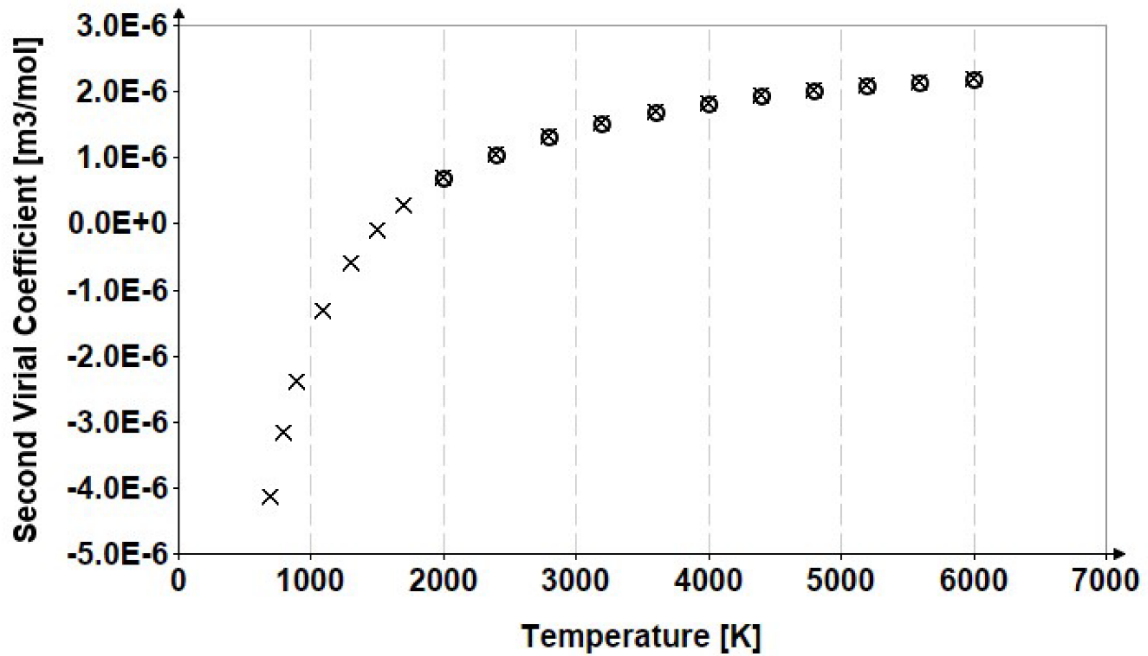


Both data and spline fit appear to be correct, so move on to generation of output vector of temperature values.

Comparing the low temperature range shapes of the second virial coefficient and the OMEGA22 curves, it appears that the temperature spacing for the final force constant vectors is driven by the steep slope of the second virial coefficient curve. Thus, define a trial temperature vector that exactly matches the Lykova (1969b) temperatures down to 2000 K and steps equal to, or less than, 400 K to result in suitable spacing of points along the curve path itself.

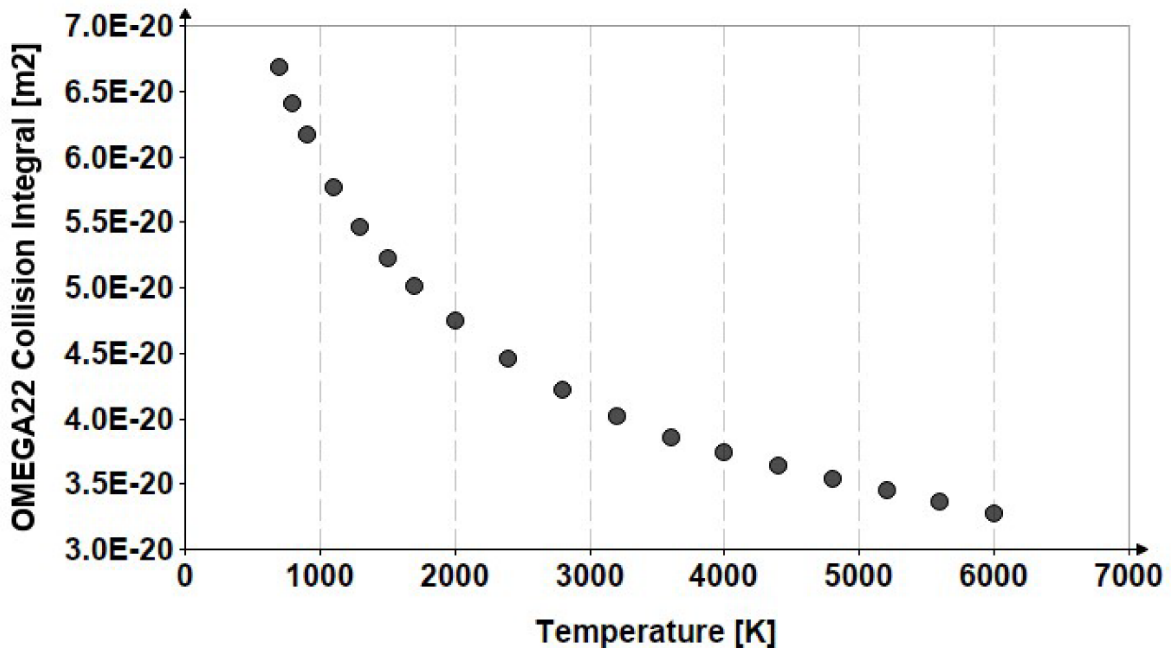
$$T\_H\_out := \begin{bmatrix} 700 \\ 800 \\ 900 \\ 1100 \\ 1300 \\ 1500 \\ 1700 \\ 2000 \\ 2400 \\ 2800 \\ 3200 \\ 3600 \\ 4000 \\ 4400 \\ 4800 \\ 5200 \\ 5600 \\ 6000 \end{bmatrix} \cdot K$$

$$B\_H\_constraint := \text{stack} \left( B \left( \left( \sigma\_H\_extrap, \varepsilon\_ovr\_k\_H\_extrap, \begin{bmatrix} 700 \\ 800 \\ 900 \\ 1100 \\ 1300 \\ 1500 \\ 1700 \end{bmatrix} \cdot K \right), B\_Hdata \right) \right)$$



This vector looks as if it possess a density suitable to the task ahead, so the next task is to define a corresponding vector of OMEGA22 constraints based on the values from Vanderslice et al. (1962).

$$\Omega_{22\_H\_constraint} := \Omega_{22\_H\_spline}(T_{H\_out})$$



## Creation of Temperature Varying Force Constant Vectors

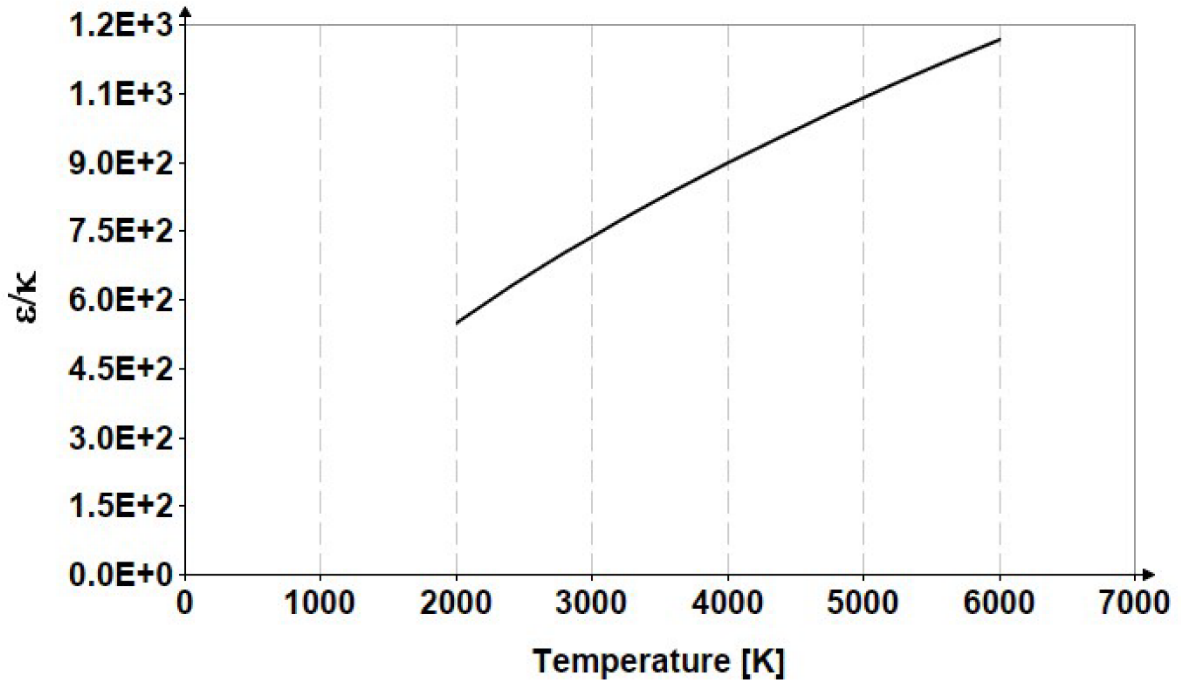
The needed constraint vectors representing variation of atomic hydrogen second virial coefficient and OMEGA22 collision integral with respect to temperature are now available. The end product of the present calculations are vectors of force constants that vary with temperature such that they recreate these constraint vectors when applied to models of the second virial coefficient and OMEGA22 integral based on the Lennard-Jones 6-12 collision interaction potential. The needed Lennard-Jones 6-12 second virial coefficient model was already defined above in the form of the quantum corrected model of Boyd (1971), since  $B_{star\_p}$  is the needed model when  $p = 0$  and  $m = 12$ . To ensure this to be the case, we now consider a handful of  $B_{star\_p}$  values tabulated in Hirschfelder et al. (1966).

For reduced temperataure, $T_{star}$	Hirschfelder et al. tabulates	Boyd (1971) $B_{star\_p}$ yields
$T_{star} := \begin{bmatrix} 0.5 \\ 1 \\ 2 \\ 5 \\ 10 \\ 20 \\ 50 \end{bmatrix}$	$\begin{bmatrix} -8.720205 \\ -2.5380814 \\ -0.62762535 \\ 0.24334351 \\ 0.46087529 \\ 0.52537420 \\ 0.50836143 \end{bmatrix}$	$B_{star\_p}(12, 0, T_{star}) = \begin{bmatrix} -8.7202054 \\ -2.5380813 \\ -0.6276253 \\ 0.2433435 \\ 0.4608753 \\ 0.5253742 \\ 0.5083614 \end{bmatrix}$

Thus, it is apparent that the Boyd model works fine.

Now a Lennard-Jones 6-12 model is needed for the OMEGA22 integral, and Hirschfelder et al. (1966) tabulate values for this as well. The Hirschfelder et al. (1966) tabulation is extensive, but only the needed range of values will be entered here. The needed range in actual temperature space is 700 K to 6500 K, and  $\epsilon/k$  from Lykova (1969b) behaves as follows.

$T_{Hdata} = \begin{bmatrix} 2000 \\ 2400 \\ 2800 \\ 3200 \\ 3600 \\ 4000 \\ 4400 \\ 4800 \\ 5200 \\ 5600 \\ 6000 \end{bmatrix} K$	$\sigma_{Hdata} := \begin{bmatrix} 2.189 \\ 2.133 \\ 2.085 \\ 2.045 \\ 2.014 \\ 1.988 \\ 1.965 \\ 1.943 \\ 1.923 \\ 1.902 \\ 1.882 \end{bmatrix} \cdot \text{Angstrom}$	$\epsilon_{ovr\_k\_Hdata} := \begin{bmatrix} 547.8 \\ 627.8 \\ 701.7 \\ 770.7 \\ 835.3 \\ 896.9 \\ 955.5 \\ 1011.8 \\ 1065.6 \\ 1116.9 \\ 1165.7 \end{bmatrix} \cdot K$
--	---	---



One may visually extrapolate the curve down to 700 K finding a corresponding characteristic temperature of about 300 K. One may estimate that the lower and upper bounds on Tstar as:

$$Tstar\_lo := \frac{700 \cdot K}{300 \cdot K} \quad Tstar\_lo = 2.333333 \quad \text{call it 2.0}$$

$$Tstar\_hi := \frac{6500 \cdot K}{1200 \cdot K} \quad Tstar\_hi = 5.416667 \quad \text{call it 6.0}$$

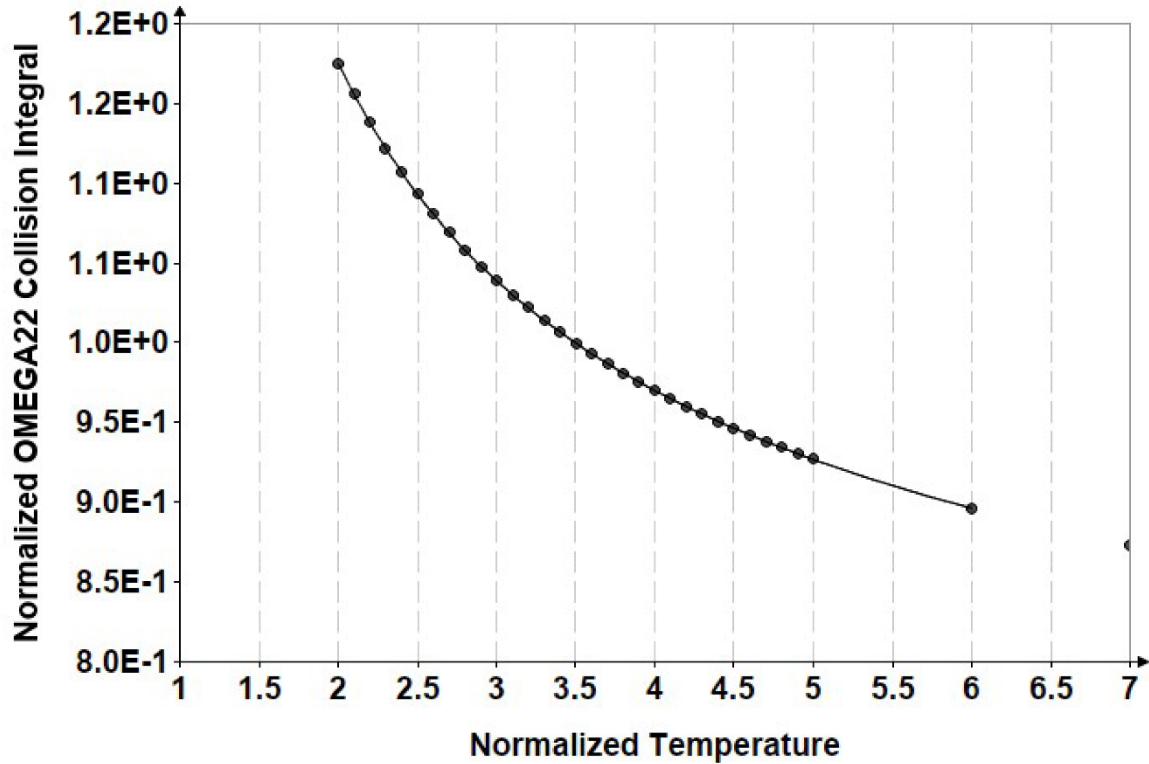
So, next enter the needed tabulated values from Hirschfelder et al. (1966)

$Tstar\_Q22\_LJ612 :=$		$Q22star\_LJ612 :=$
2.0		1.175
2.1		1.156
2.2		1.138
2.3		1.122
2.4		1.107
2.5		1.093
2.6		1.081
2.7		1.069
2.8		1.058
2.9		1.048
3.0		1.039
3.1		1.030
3.2		1.022
3.3		1.014
3.4		1.007
3.5		0.9999
3.6		0.9932
3.7		0.9870
3.8		0.9811
3.9		0.9755
4.0		0.9700
4.1		0.9649
4.2		0.9600
4.3		0.9553
4.4		0.9507
4.5		0.9464
4.6		0.9422
4.7		0.9382
4.8		0.9343
4.9		0.9305
5		0.9269
6		0.8963
7		0.8727

The characteristic temperature value was stretched up to 7, since the spacing is sparse near the intended 6 value and extension to 7 will ensure the spline fit will behave well up through the desired value of roughly 5.4.

Define a cubic spline model

$Q22star\_spline(Tstar) := \text{interp}(\text{cspline}(Tstar\_Q22\_LJ612, Q22star\_LJ612), Tstar\_Q22\_LJ612, Tstar)$



It is now possible to calculate the temperature varying force constants for each temperature in the output vector. Define the second virial coefficient and OMEGA22 collision integral constraint relations as residuals to be driven to 0.

Guess Values	$\sigma_H := 2.2 \cdot \text{Angstrom}$ $\varepsilon_{ovr\_k\_H} := 550 \cdot K$
Constraints	$\frac{b0(\sigma_H) \cdot Bstar\_p(12, 0, Tstar(\varepsilon_{ovr\_k\_H}, T_{H\_out})) - B\_H\_constraint}{B\_H\_constraint} = 0$ $\frac{\sigma_H^2 \cdot \Omega22star\_spline(Tstar(\varepsilon_{ovr\_k\_H}, T_{H\_out})) - \Omega22\_H\_constraint}{\Omega22\_H\_constraint} = 0$
Solver	$Result(T_{H\_out}, B\_H\_constraint, \Omega22\_H\_constraint) := \mathbf{find}(\sigma_H, \varepsilon_{ovr\_k\_H})$

Define a Result vector to force solutions to be carried out at each temperature in T\_H\_out.

$$Result := \overrightarrow{Result(T_{H\_out}, B\_H\_constraint, \Omega22\_H\_constraint)}$$

and unpack the results into individual output variables.  $i := 0 .. \text{length}(T\_H\_out) - 1$

$$\sigma\_H\_out_i := \left( \text{Result}_i \right)_0 \quad \epsilon\_ovr\_k\_H\_out_i := \left( \text{Result}_i \right)_1$$

Let us now use these temperature varying force constants to recreate atomic hydrogen second virial coefficient, compare the resulting curve with the data from Lykova (1969b), and also with the curve that resulted from the earlier method of McDonald (2017) that is to be replaced by the current temperature varying force constants.

$$\sigma\_H\_spline(T) := \text{interp}(\text{cspline}(T\_H\_out, \sigma\_H\_out), T\_H\_out, \sigma\_H\_out, T)$$

$$\epsilon\_ovr\_k\_H\_spline(T) := \text{interp}(\text{cspline}(T\_H\_out, \epsilon\_ovr\_k\_H\_out), T\_H\_out, \epsilon\_ovr\_k\_H\_out, T)$$

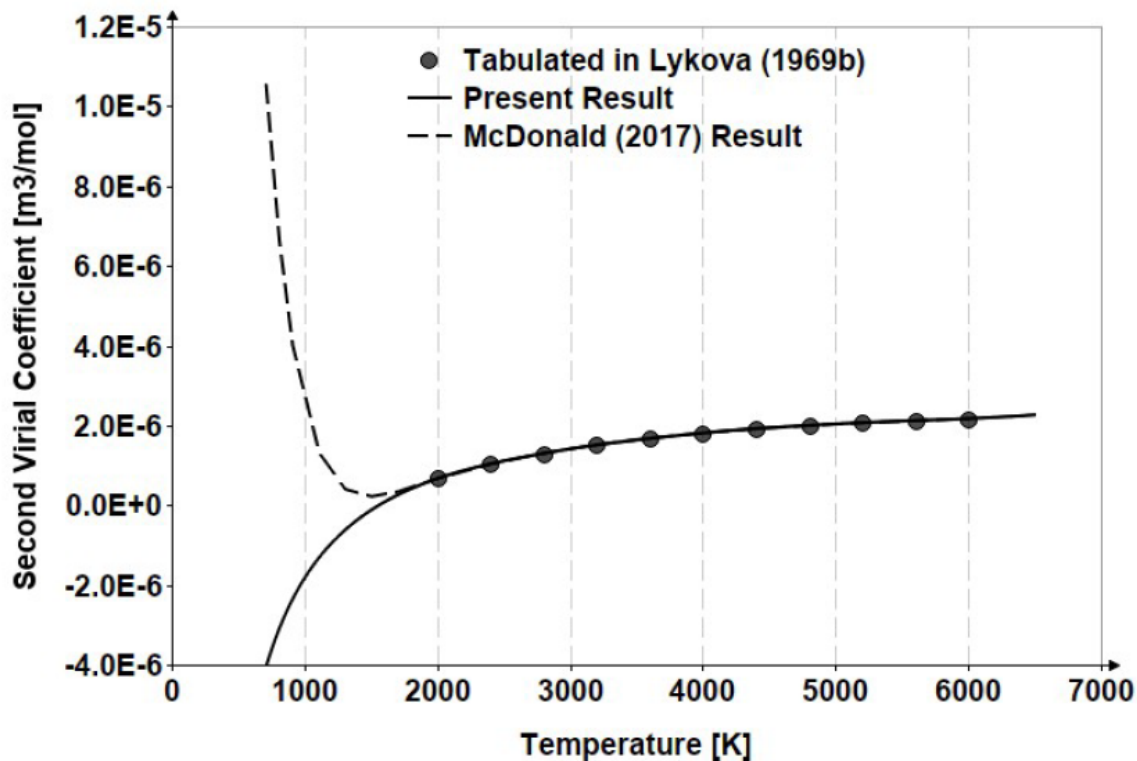
and calculate the resulting second virial coefficient

$$B\_H\_out := \overline{b0}(\sigma\_H\_spline(Tplot)) \cdot Bstar\_p(12, 0, Tstar(\epsilon\_ovr\_k\_H\_spline(Tplot), Tplot))$$

Define the second virial coefficient values from McDonald (2017) for comparison.

$$B\_H\_McD2017 := \begin{bmatrix} 1.056387 \cdot 10^{-5} \\ 6.652810 \cdot 10^{-6} \\ 4.026377 \cdot 10^{-6} \\ 1.331818 \cdot 10^{-6} \\ 4.000256 \cdot 10^{-7} \\ 2.179264 \cdot 10^{-7} \\ 3.398769 \cdot 10^{-7} \\ 6.714385 \cdot 10^{-7} \\ 1.030911 \cdot 10^{-6} \\ 1.304507 \cdot 10^{-6} \\ 1.519367 \cdot 10^{-6} \\ 1.682096 \cdot 10^{-6} \\ 1.811282 \cdot 10^{-6} \\ 1.913919 \cdot 10^{-6} \\ 1.996525 \cdot 10^{-6} \\ 2.064021 \cdot 10^{-6} \\ 2.119696 \cdot 10^{-6} \\ 2.165817 \cdot 10^{-6} \end{bmatrix} \frac{m^3}{mol}$$

The comparison plot is on the next page.



The second virial coefficient behavior resulting from the current temperature varying force constants applied to a Lennard-Jones 6-12 potential proves an excellent representation of the data tabulated in Lykova (1969b). Below 2000 K, we have no idea if the extrapolation down to 700 K is representative of the calculation methods that resulted in the values tabulated in Lykova (1969b); since the exact methods are only related in the missing Kessel'man dissertation. Yet, the behavior is qualitatively typical of second virial coefficient behavior - unlike the behavior of the method employed in McDonald (2017) which exhibits erroneous behavior below roughly 1500 K. Results are listed on the next page.

List the resulting temperature-varying force constants.

$T_{H\_out} =$	$\begin{bmatrix} 700 \\ 800 \\ 900 \\ 1100 \\ 1300 \\ 1500 \\ 1700 \\ 2000 \\ 2400 \\ 2800 \\ 3200 \\ 3600 \\ 4000 \\ 4400 \\ 4800 \\ 5200 \\ 5600 \\ 6000 \end{bmatrix}$	<i>K</i>	$\sigma_{H\_out} =$	$\begin{bmatrix} 2.50468640332522 \\ 2.46627380552282 \\ 2.43014397358195 \\ 2.36824432499839 \\ 2.31808674120397 \\ 2.27605716073011 \\ 2.23858294932165 \\ 2.18861476684896 \\ 2.13237691699302 \\ 2.08547178138944 \\ 2.04441186872117 \\ 2.01066064153450 \\ 1.98682486257900 \\ 1.96534134917912 \\ 1.94504939755092 \\ 1.92607893789974 \\ 1.90652134545199 \\ 1.88622489404564 \end{bmatrix}$	<i>Angstrom</i>
----------------	---	----------	---------------------	--	-----------------

$T_{H\_out} =$	$\begin{bmatrix} 700 \\ 800 \\ 900 \\ 1100 \\ 1300 \\ 1500 \\ 1700 \\ 2000 \\ 2400 \\ 2800 \\ 3200 \\ 3600 \\ 4000 \\ 4400 \\ 4800 \\ 5200 \\ 5600 \\ 6000 \end{bmatrix}$	<i>K</i>	$\varepsilon_{ovr\_k\_H\_out} =$	$\begin{bmatrix} 256.052673923215 \\ 281.064787024414 \\ 305.598912030394 \\ 353.130383544949 \\ 398.862128373436 \\ 443.110790463143 \\ 486.071380370679 \\ 548.253558204184 \\ 627.364861230457 \\ 701.882484340774 \\ 769.964733353094 \\ 834.669236329593 \\ 896.161940437369 \\ 955.419707449369 \\ 1013.778279697640 \\ 1068.696327184160 \\ 1121.803614791310 \\ 1168.116099402920 \end{bmatrix}$	<i>K</i>
----------------	---	----------	----------------------------------	--	----------

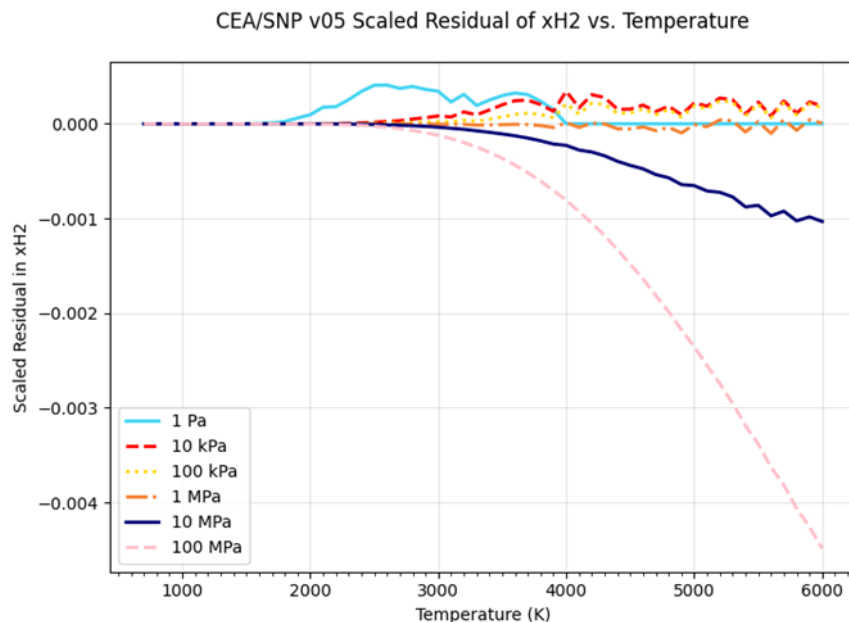
## APPENDIX D.

### VALIDATION OF THERMODYNAMIC PROPERTY RESULTS AGAINST CHEMICAL EQUILIBRIUM WITH APPLICATIONS

Chemical Equilibrium with Applications is a decades-old program for calculation of equilibrium compositions under the assumption that reacting species obey the ideal gas law. The CEA entry for dihydrogen is based on equilibrium hydrogen. When requesting equilibrium properties of dissociating dihydrogen at specified pressure and temperature states, CEA outputs enthalpy in a 298.15 K reference state and entropy in a 0 K and 1 bar reference state. Thus, the entropy output is already in the reference state used for the dissociating properties calculated in Section 5.3; but enthalpy must be shifted from CEA's 298.15 K reference to the desired 0 K reference. Also, note that if the reader tries to recreate the validation results in this appendix from the database output, they must remove the shift that moves the results based on Section 5.3 calculations to the REFPROP 10 Normal Boiling Point reference state (Section 5.4 and Appendix B).

The goal of this section is to compare the current database results with those from CEA to help discover errors in coding/methods that might have otherwise gone unnoticed. Residual errors are defined on the basis of the validation source being the reference for the normalized residual error. Here that means  $\text{Residual Error} = (\text{Present Database Value} - \text{CEA Value}) / (\text{CEA Value})$ .

#### Dihydrogen Mole Fraction



All curves are in excellent agreement up to around 2000 K, where the 1 Pa curve begins to exhibit considerable error. Higher pressure curves begin to exhibit similar error/sketchiness on attaining temperature where dihydrogen has nearly completely dissociated into atomic hydrogen. This

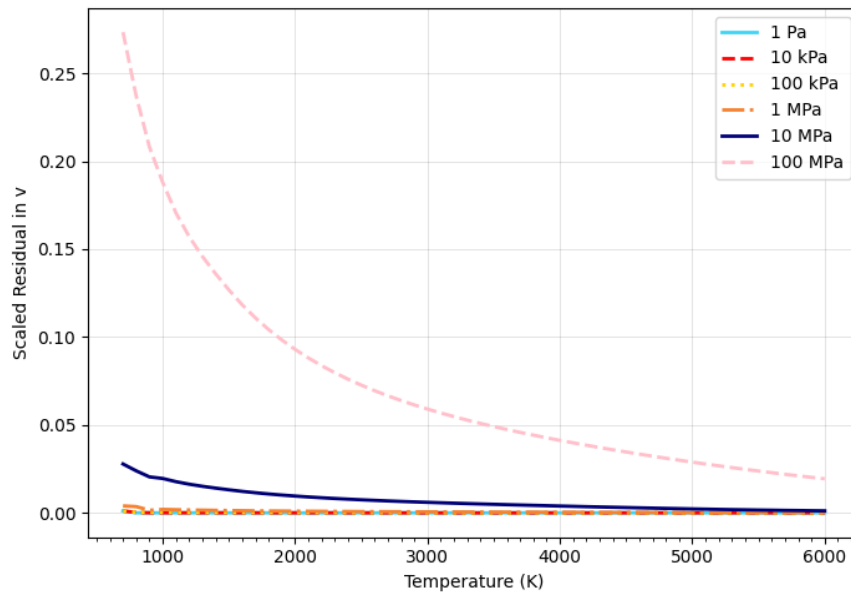
Revision: Baseline/Revision Level	Document Number: SNP-DOC-0046
Effective Date: 07/01/2024	Page: 119 of 149
Title: Parahydrogen Thermophysical Properties V05 Final Report	

behavior occurs because the CEA approach for determining equilibrium composition is not as precise as our present use of a single algebraic relation that directly applies tabulated equilibrium constant values. The CEA approach permits good estimates of composition for complex systems, but at some cost in accuracy of predicted composition. Above roughly 3000 K, the 10 MPa and 100 MPa curves move steadily downwards, since the present calculations account for fugacity effects on composition – whereas CEA does not.

### Mass-Specific Volume

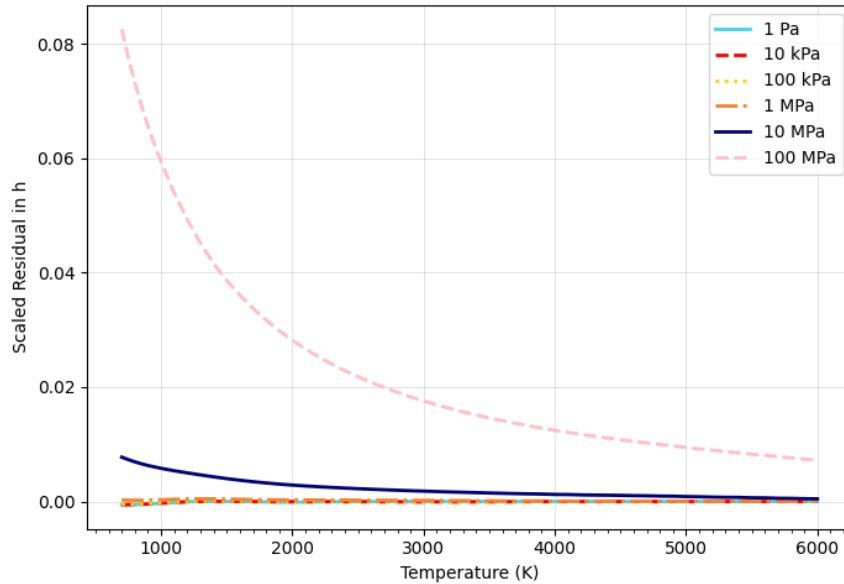
Though the database provides mass density, this validation discussion works with its inverse – mass-specific volume. Since CEA assumes ideal gas behavior, one may add 1.0 to the resulting residual value to arrive at compressibility factor (commonly referred to by the variable name  $Z$ ).

CEA/SNP v05 Scaled Residual of  $v$  vs. Temperature



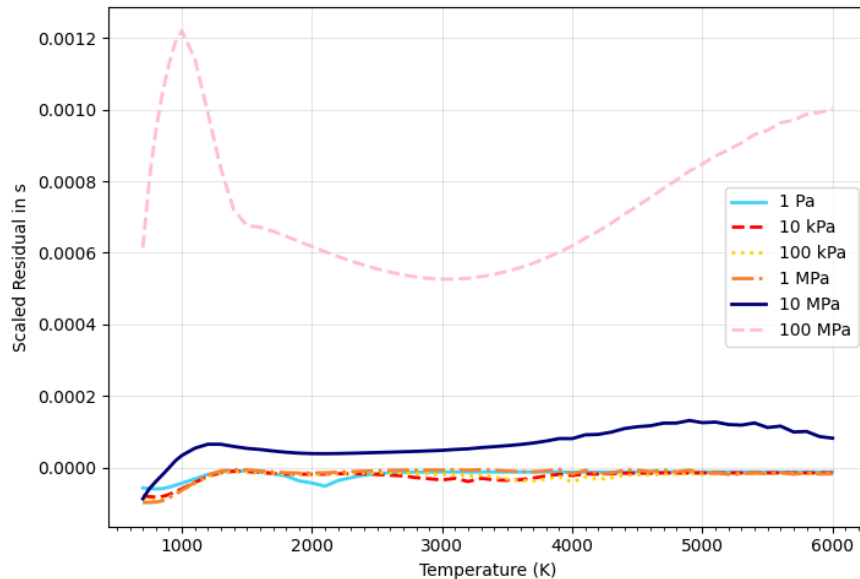
All the density isobars appear correct. If one adds 1.0 to the resulting 100 MPa curve, it matches  $Z$  output by REFPROP 10 at 1000 K where dissociation is negligible.

### Mass-Specific Enthalpy

CEA/Python Scaled Residual of  $h$  vs. Temperature

All curves appear well-behaved and the slightly under 0.06 value for residual at 1000 K agrees well with the ratio of real-gas to ideal gas enthalpy equal to 1.059 output by REFPROP 10.

### Mass-Specific Entropy

CEA/Python Scaled Residual of  $s$  vs. Temperature

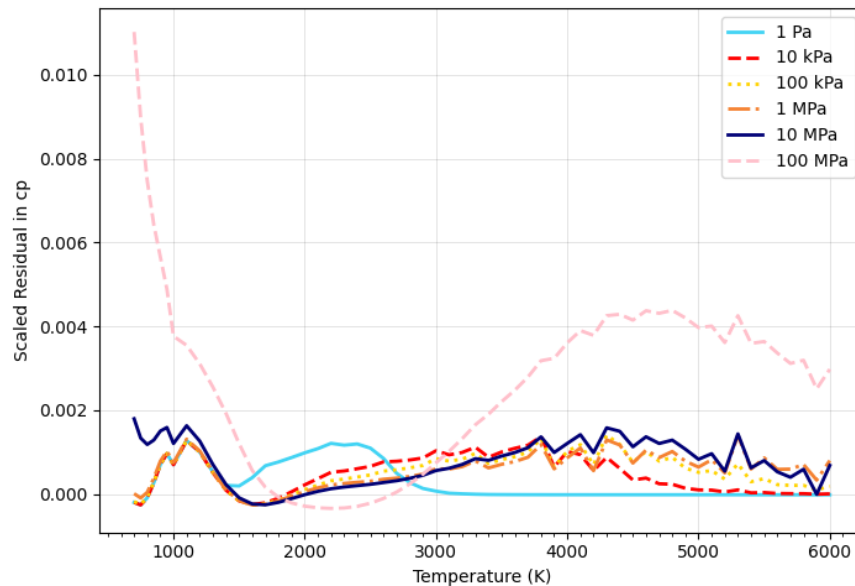
The entropy residual plot exhibits a handful of interesting behaviors. Each curve begins at 700 K, a temperature at which dissociation is negligible – even at 1 Pa. All of the curves, except for 100 MPa, exhibit a residual of roughly 0.0001 at 700 K – this is due mostly to small differences in zero-pressure entropy between the two datasets. As temperature approaches the 1500 K upper

bound on the bridging region, the lower pressure entropy curves exhibit very small residuals. All except the 100 MPa curve also exhibit some of the sketchiness discussed above in the section on dihydrogen mole fraction.

The 100 MPa curve behavior up to 1000 K behaves exactly the same as that for REFPROP, since up to just under 1000 K (100 MPa Bridging Temperature is 981 K) the source data is, in fact, REFPROP 10. As soon as the current database calculation methods begin being used above 1000 K, the residual curve drops sharply until the 1500 K upper end of the bridging region is reached. This sharp drop is mostly due to the fact that the methodology used to bridge/meld the REFPROP 10 and current methods together works rather poorly for entropy above about 30 MPa. The more gradual decrease in residual above 1500 K is simply the result of the current database accounting for real-gas effects on whereas CEA is ideal gas in nature. Above 3000 K, the 100 MPa curve begins to increase due to the impact of real-gas effects on equilibrium composition – fugacity.

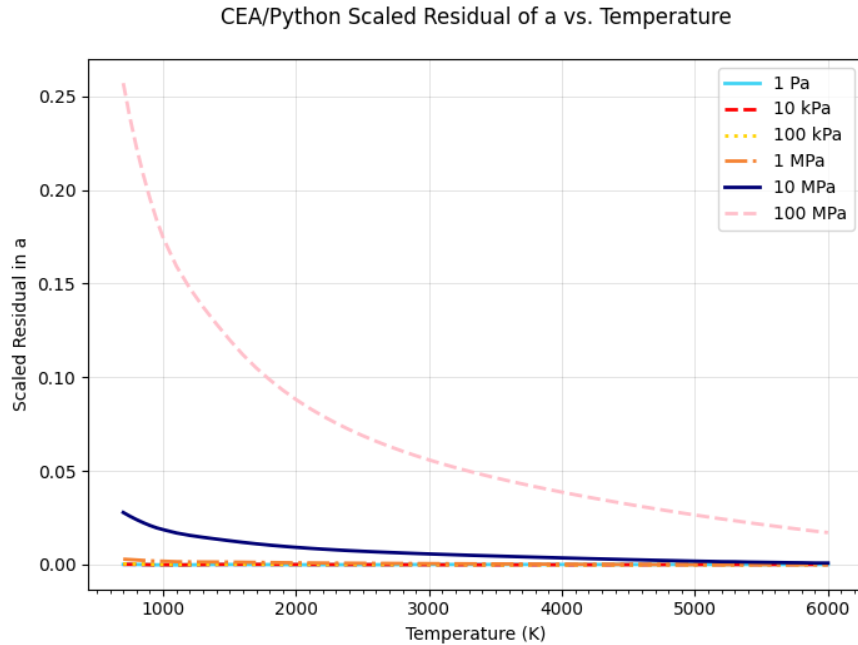
### Isobaric Mass-Specific Heat

CEA/Python Scaled Residual of cp vs. Temperature



This residual comparison shows an interesting trend in the bridging region for all pressure steps due to the newly identified bridging methodology. Additionally, the residuals begin to increase in a parabolic fashion after roughly 1500 K before returning to zero. This effect is observed due to the real-gas effects in the dissociation region prior to returning to an equilibrium state with the monatomic hydrogen. For example, the light blue curve for 1 Pa has a very short parabolic peak and returns to zero given that the dissociation occurs significantly faster in this low pressure region. As such, the higher pressure curves show a peak at higher and higher temperatures as the dissociation requires more temperature rise to reach the same dihydrogen mole fraction. The 100 MPa curve yields the highest residual throughout, but its value does not exceed ~0.01.

## Sound Speed



The plot above clearly depicts the importance of real-gas effects on sound speed. All of the results appear well-behaved. The comparisons with the tabulations of Vargaftik et al. (1996) will provide a more quantitative idea of the validity of the present calculations. But, the 1000 K, 100 MPa value of 0.17 above agrees with the same residual calculation based on sound speed from REFPROP 10.

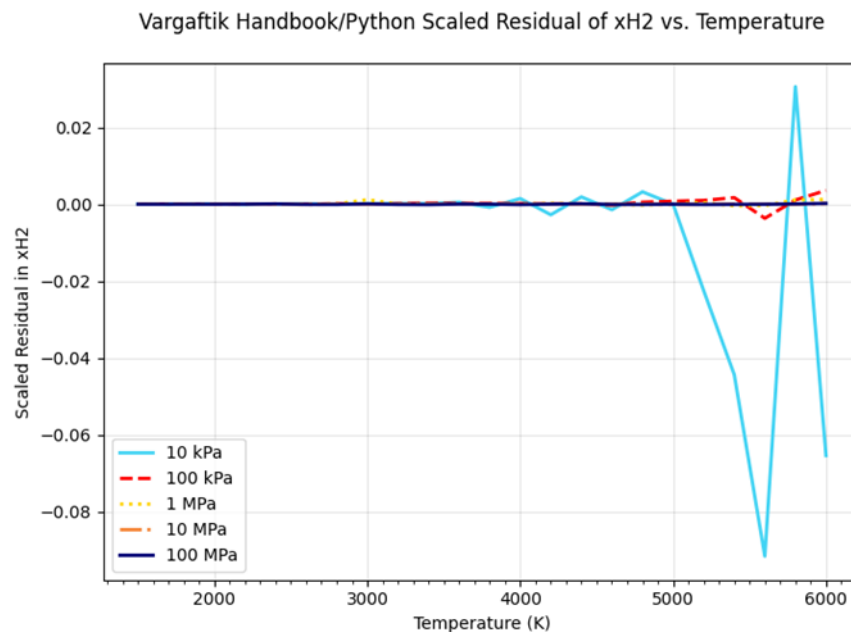
## APPENDIX E.

### VALIDATION OF THERMODYNAMIC PROPERTY RESULTS AGAINST VARGAFTIK ET AL. (1996) TABULATIONS

Vargaftik et al. (1996) provides thermophysical properties for dissociation dihydrogen. The methods behind the current SNP parahydrogen property calculations were largely based on the methods believe to have been used to create the Vargaftik tabulations. Vargaftik et al. (1996) exhibits area of missing data and several datum points for various properties were found to be erroneous (typically probable transcription errors) when reviewed by McDonald (2017). All such erroneous datum points are removed from the comparisons in this appendix. Vargaftik et al. (1996) provides enthalpy in a 0 K reference state and entropy in a 0 K, 1 bar reference state. Note that if the reader tries to recreate the validation results in this appendix from the database output, they must remove the shift that moves the results based on Section 5.3 calculations to the REFPROP 10 Normal Boiling Point reference state (Section 5.4 and Appendix B).

The goal of this section is to compare the current database results with those from Vargaftik et al. (1996) to help discover errors in coding/methods that might have otherwise gone unnoticed while providing quantitative insight into the accuracy of our newer SNP calculations. Residual errors are defined based on the validation source being the reference for the normalized residual error. Here that means – Residual Error = (Present Database Value – Vargaftik Value)/(Vargaftik Value).

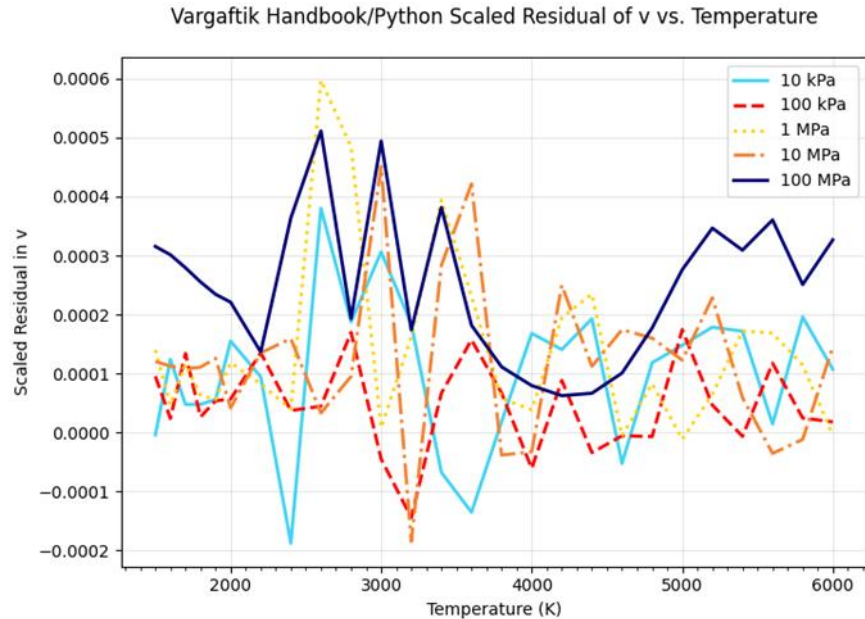
#### Dihydrogen Mole Fraction



Agreement is excellent. The large deviations above 5000 K result from Vargaftik only tabulating those results to the fourth decimal place resulting in only one significant figure at/above 5000 K at 10 kPa.

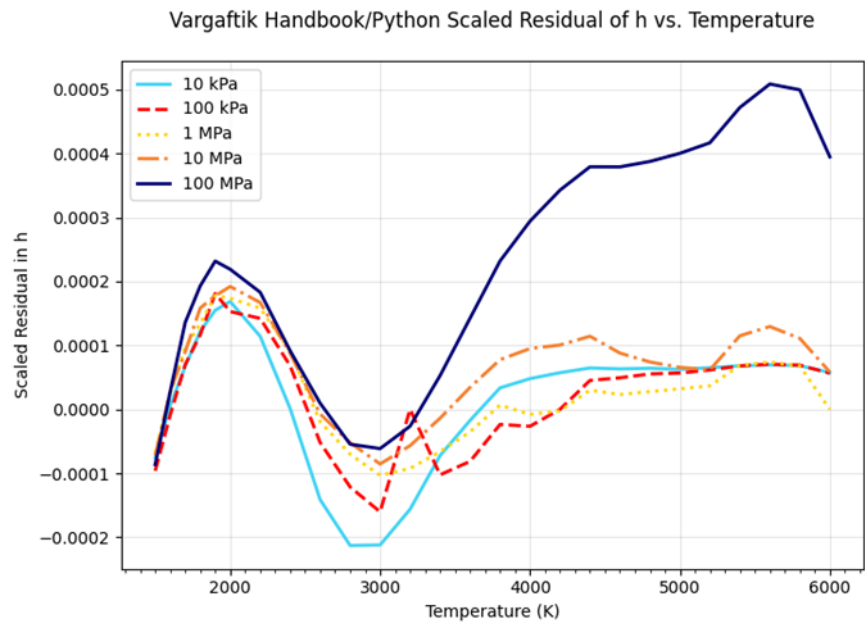
## Mass-Specific Volume

Though the database provides mass density, this validation discussion works with its inverse – mass-specific volume, since Vargaftik et al. (1996) tabulates specific volume.

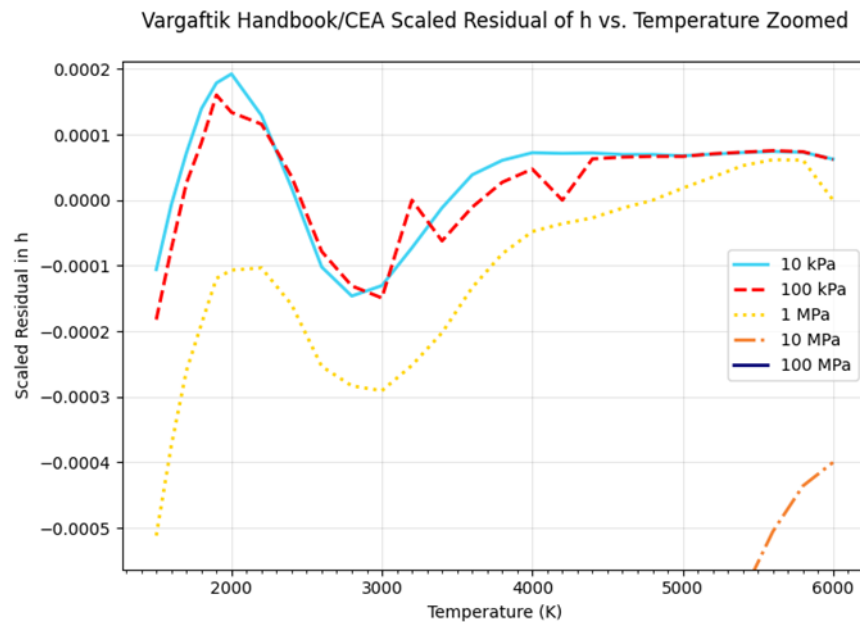


The errors observed are in accord with Vargaftik only tabulating 4 significant figures. No evidence of a systemic error is apparent in the residual plot.

## Mass-Specific Enthalpy

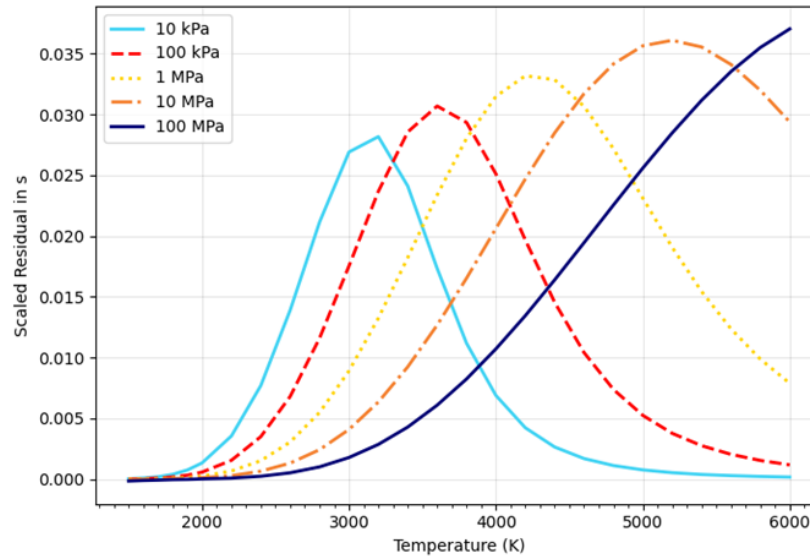


Though none of the residuals are large – most are less than 0.02% in magnitude – there is obviously something of a systemic nature at play. Each curve exhibits a common behavior with respect to temperature. While the 100 MPa curve exhibits the same basic behavior with respect to temperature as the lower pressures, above 3000 K it rises above the remaining curves. The fact that the enthalpy residual from the CEA comparisons in the last appendix exhibit no similar trends suggests that the issue might be with the Vargaftik dataset itself. Thus, a similar residual plot was made that compares Vargaftik to CEA, and this plot is found to exhibit exactly the same behavior – except that the highest pressure curves are no longer visible since CEA doesn't account for real-gas effects. It would seem that something odd is going on with the Vargaftik tabulation.



## Mass-Specific Entropy

Vargaftik Handbook/Python Scaled Residual of s vs. Temperature

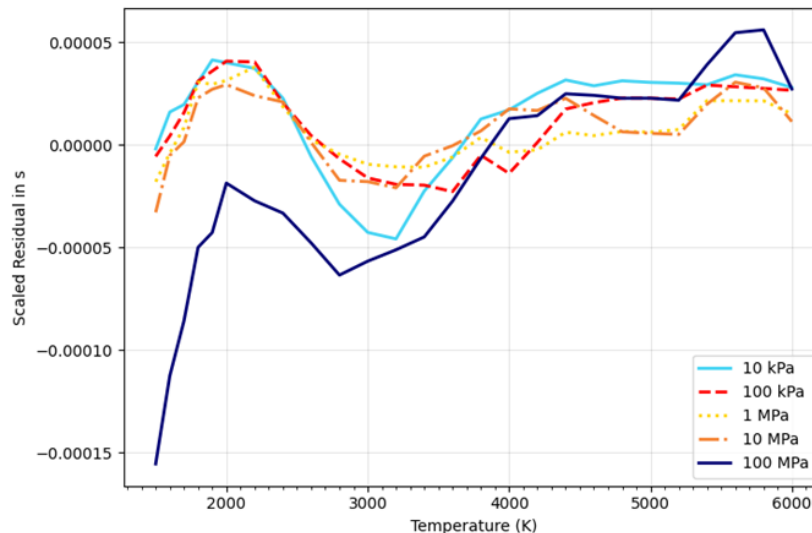


There is obviously some systemic error at play in the plot above. This behavior was first noticed in McDonald (2017) where it was surmised that the Vargaftik tabulations might have failed to include the terms associated with mixing of the individual species

$$-R_u \cdot x_{H_2} \cdot \ln(x_{H_2}) - R_u \cdot x_H \cdot \ln(x_H)$$

So, those terms were removed from the Python source code with the following result

Vargaftik Handbook/Python Scaled Residual of s vs. Temperature



which strongly suggests that Vargaftik et al. (1996) did fail to include the mixing terms in their tabulated entropy results.

Revision: Baseline/Revision Level	Document Number: SNP-DOC-0046
Effective Date: 07/01/2024	Page: 127 of 149
Title: Parahydrogen Thermophysical Properties V05 Final Report	

## APPENDIX F.

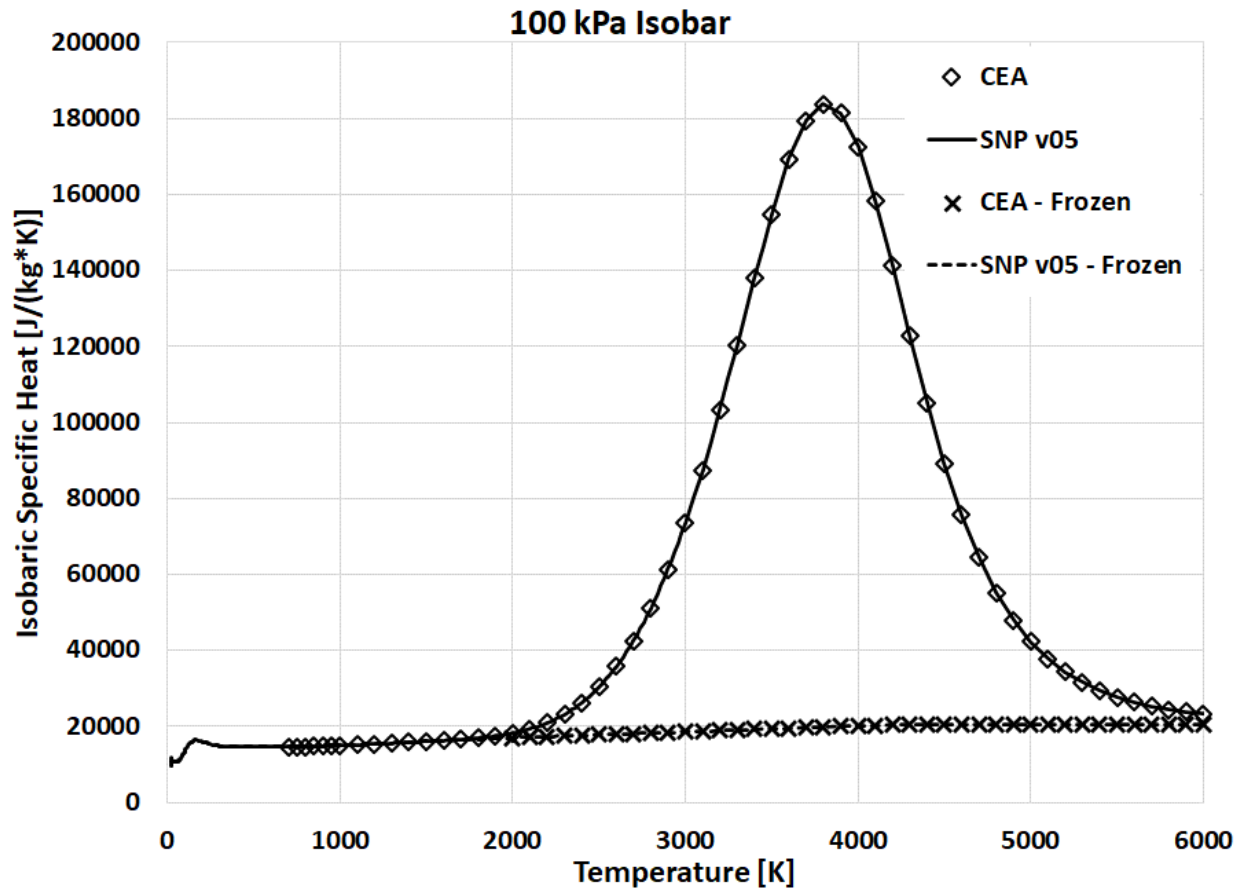
### VALIDATION OF TRANSPORT PROPERTY RESULTS

Transport properties calculated for inclusion in the SNP v05 database are compared for validation purposes against values from REFPROP 10 (NIST, 2018), Chemical Equilibrium with Applications (CEA, 2004), Vargaftik et al. (1996) for pressures up to 20 MPa, and Vargaftik and Vasilevskaya (1975) above 20 MPa – these latter two are simply referred to as Vargaftik in the plots that follow. Both Vargaftik sources apply the same Vanderslice et al. (1962) methods used for the present SNP v05 database. Unlike the thermodynamic property validation plots which compare normalized residuals, the present transport property validation plots compare curves of the property values themselves. The transport properties are not expected to agree as well with validation sources as were the thermodynamic properties. For the transport properties, the most important validation outcomes are that the transition from lower temperature REFPROP values to the higher temperature dissociating calculations be smooth/well-behaved and that there is good qualitative agreement between SNP v05 values and validation sources.

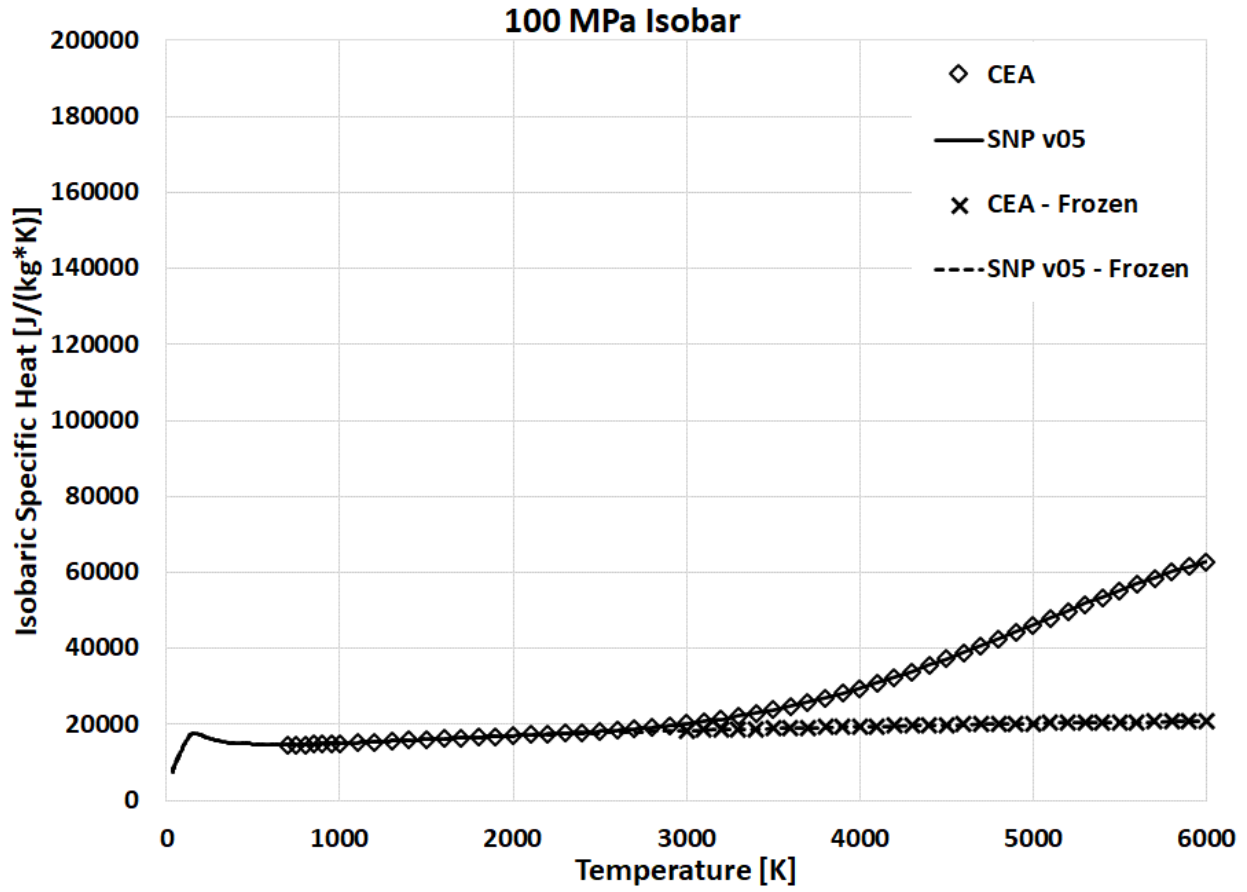
#### Isobaric Specific Heat

The main body of validation regarding isobaric specific heat is found in Appendix F, but two plots are provided here to ensure that the so-called ‘frozen’ version was calculated correctly. These plots also help one to understand the relationship between the equilibrium and frozen values.

The 100 kPa isobar is provided below. At this pressure, one can see almost the entire hump associated with dissociation of H<sub>2</sub> to H. This hump results from the progressive expression of H atom formation enthalpy. The lower curves depict the frozen values where this expression of formation enthalpy is not included in the result. The SNP v05 frozen curve does account for real-gas effects, whereas the CEA frozen curve does not; but real-gas effects are minimal at 100 kPa.

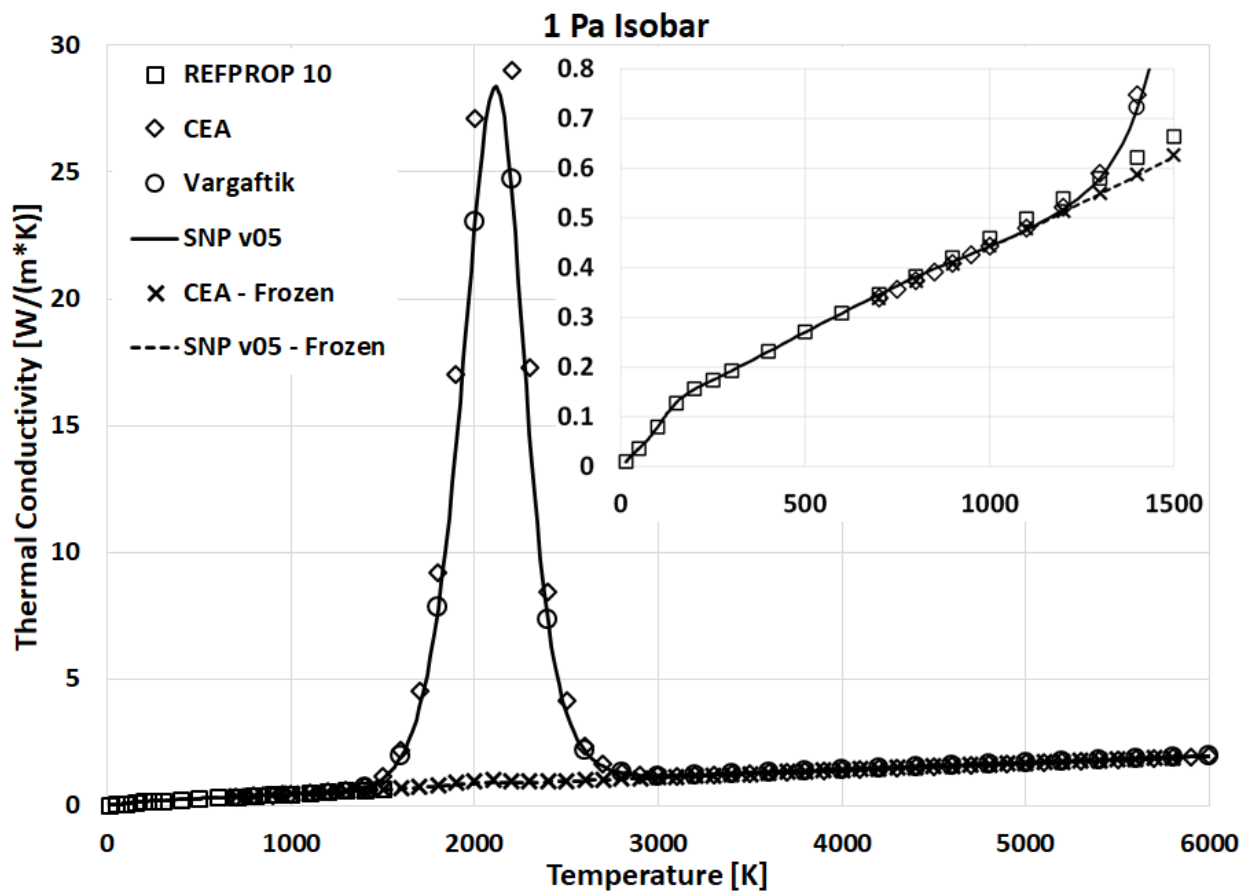


The highest pressure isobar is considered in the plot on the next page. The isobaric specific heat scale is kept the same as for the 100 kPa plot, so that one may more readily compare these isobars – if desired. Even at 100 MPa, real-gas effects on isobaric specific heat are really not noticeable in the plot.



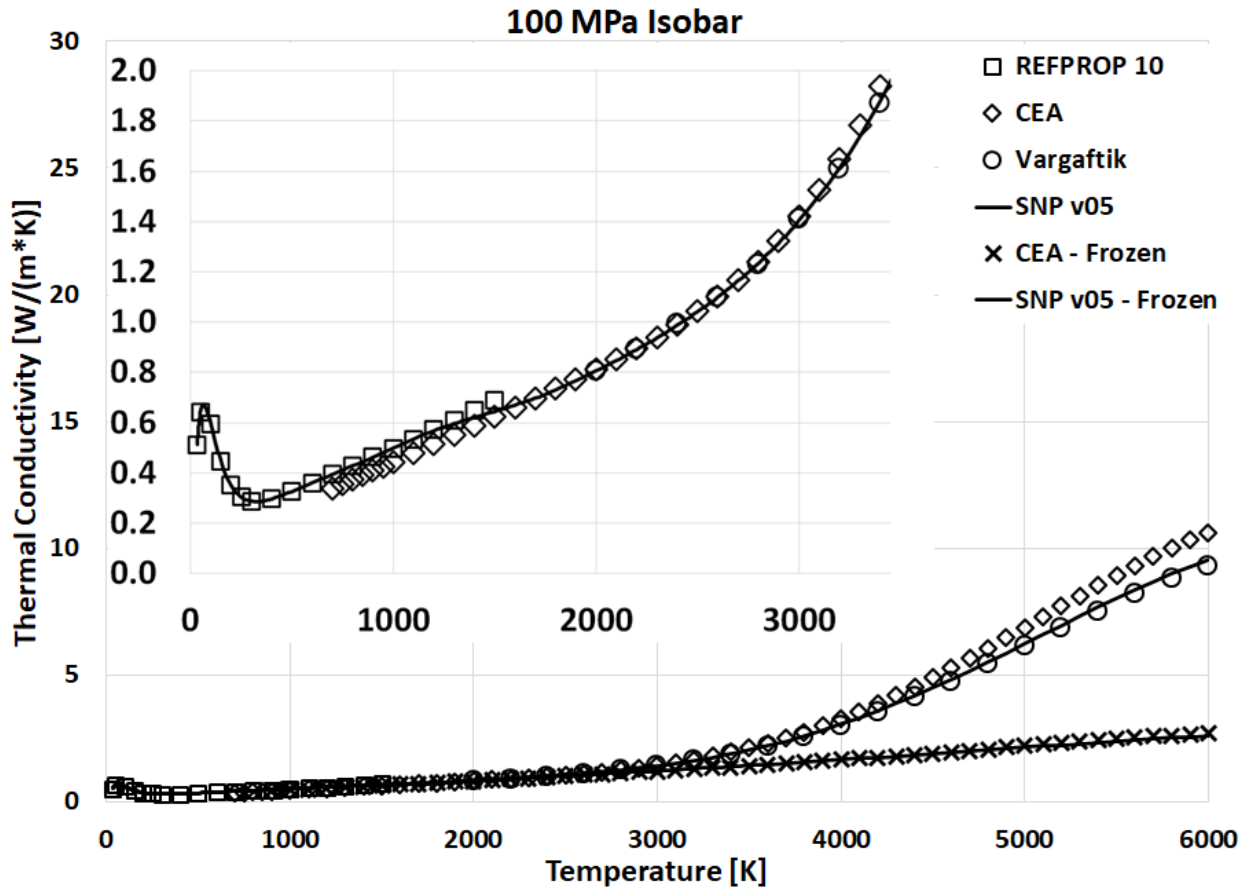
## Thermal Conductivity

For the lowest pressure considered in the SNP v05 database, 1 Pa, the figure below depicts values from the various validation sources. The figure depicts the full temperature range in which one may observe almost exact agreement between SNP v05 and Vargaftik curves – as should be the case since both are based on the methods of Vanderslice et al. (1962). An inset plot zooms into the lower temperature region where one sees that SNP v05 values are taken directly from REFPROP 10 up to roughly 700 K above which the SNP v05 curve gradually transitions to the methods of Vanderslice et al. (1962), thus, rising above the REFPROP 10 values primarily due to the reaction contribution to thermal conductivity for which REFPROP 10 does not account. Frozen curves are also depicted to provide an idea of their relationship to equilibrium values.

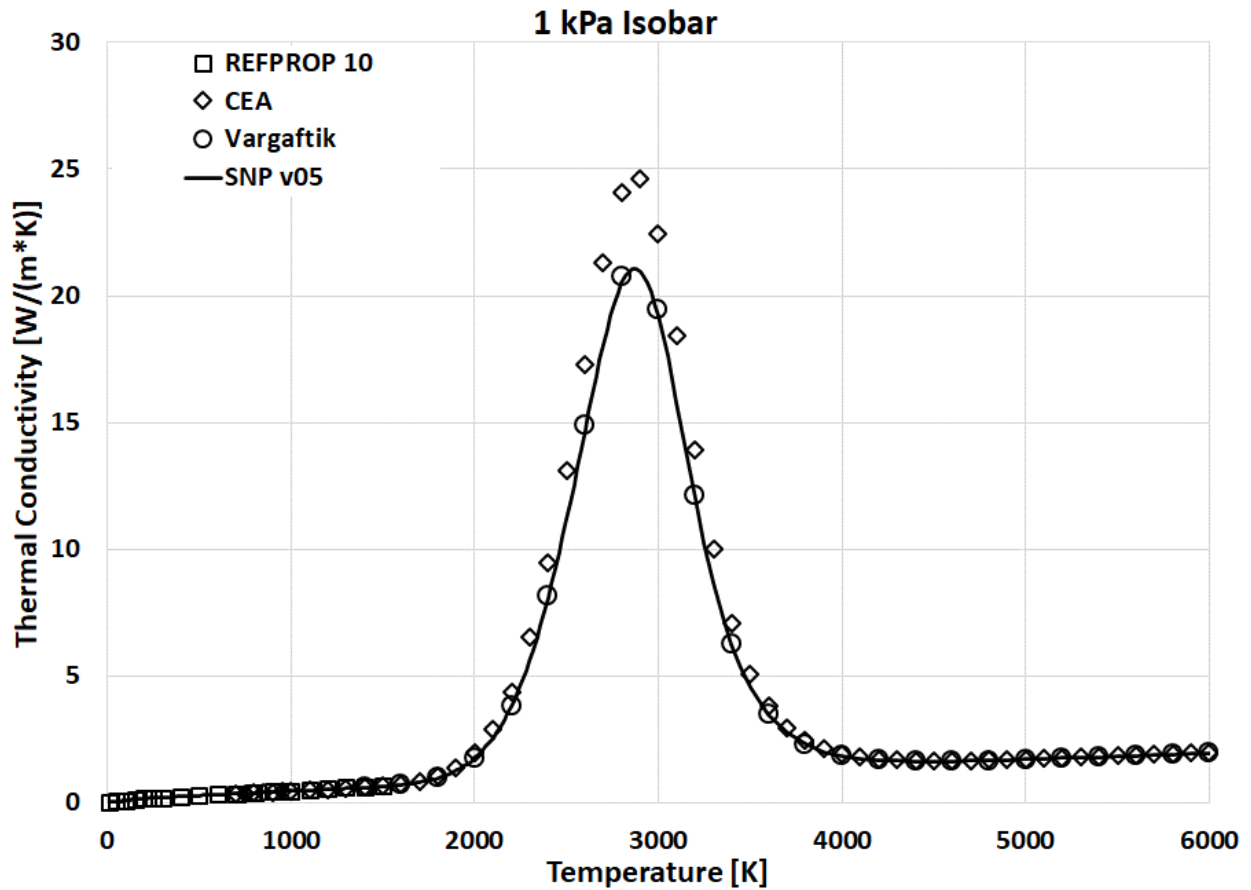


From the lowest pressure considered in the SNP v05 database, we jump straight to the highest pressure of 100 MPa in the plot immediately below. At the lowest pressure of 1 Pa, the REFPROP 10 and CEA/Vargaftik values are in quite good agreement at the roughly 700 K Bridging Temperature above which reaction effects begin to become important to thermal conductivity; thus, the SNP v05 curve makes a quite smooth transition from REFPROP 10 values to those from the dissociating methods of Vanderslice et al. (1962). The inset plot for the 100 MPa isobar reveals that this same transition is more tortuous due to the REFPROP 10 values laying upwards of 20% above those of the dissociating methods. Yet, the SNP v05 curve still appears very acceptable.

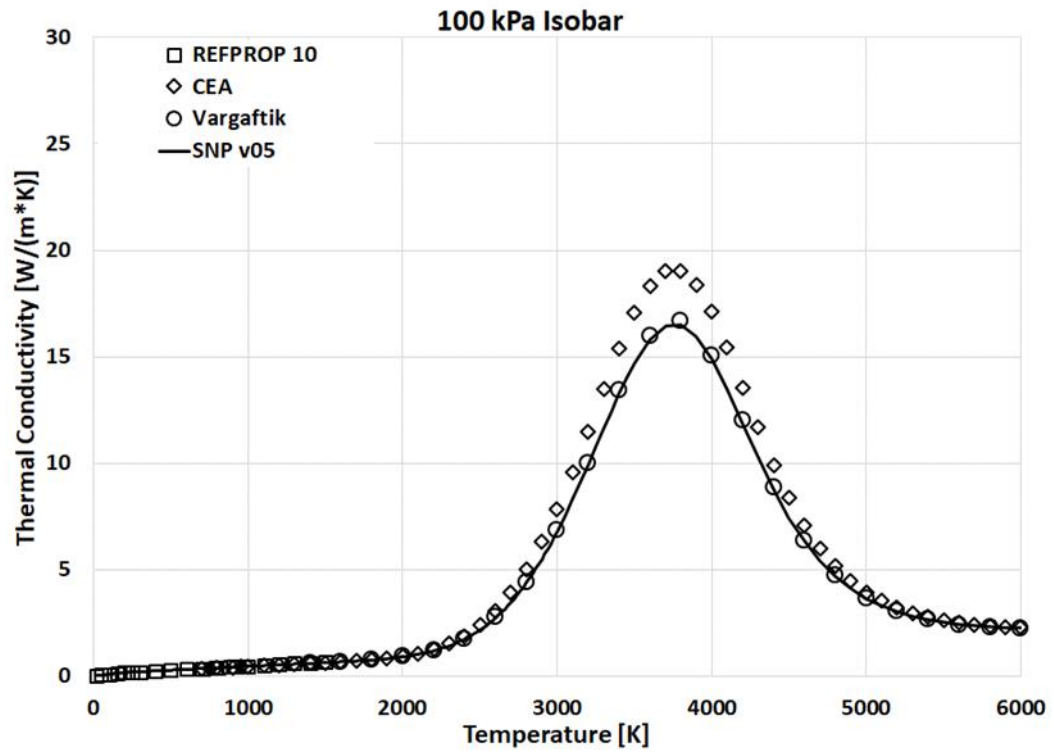
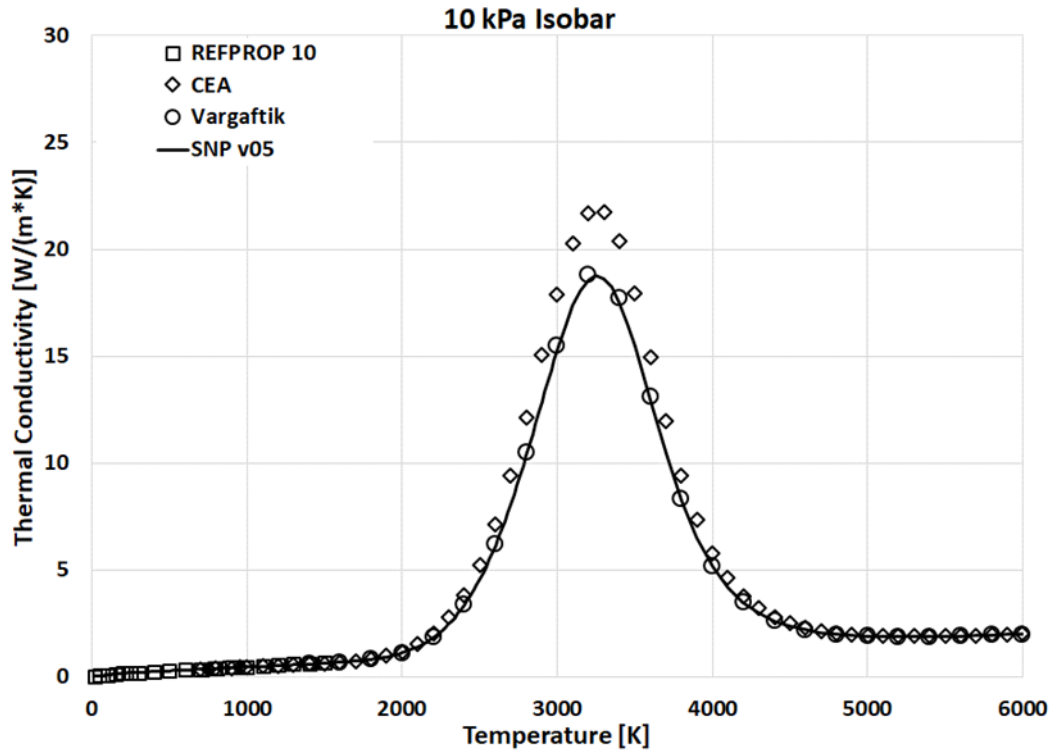
The fact that the CEA curve lies noticeably above the Vargaftik/SNP v05 curves is readily apparent in the 100 MPa isobar plot – far more so than was evident in the 1 Pa isobar plot. This behavior is discussed briefly below.

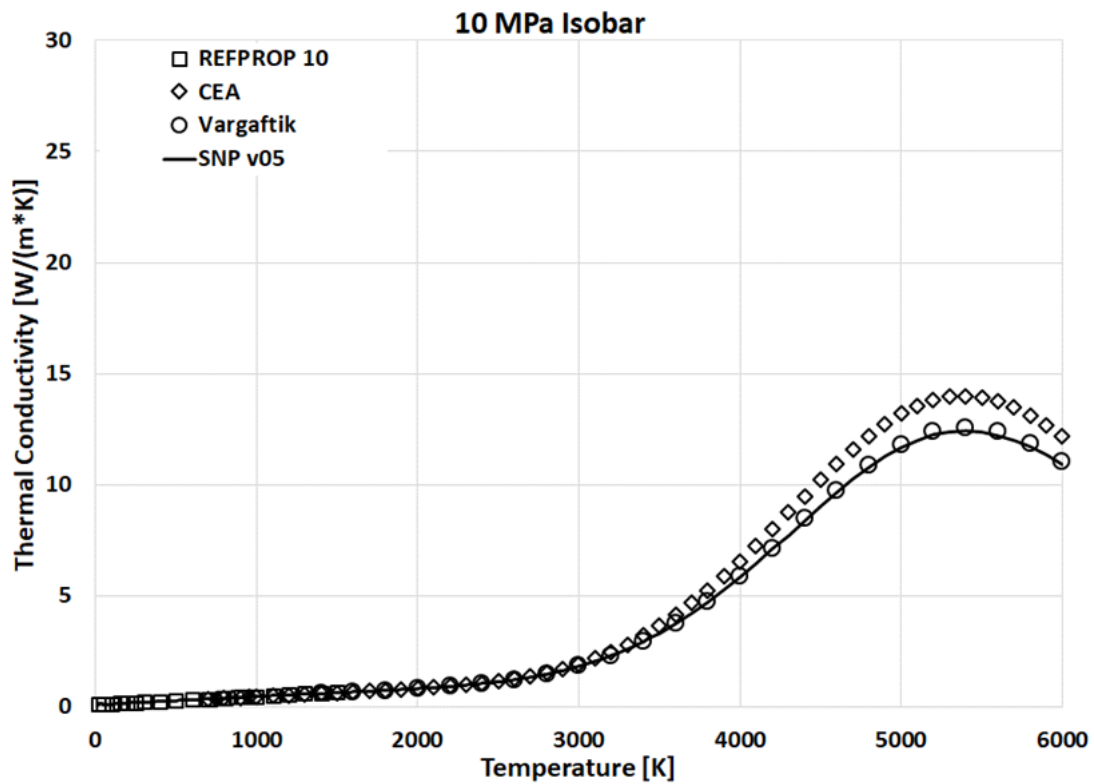
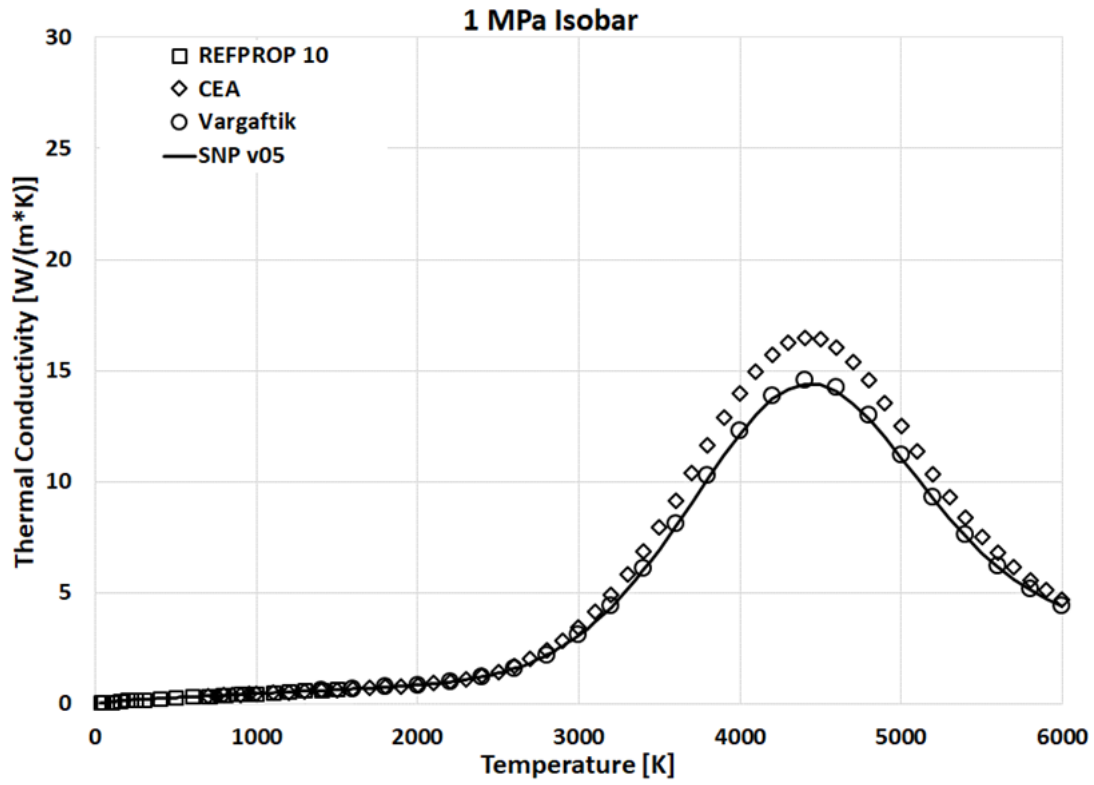


We next review the 1 kPa isobar, as it best illustrates the extent to which the CEA curve lies above those of Vargaftik and SNP v05 in the dissociation region (large hump). The primary reason for the difference, often quite large at the relative maxima in thermal conductivity, is that CEA obtains its unlike interaction diffusion coefficient from Tang and Wei (1974) instead of Vanderslice et al. (1962). Tang and Wei (1974) values for this diffusion coefficient are as much as 35% higher than those from Vanderslice et al. (1962). Though Tang and Wei (1974) is newer by 12 years, neither Tang and Wei (1974) nor Vanderslice et al. (1962) values are anchored to or validated by experimental results. Kjelstrup et al. (2016) arrive at the same diffusion coefficient via direct simulation of molecular dynamics resulting in values at least an order of magnitude smaller than those of Tang and Wei (1974). The best approach for arriving at the unlike interaction diffusion coefficient is unknown, but the method of Vanderslice et al. (1962) used for the SNP v05 calculations do represent a middle-ground between the other approaches.



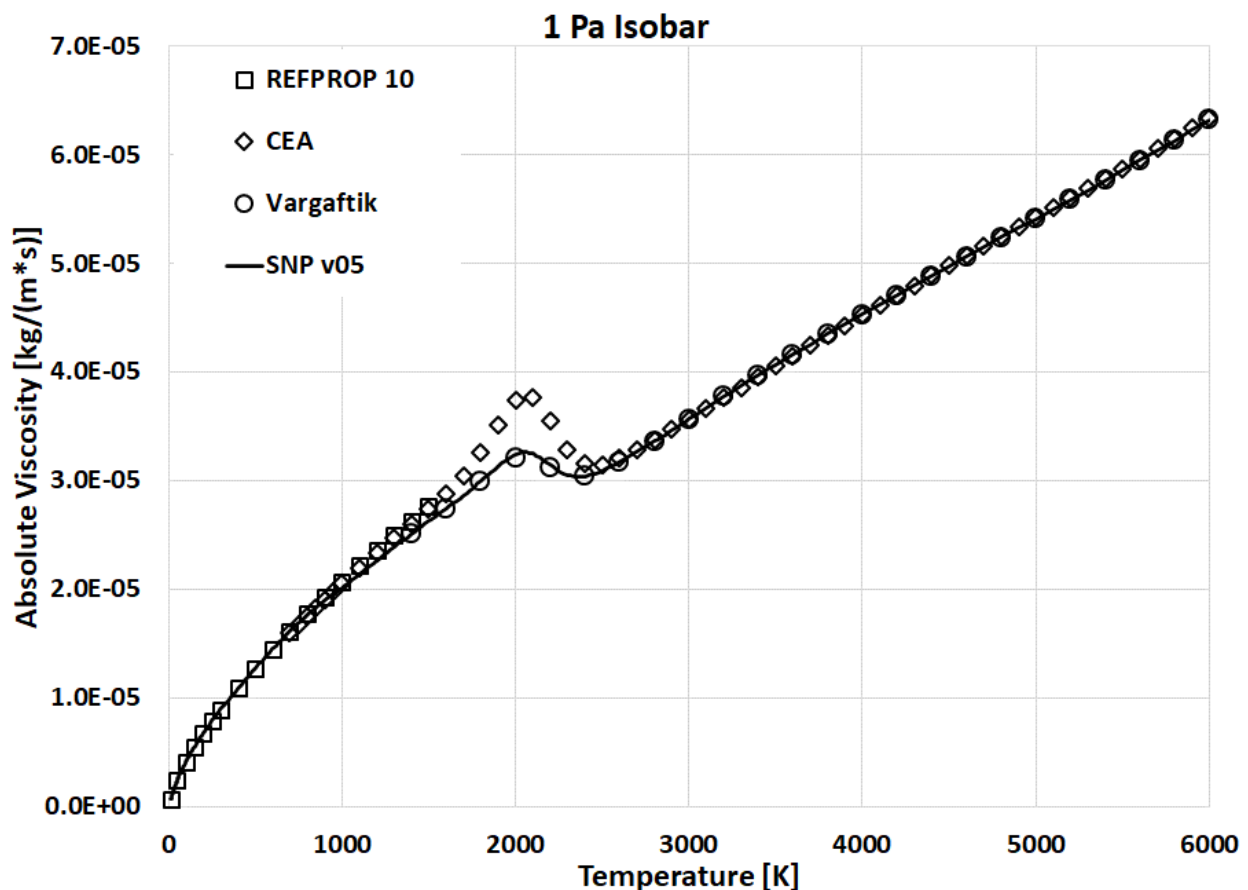
The remaining thermal conductivity isobar plots are supplied without further discussion as validation that the calculation methods result in reasonable behavior across the range of pressure and temperature considered in the SNP v05 database.



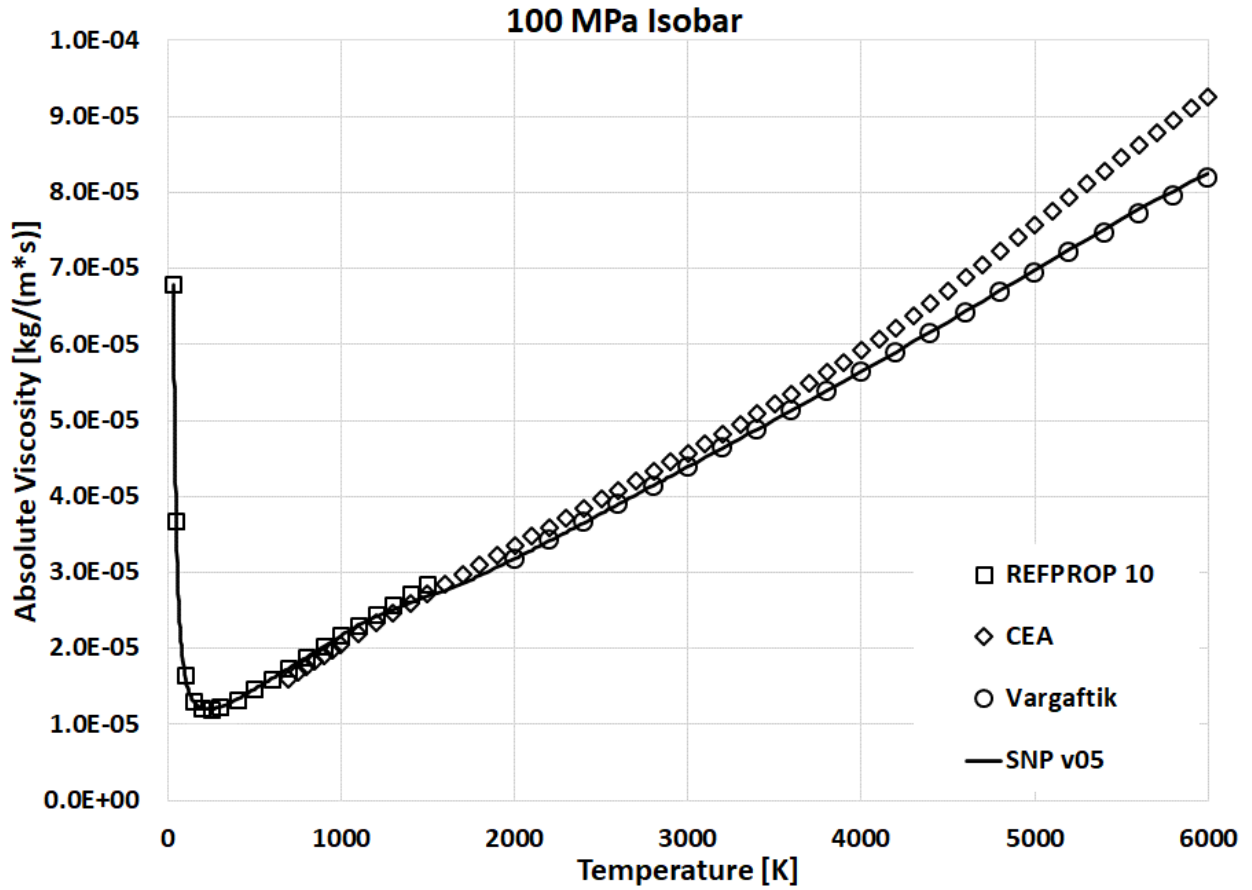


## Absolute Viscosity

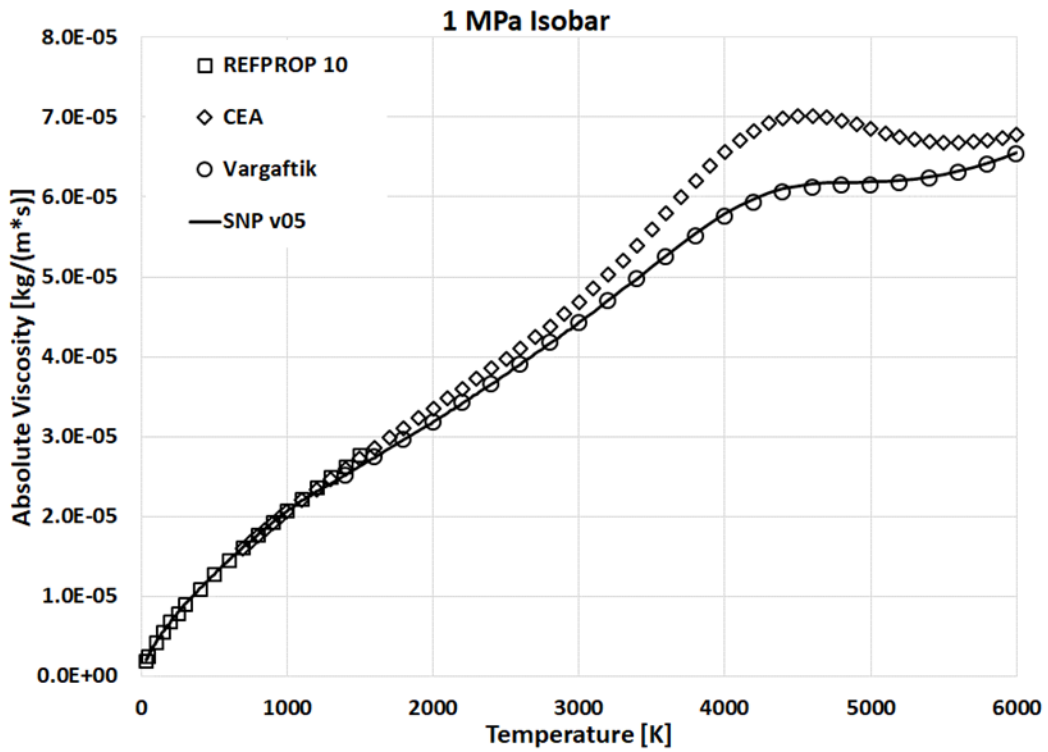
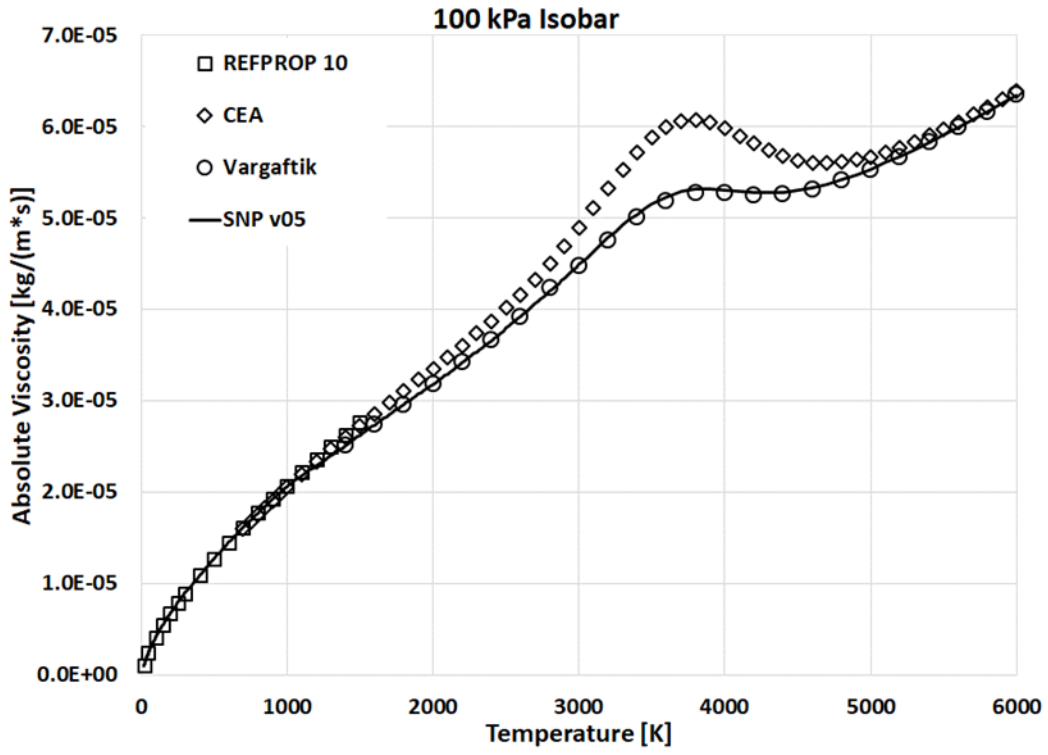
For the lowest pressure considered in the SNP v05 database, 1 Pa, the figure below depicts values from the various validation sources. The figure depicts the full temperature range in which one may observe almost exact agreement between SNP v05 and Vargaftik curves – as should be the case since both are based on the methods of Vanderslice et al. (1962). The SNP v05 curve makes a smooth transition from the REFPROP 10 curve to the Vargaftik curve. Note that at 2000 K, the CEA value is roughly 30 percent larger than the SNP v05 and Vargaftik curves. This behavior is due to the same differences in unlike interaction diffusion coefficient discussed at the end of the Thermal Conductivity section above.

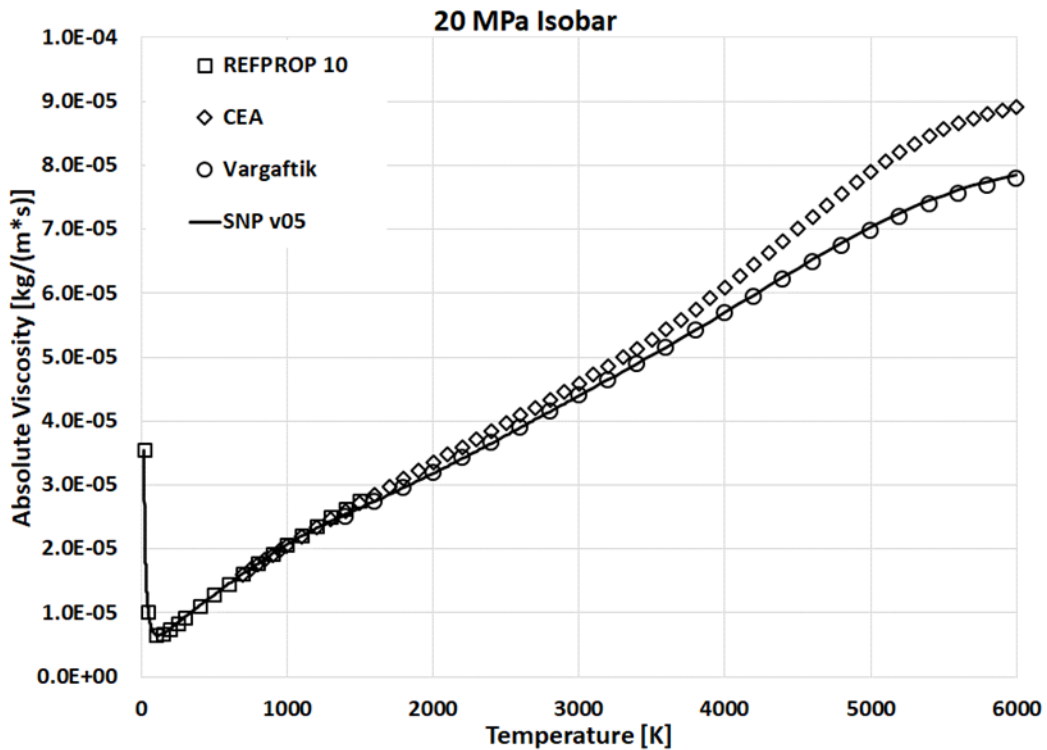
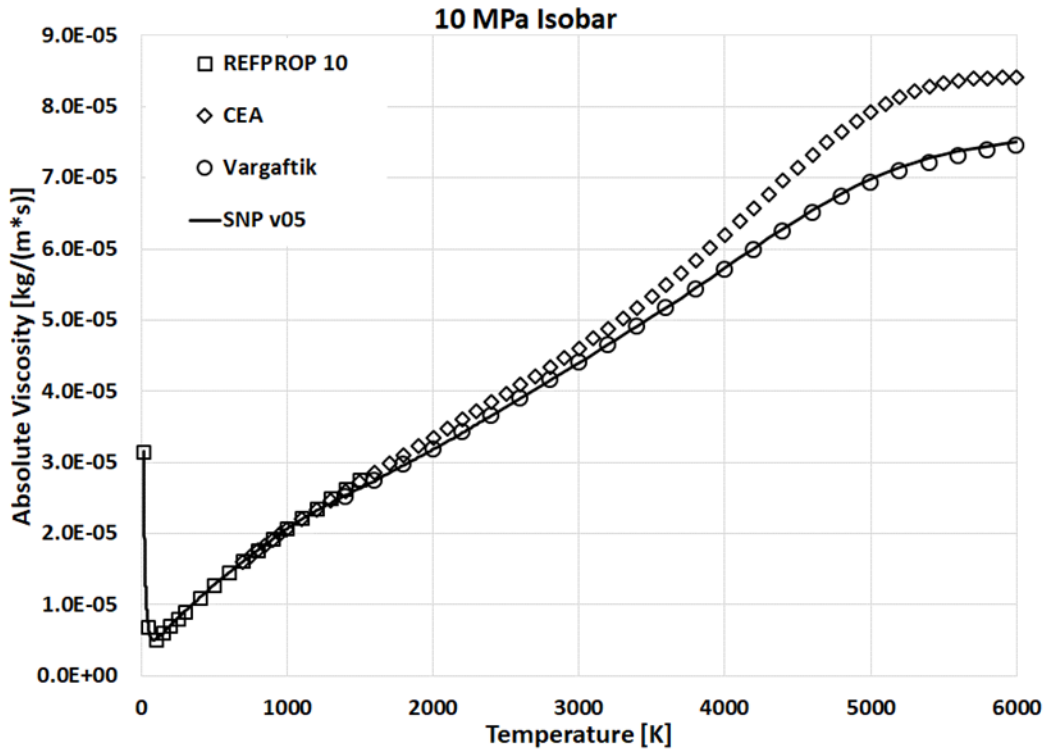


Next, the 100 MPa isobar is considered where, as was also the case for thermal conductivity, the REFPROP 10 values lie much farther above the Vargaftik values than was the case at 1 Pa. As a result, the transition between these two curves/datasets is far less smooth than for the 1 Pa case. Yet, the 100 MPa isobar SNP v05 is deemed acceptable, and the same transitions for lower pressures only get better. Here again, the CEA curve lay well above the other curves due to the higher unlike interaction diffusion coefficient applied by CEA.



The remaining isobars are provided without further discussion.





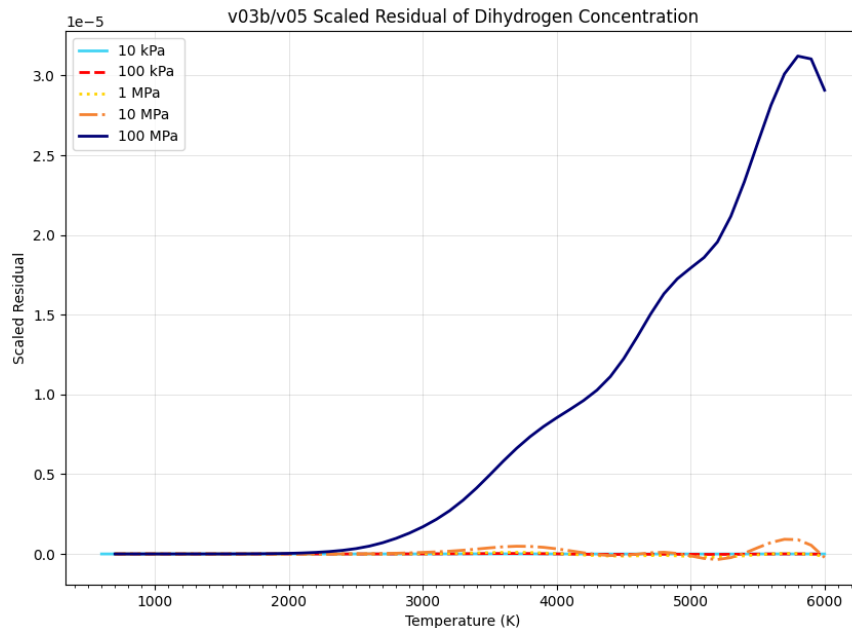
## APPENDIX G.

### COMPARISON OF V05 WITH V03B

This appendix compares the current SNP v05 database results with those of the v03b database in wide use within the SNP community. As was the case in Appendix F for thermodynamic properties, this section considers normalized residual errors defined as  $(v03b \text{ value} - v05 \text{ value}) / (v05 \text{ value})$ .

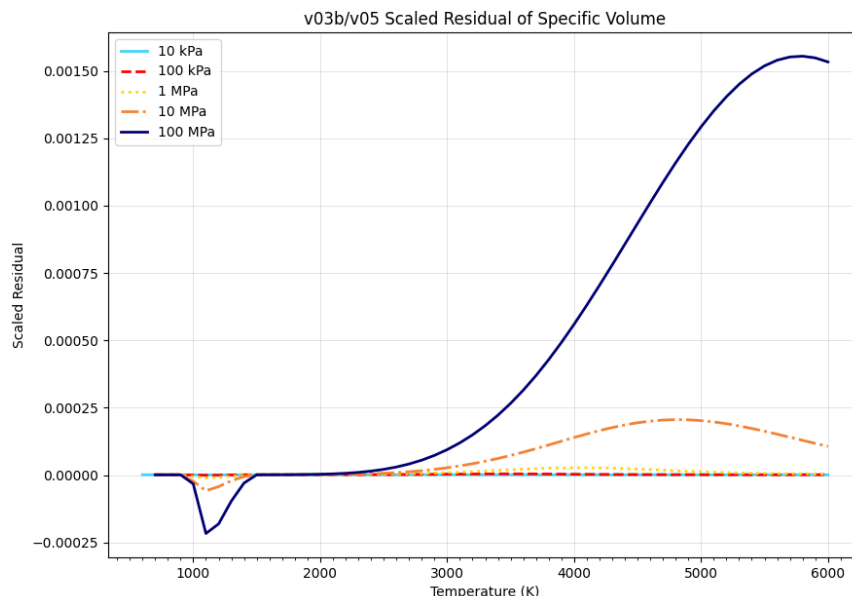
#### Dihydrogen Mole Fraction

First note that the error values on the plot are to be multiplied by  $1E-05$  as denoted by the  $1e-05$  found at the top left of the plot. Thus, the peak error magnitude observed in the plot is  $3E-05$  and not 3.0. The observed error is due to the typographical error in the fugacity calculation discussed back in Section 3.3.3.1. Though now corrected, this error would not have been greater than roughly  $2E-06$  at 3000 K – 3000 K representing the highest temperature considered by any recent nuclear thermal propulsion systems analyses.



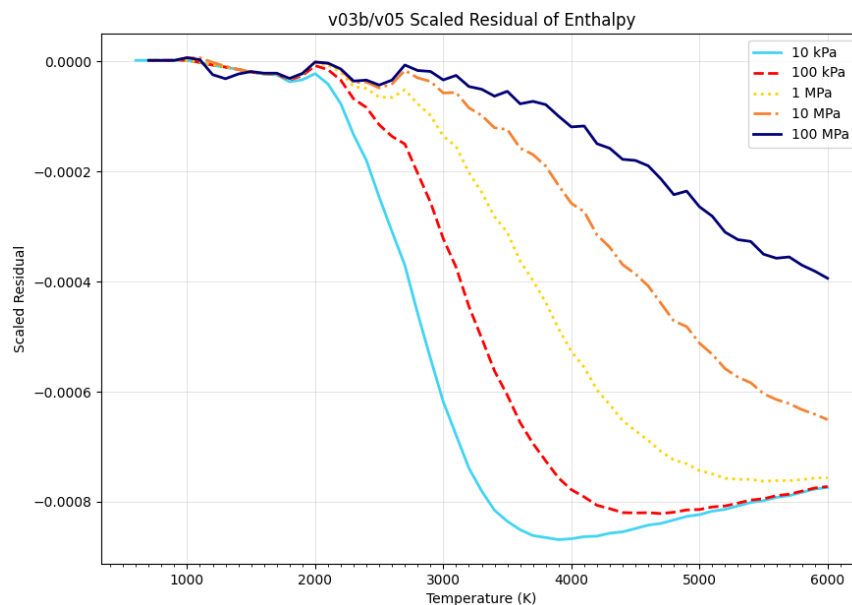
#### Mass-Specific Volume

The highest pressure isobars exhibit humps that originate at 1000 K. This 1000 K origin is because v03b joined the REFPROP 9.1 and higher temperature methods at 1000 K. These humps just above 1000 K are the result of a greatly improved bridging process for v05 compared to v03b. The residual error near 6000 K for the 100 MPa isobar peaks at only 0.16%, and the error of greater practical interest for nuclear thermal propulsion systems analyses at roughly 3000 K and 10 MPa is only about 0.001%.



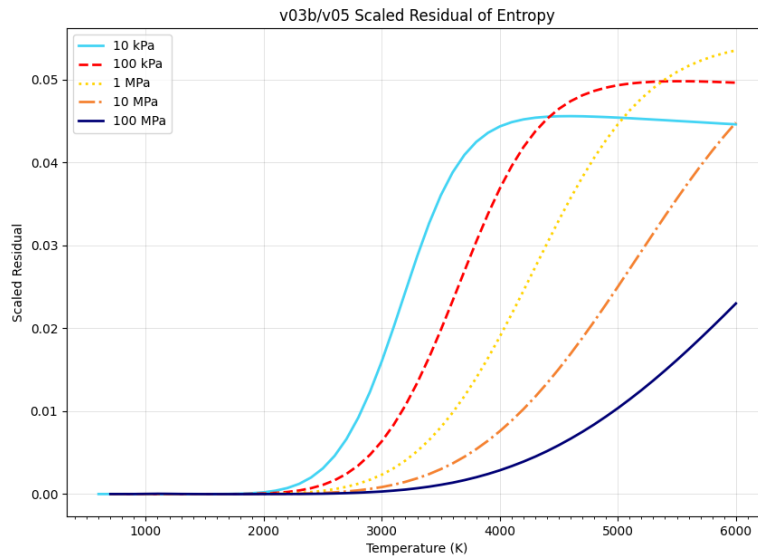
## Mass-Specific Enthalpy

The largest difference in enthalpy occurs at the lowest pressures and is never greater than 0.1% in magnitude.



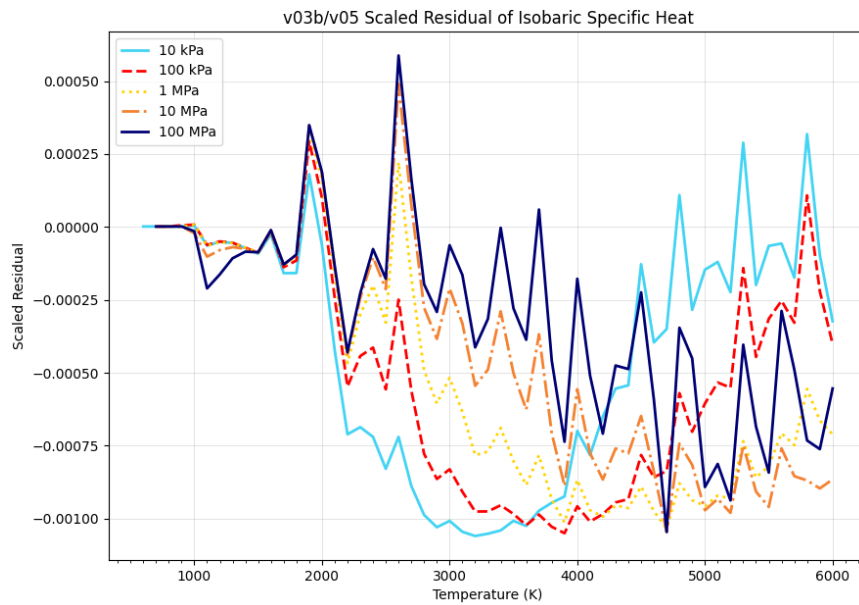
## Mass-Specific Entropy

Entropy differences between v03b and v05 are quite large for states where mostly H atom is present. The reason for these large entropy differences is the erroneous manner in which McDonald (2017, 2018) shifted H atom entropy in addition to shifting parahydrogen entropy to match the REFPROP reference state. For v05, the entire database is calculated in a 0 K reference state and then all results are shifted to the REFPROP 10 default reference state.



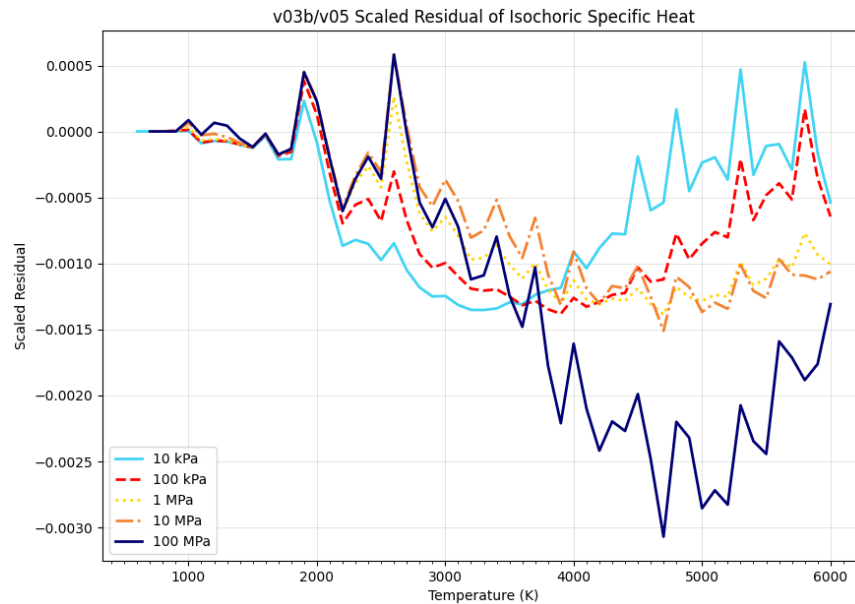
### Isobaric Mass-Specific Heat

Maximum differences here are around 0.1% in magnitude. Exact error sources are not known.



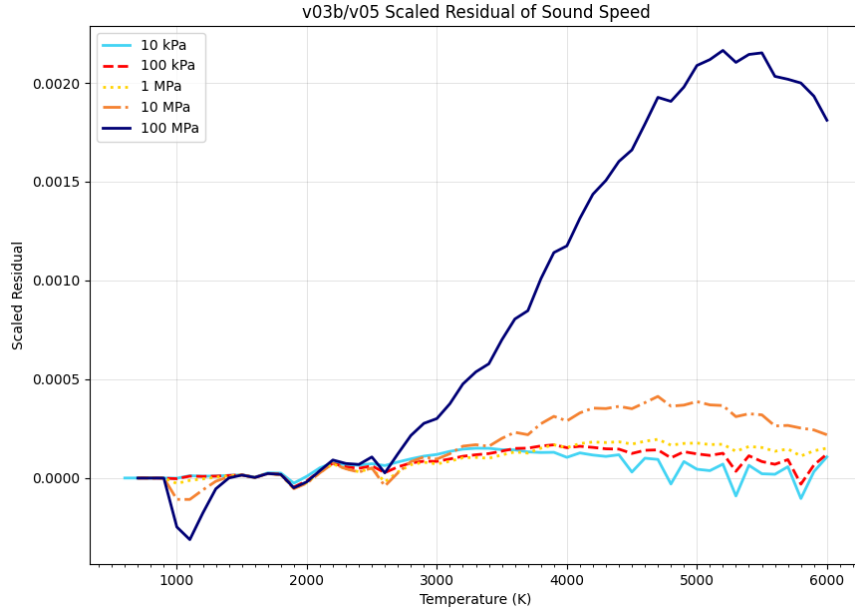
### Isochoric Mass-Specific Heat

Maximum differences here are around 0.3%. Exact sources of error are unknown.



## Sound Speed

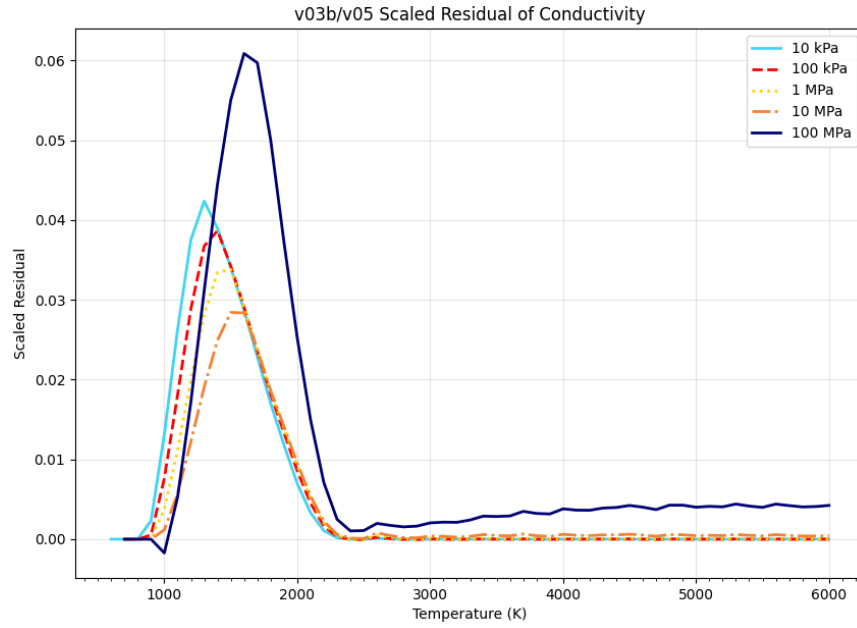
Differences in sound speed are also quite small except for the 100 MPa isobar. Exact cause(s) for the error is unknown.



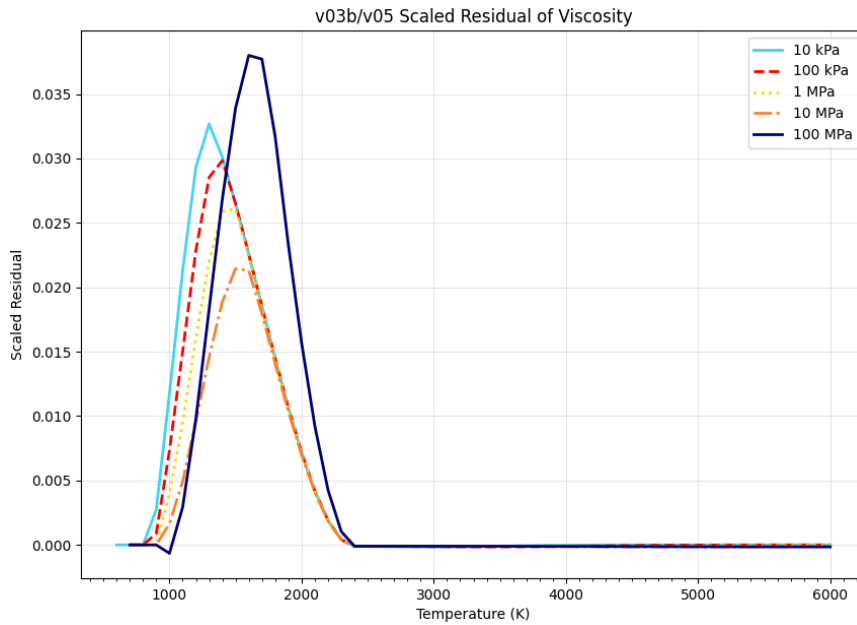
## Thermal Conductivity

Both thermal conductivity and absolute viscosity exhibit peaks in their v03b vs v05 residuals in the region of each isobar where dissociation of H<sub>2</sub> to H first occurs with increasing temperature. The v05 process for bridging/joining REFPROP 10 values to the dissociation values calculated using the methods of Vanderslice et al. (1962) is much better than that applied for the v03b

database release. The SNP v05 database forces bridging to be complete before any substantial dissociation occurs with increasing temperature.



### Absolute Viscosity



Revision: Baseline/Revision Level	Document Number: SNP-DOC-0046
Effective Date: 07/01/2024	Page: 144 of 149
Title: Parahydrogen Thermophysical Properties V05 Final Report	

## APPENDIX H.

### OVERVIEW OF THE BRIDGING PROCESS

A great deal of care is taken with regards to how the lower temperature REFPROP 10 parahydrogen properties results are joined to the higher temperature dissociating results from Section 5.3. The REFPROP 10 Pressure-Volume-Temperature surface in the near region of the Bridging Line (Sections 3.3.2.3.1 and 5.5) exhibits much greater curvature than that available from the cubic virial equation of state the higher temperature methods apply for dihydrogen. Thus, in the end, any attempt to join these two datasets will be imperfect. The question becomes one of where to allow the imperfections to manifest themselves to result in the best possible combined working database.

The present bridging approach demands smooth union of the REFPROP and dissociating P-V-T surfaces along the Bridging Line. Thus, the following constraints are always applied in the solution for Bridging Parameters – exact matching of Molar Specific Volume,  $V$ , and the first partial derivatives of  $V$  with respect to temperature at constant pressure,  $(\delta V/\delta T)_P$ , and its complement,  $(\delta V/\delta P)_T$ . The remaining properties to be matched are enthalpy,  $H$ , entropy,  $S$ , and specific heat,  $C_p$ . Isochoric specific heat and sound speed are also important, but these are found to just fall into place if the former are matched. Five Bridging Parameters are attached directly to the virial equation of state, so it is possible to use these to satisfy two of enthalpy, entropy, and isobaric specific heat but not all three – especially not all three at higher pressures.

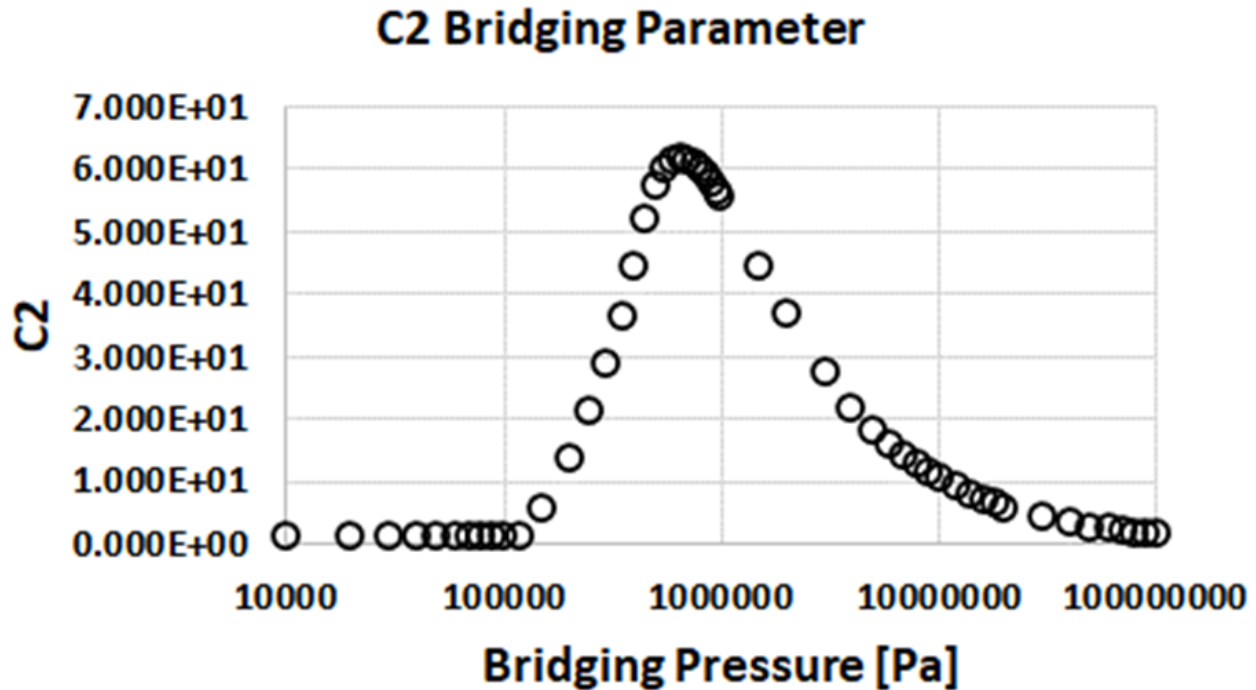
At high pressure (definitely for  $> 10$  MPa, the best overall solution approach is directly satisfy  $V$ ,  $(\delta V/\delta T)_P$ ,  $(\delta V/\delta P)_T$ ,  $H$ ,  $C_p$  and apply an additive correction to  $S$  that forces matching the REFPROP 10 value. Yet, experience also reveals that this approach works poorly at lower pressures ( $< 1$  MPa) – this behavior occurs because the zero-pressure isobaric specific heat extracted by differentiation of  $H_0$  is not exactly the same as that from REFPROP 10. Thus, a strategy is needed by which to transition from application of constraint sets

$V$ ,  $(\delta V/\delta T)_P$ ,  $(\delta V/\delta P)_T$ ,  $H$ ,  $C_p$  ..... at higher pressures  
to

$V$ ,  $(\delta V/\delta T)_P$ ,  $(\delta V/\delta P)_T$ ,  $H$ ,  $S$  ..... at lower pressures.

#### Constraint Application Details

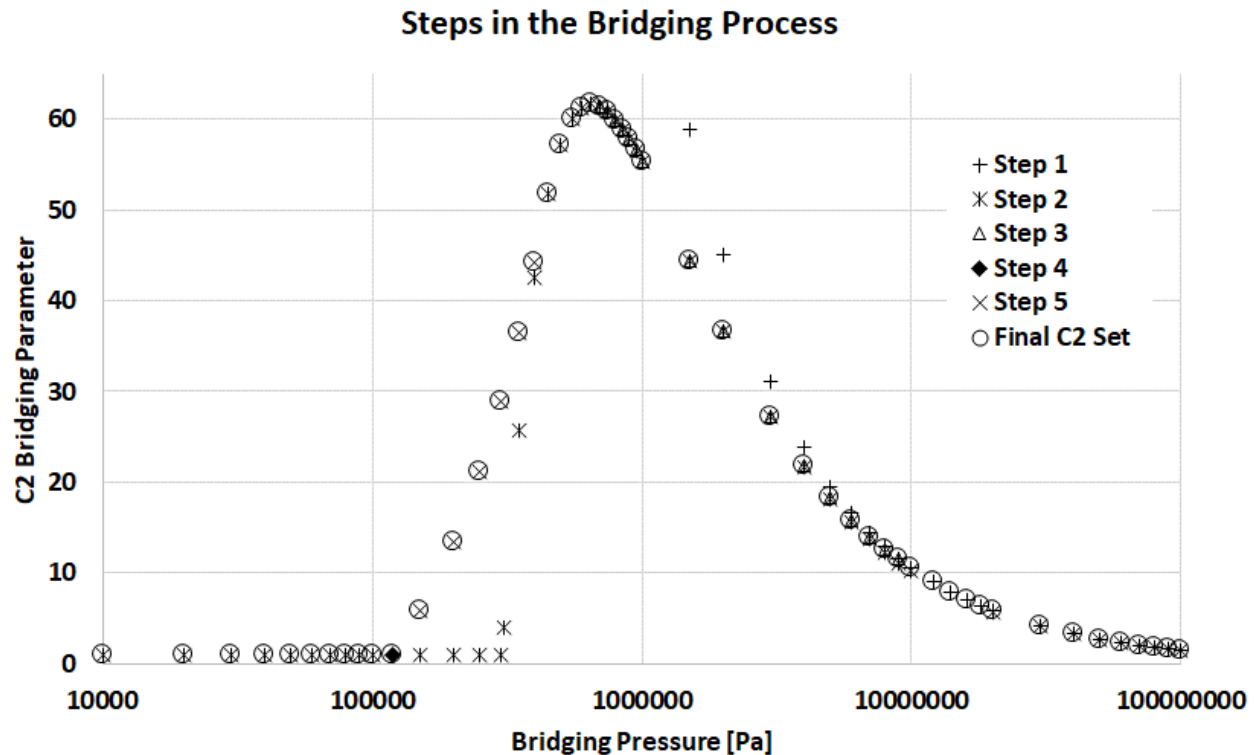
Bridging Parameters are calculated for a suitably dense vector of pressure, temperature pairs along the Bridging Line – the chosen density may be viewed in the plots of Section 5.5.3. The plot of C2 Bridging Parameter values versus pressure is repeated here for reader convenience.



Bridging Parameters are found by simultaneous solution of the property relations to satisfy the constraints related in Section 5.5.2.1 by varying the Bridging Parameters related in Section 5.5.2.2. This solution process begins at the highest pressure in the database, 100 MPa, and proceeds down the 52 Bridging Pressures denoted in the C2 versus Bridging Pressure plot above. Broken down into numbered steps, the bridging process is:

0. Establish a vector of Bridging Temperature values by satisfying constraints 1-7 from Section 5.5.2.1 ( $V$ ,  $H$ ,  $S$ ,  $DVDT$ ,  $DVDP$ ,  $C_p$ ,  $C_{p\_rxn}/C_{p\_mix} = 1E-08$ ) by simultaneously varying parameters 1-7 ( $\sigma$ ,  $\epsilon/k$ ,  $C_0$ ,  $C_1$ ,  $C_2$ ,  $\Delta S_{bridge}$ ,  $T_{bridge}$ ) from Section 5.5.2.2 to minimize constraint errors. Note a simplified nomenclature is used in this appendix. The Bridging Temperature values obtained in this matter will be used throughout the rest of this process, as they are good enough due to the very strong coupling of constraint 7 ( $C_{p\_rxn}/C_{p\_mix} = 1E-08$ ) with parameter 7 ( $T_{bridge}$ ).

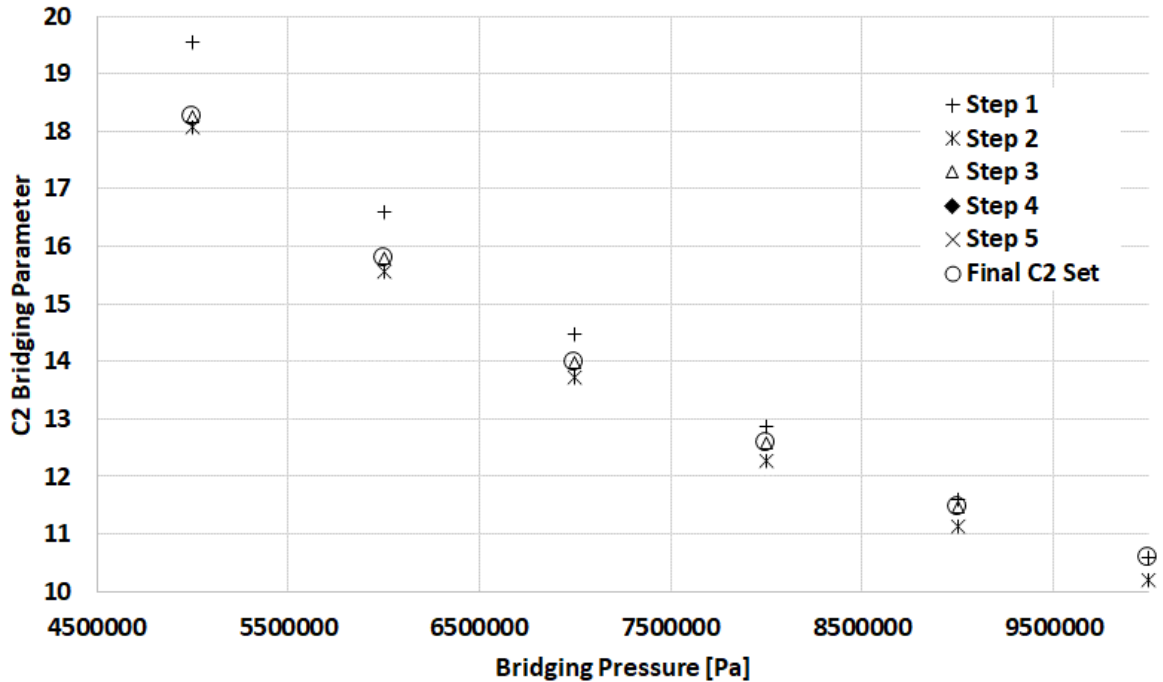
Figure to which the remaining numbered steps make reference



- From 100 MPa down to 10 MPa, constraints for V, H, DVDT, DVDP, Cp are satisfied by solving for optimal values of  $\sigma$ ,  $\epsilon/k$ , C0, C1, C2, which results in very small normalized residual errors for the 5 constraints – typically  $< 1E-15$ . The resulting values for C2 are depicted by plus signs (mostly obscured by asterisks) in the reference plot above. The entropy, S, constraint is then satisfied by calculating the  $\Delta S_{\text{bridge}}$  directly as the difference between the current (SNP v05) method result and the corresponding REFPROP 10 entropy value. As evident in the C2 plot above, C2 rises increasingly rapidly below 10 MPa and, were this solution process continued, C2 values upwards of 10000 results at 10 kPa. Such large C2 values do not allow the temperature variation scheme related back in Section 5.5.4 to work well, so something must be done to control the C2 behavior with decreasing Bridging Pressure. The approach taken here is to define an acceptable normalized residual error in the Cp constraint (taken to be  $-1E-05$ ) and find Bridging Parameter sets that just achieve this  $-1E-05$  constraint. This consistently slightly underpredicts Cp, but reins in the C2 values.
- Below 10 MPa, constraints V, H, DVDT, DVDP are satisfied by simultaneous variation of  $\sigma$ ,  $\epsilon/k$ , C0, C1, and C2 is varied separately to satisfy the  $-1E05$  normalized error constraint on Cp. These C2 values are depicted by asterisks in the reference plot above. This eventually results in C2 passing through a relative maximum at roughly 650 kPa. The resulting Bridging Parameter values are mostly not directly used, but rather a ‘working’ C2 curve is created in the next step.

- The outcome of this step is noticeable in the reference plot, so the plot immediately below depicts a sub-portion that better reveals the purpose of Step 3.

**Zoom in to Step 3 in the Bridging Process**



Step 3 blends the curves resulting from Steps 1 (plus signs) and 2 (asterisks) by linearly decreasing the difference between the C2 values at 10 MPa resulting from Step 1 (plus sign) and Step 2 (asterisk) such that it vanishes at the relative maxima – or in equation form

$$C2(P) = C2_{10MPa\_step2} + (C2_{10MPa\_step1} - C2_{10MPa\_step2}) \cdot \frac{(P - 650000)}{(10000000 - 650000)}$$

which yields the Step 3 curve (triangles) readily noticeable in the plot immediately above, but much less noticeable in the earlier reference plot covering the full C2-Bridging Pressure range.

Use of the above C2 relation for  $650000 < P < 10000000$  results in Cp normalized error values better than  $-1E-05$ , when V, H, DVDT, DVDP are satisfied by simultaneous variation of  $\sigma$ ,  $\epsilon/k$ , C0, C1. The entropy, S, constraint is then satisfied by calculating the  $\Delta S_{bridge}$  directly as the difference between the current (SNP v05) method result and the corresponding REFPROP 10 entropy value.

- Not really a step but on the interval  $450000 \leq P \leq 650000$  the Bridging Parameter values used are those from Step 2. The entropy, S, constraint is then satisfied by calculating the

Revision: Baseline/Revision Level	Document Number: SNP-DOC-0046
Effective Date: 07/01/2024	Page: 148 of 149
Title: Parahydrogen Thermophysical Properties V05 Final Report	

$\Delta S_{\text{bridge}}$  directly as the difference between the current (SNP v05) method result and the corresponding REFPROP 10 entropy value.

- On the interval  $118566 < P < 450000$ , the methodology transitions away from satisfying a  $C_p$  constraint towards application of the  $S$  constraint. To aid this transition, Step 5 finds the Bridging Pressure value at which satisfying  $V$ ,  $H$ ,  $S$ ,  $DVDT$ ,  $DVDP$  constraints by simultaneous variation of  $\sigma$ ,  $\epsilon/k$ ,  $C_0$ ,  $C_1$  with  $C_2 = 1.0$  results in the  $C_p$  constraint error equal to  $-1E-05$  applied in Step 2 above. See black diamond in the reference plot above.
- In this step,  $C_2$  values are defined by linearly fitting the  $(P_{\text{bridge}}, C_2)$  pairs at 118566 Pa and 450000 Pa. The upper bound of 450000 Pa is simply the existing Bridging Pressure vector point at which the slope of the line defined here ( $x$ 's in the reference plot) most closely matches the slope of the curve from Step 2; there is no need to exactly match the slope as the idea here to is ride a curve on which normalized  $C_p$  error is roughly  $-1E-05$ . There is nothing magic about  $-1E-05$ , so we didn't make this harder than it had to be. The task now is to transition from applying  $V$ ,  $H$ ,  $DVDT$ ,  $DVDP$ ,  $C_p$  constraints at 450000 Pa to applying  $V$ ,  $H$ ,  $S$ ,  $DVDT$ ,  $DVDP$  constraints at 118566 Pa. This task is accomplished by defining a weighting factor,  $C_p_{\text{weight}}$ , as follows:

$$\text{Entropy Constraint: } (S_{\text{mix}} - S_{\text{REFPROP}})/S_{\text{REFPROP}} * (1 - C_p_{\text{weight}}) = 0$$

$$C_p \text{ Constraint: } (C_{p_{\text{mix}}} - C_{p_{\text{REFPROP}}})/C_{p_{\text{REFPROP}}} * C_p_{\text{weight}} = 0$$

The solution methodology satisfies  $V$ ,  $H$ ,  $DVDT$ ,  $DVDP$  and the above weighted versions of the  $S$  and  $C_p$  constraints by simultaneously varying  $\sigma$ ,  $\epsilon/k$ ,  $C_0$ ,  $C_1$  with  $C_2$  coming from the linear fit defined between 118566 Pa and 450000 Pa points. The entropy,  $S$ , constraint is then satisfied by calculating the  $\Delta S_{\text{bridge}}$  directly as the difference between the current (SNP v05) method result and the corresponding REFPROP 10 entropy value.

- Below the 118566 Pa Bridging Pressure value,  $C_2 = 1.0$  and  $\Delta S_{\text{bridge}} = 0$ . The remaining Bridging Parameters,  $\sigma$ ,  $\epsilon/k$ ,  $C_0$ ,  $C_1$ , are simultaneously varied to satisfy  $V$ ,  $H$ ,  $S$ ,  $DVDT$ ,  $DVDP$  constraints.

The above 7 steps enable calculation of the complete set of needed Bridging Parameter which are depicted by open circles in the reference plots above.

Revision: Baseline/Revision Level	Document Number: SNP-DOC-0046
Effective Date: 07/01/2024	Page: 149 of 149
Title: Parahydrogen Thermophysical Properties V05 Final Report	

## APPENDIX I.

### PYTHON SOURCE CODE LISTING(S)

The following python source code files are included in the distribution with this report. A general description of each file and its application to the total code suite is tabulated below:

File Name	Description
<b>parahydrogen.py</b>	This script includes all relevant real-gas property calculations, bridging parameters, interpolators, and required helper functions.
<b>parahydrogen_caller.py</b>	This file serves as the wrapper function to call parahydrogen.py, plotter.py, interpolate.py, etc. Several unit tests are included for viewing.
<b>interpolate.py</b>	Generates multidimensional interpolators for each fluid property based on the input dataframe provided by the user.
<b>plotter.py</b>	Provides all 2D and 3D plotting features for each fluid property as well as the verification activities.
<b>read_data.py</b>	Reads input data and stores in python dataframes for usage by other scripts. Includes all calls to parse the saturation pairs and REFPROP reference data.
<b>write_data.py</b>	Serves as the primary tool for storing output data into CSV files
<b>saturation_data.zip</b>	Includes the interpolators to call the saturation liquid / vapor data pairs as well as the solidus temperature (lowest T available for each P).
<b>interpolators.zip</b>	Includes the REFPROP interpolators below the bridging dissociation temperatures for all accepted pressure steps (1 Pa – 100 MPa).